

# Flavor Generation in Food Processing

Lead Guest Editor: Tao Feng

Guest Editors: Zhimin Xu and Jun Lu



---



# **Flavor Generation in Food Processing**

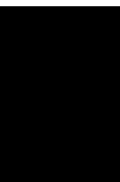
Journal of Food Quality

---

## **Flavor Generation in Food Processing**

Lead Guest Editor: Tao Feng

Guest Editors: Zhimin Xu and Jun Lu




---






Copyright © 2022 Hindawi Limited. All rights reserved.

This is a special issue published in "Journal of Food Quality." All articles are open access articles distributed under the Creative Commons Attribution License, which permits unrestricted use, distribution, and reproduction in any medium, provided the original work is properly cited.

# Chief Editor

Anet Režek Jambrak , Croatia



























## Associate Editors

Ángel A. Carbonell-Barrachina , Spain  
Ilija Djekić , Serbia  
Alessandra Durazzo , Italy  
Jasenka Gajdoš-Kljusurić, Croatia  
Fuguo Liu , China  
Giuseppe Zeppa, Italy  
Yan Zhang , China

## Academic Editors

Ammar AL-Farga , Saudi Arabia  
Leila Abaza , Tunisia  
Mohamed Abdallah , Belgium  
Parise Adadi , New Zealand  
Mohamed Addi , Morocco  
Encarna Aguayo , Spain  
Sayeed Ahmad, India  
Ali Akbar, Pakistan  
Pravej Alam , Saudi Arabia  
Yousef Alhaj Hamoud , China  
Constantin Apetrei , Romania  
Muhammad Sajid Arshad, Pakistan  
Md Latiful Bari BARI , Bangladesh  
Rafik Balti , Tunisia  
José A. Beltrán , Spain  
Saurabh Bhatia , India  
Saurabh Bhatia, Oman  
Yunpeng Cao , China  
ZhenZhen Cao , China  
Marina Carcea , Italy  
Marcio Carcho , Portugal  
Rita Celano , Italy  
Maria Rosaria Corbo , Italy  
Daniel Cozzolino , Australia  
Alessandra Del Caro , Italy  
Engin Demiray , Turkey  
Hari Prasad Devkota , Japan  
Alessandro Di Cerbo , Italy  
Antimo Di Maro , Italy  
Rossella Di Monaco, Italy  
Vita Di Stefano , Italy  
Cüneyt Dinçer, Turkey  
Hüseyin Erten , Turkey  
Yuxia Fan, China




Umar Farooq , Pakistan  
Susana Fiszman, Spain  
Andrea Galimberti , Italy  
Francesco Genovese , Italy  
Seyed Mohammad Taghi Gharibzahedi ,  
Germany  
Fatemeh Ghiasi , Iran  
Efsthios Giaouris , Greece  
Vicente M. Gómez-López , Spain  
Ankit Goyal, India  
Christophe Hano , France  
Hadi Hashemi Gahrui , Iran  
Shudong He , China  
Alejandro Hernández , Spain  
Francisca Hernández , Spain  
José Agustín Tapia Hernández , Mexico  
Amjad Iqbal , Pakistan  
Surangna Jain , USA  
Peng Jin , China  
Wenyi Kang , China  
Azime Özkan Karabacak, Turkey  
Pothiyappan Karthik, India  
Rijwan Khan , India  
Muhammad Babar Khawar, Pakistan  
Sapna Langyan, India  
Mohan Li, China  
Yuan Liu , China  
Jesús Lozano , Spain  
Massimo Lucarini , Italy  
Ivan Luzardo-Ocampo , Mexico  
Nadica Maltar Strmečki , Croatia  
Farid Mansouri , Morocco  
Anand Mohan , USA  
Leila Monjazez Marvdashti, Iran  
Jridi Mourad , Tunisia  
Shaaban H. Moussa , Egypt  
Reshma B Nambiar , China  
Tatsadjieu Ngouné Léopold , Cameroon  
Volkan Okatan , Turkey  
Mozaniel Oliveira , Brazil  
Timothy Omara , Austria  
Ravi Pandiselvam , India  
Sara Panseri , Italy  
Sunil Pareek , India  
Pankaj Pathare, Oman

María B. Pérez-Gago , Spain  
Anand Babu Perumal , China  
Gianfranco Picone , Italy  
Witoon Prinyawiwatkul, USA  
Eduardo Puértolas , Spain  
Sneh Punia, USA  
Sara Ragucci , Italy  
Miguel Rebollo-Hernanz , Spain  
Patricia Reboredo-Rodríguez , Spain  
Jordi Rovira , Spain  
Swarup Roy, India  
Narashans Alok Sagar , India  
Rameswar Sah, India  
El Hassan Sakar , Morocco  
Faouzi Sakouhi, Tunisia  
Tanmay Sarkar , India  
Cristina Anamaria Semeniuc, Romania  
Hiba Shaghaleh , China  
Akram Sharifi, Iran  
Khetan Shevkani, India  
Antonio J. Signes-Pastor , USA  
Amarat (Amy) Simonne , USA  
Anurag Singh, India  
Ranjna Sirohi, Republic of Korea  
Slim Smaoui , Tunisia  
Mattia Spano, Italy  
Barbara Speranza , Italy  
Milan Stankovic , Serbia  
Maria Concetta Strano , Italy  
Antoni Szumny , Poland  
Beenu Tanwar, India  
Hongxun Tao , China  
Ayon Tarafdar, India  
Ahmed A. Tayel , Egypt  
Meriam Tir, Tunisia  
Fernanda Vanin , Brazil  
Ajar Nath Yadav, India  
Sultan Zahiruddin , USA  
Dimitrios I. Zeugolis , Ireland  
Chu Zhang , China  
Teresa Zotta , Italy





## Contents

---


**Panelist Acceptance, Proximate Characteristics of Amino Acids and Volatile Compounds, and Color Profile of Fermented Cempedak (*Artocarpus champeden*) and Oyster Mushroom (*Pleurotus ostreatus*) Seasoning**

Miftakhur Rohmah , Bernatal Saragih, Nur Amaliah , Rimbawan Apriadi, and Anton Rahmadi   
Research Article (13 pages), Article ID 3092246, Volume 2022 (2022)

**Relationships between Shanghai Five Different Home-Brewed Wines Sensory Properties and Their Volatile Composition Assessed by GC-MS**

Xin Dang , Tao Feng , LingYun Yao , and Da Chen   
Research Article (12 pages), Article ID 3307160, Volume 2022 (2022)




**Analysis of Volatile Components in *Tremella fuciformis* by Electronic Nose Combined with GC-MS**

Lijun Fu , Jing Tian , Li Liu , Yongzheng Ma , Xiumin Zhang , Changyang Ma , Wenyi Kang , and Yong Sun   
Research Article (11 pages), Article ID 9904213, Volume 2022 (2022)


**Response Surface Methodology for Optimization of L-Arabinose/Glycine Maillard Reaction through Microwave Heating**

Qingru Xiang , Tao Feng , Qiang Su , and Lingyun Yao   
Research Article (10 pages), Article ID 1535296, Volume 2022 (2022)

**Comparison of the Nutritional and Taste Characteristics of 5 Edible Fungus Powders Based on the Composition of Hydrolyzed Amino Acids and Free Amino Acids**




Jian Li, Junmei Ma , Sufang Fan, Shengquan Mi , and Yan Zhang   
Research Article (10 pages), Article ID 3618002, Volume 2022 (2022)

**Structure and Menthone Encapsulation of Corn Starch Modified by Octenyl Succinic Anhydride and Enzymatic Treatment**

Xuan Ji, Jing Du, Jiaying Gu, Jie Yang, Li Cheng, Zhaofeng Li, Caiming Li, and Yan Hong   
Research Article (10 pages), Article ID 4556827, Volume 2022 (2022)

## Research Article

# Panelist Acceptance, Proximate Characteristics of Amino Acids and Volatile Compounds, and Color Profile of Fermented Cempedak (*Artocarpus champeden*) and Oyster Mushroom (*Pleurotus ostreatus*) Seasoning

Miftakhur Rohmah <sup>1</sup>, Bernatal Saragih,<sup>1</sup> Nur Amaliah <sup>1</sup>, Rimbawan Apriadi,<sup>2</sup> and Anton Rahmadi <sup>1,3</sup>

<sup>1</sup>Department of Agricultural Products Technology, Faculty of Agriculture, Mulawarman University, Samarinda, East Kalimantan 75119, Indonesia

<sup>2</sup>Master Program of Humid Tropical Agriculture, Faculty of Agriculture, Mulawarman University, Samarinda, East Kalimantan 75119, Indonesia

<sup>3</sup>Research Center for Medicine and Cosmetics from Tropical Rain Forests (PUI-PT Oktal), Mulawarman University, Samarinda, East Kalimantan 75119, Indonesia

Correspondence should be addressed to Anton Rahmadi; arahmadi@unmul.ac.id

Received 24 January 2022; Accepted 18 May 2022; Published 7 July 2022

Academic Editor: Tao Feng

Copyright © 2022 Miftakhur Rohmah et al. This is an open access article distributed under the Creative Commons Attribution License, which permits unrestricted use, distribution, and reproduction in any medium, provided the original work is properly cited.

The potential of mandai cempedak (*Artocarpus champeden*) powder to be mixed with other abundant raw materials such as oyster mushroom (*Pleurotus ostreatus*) as a flavoring ingredient is an exciting thing to study as a unique flavor source for the archipelago. This study aims to observe panelist acceptance, proximate characteristics of amino acid, volatile compounds, and color profiles on five mixed formulas of fermented cempedak (*Artocarpus champeden*) and oyster mushroom (*Pleurotus ostreatus*) seasoning. The five seasoning formulas combine 30–70% flavored mushroom powder and 30–70% mandai cempedak powder with control of commercial mushroom powder and pure mandai powder. Hedonic quality assessment on seasoning samples of flavored mushroom powder and mandai cempedak powder played a more critical role in the acceptance of the final product, with a slightly reddish yellow color tendency with a paleness level of around 66–67%. Seasoning samples had a savory taste with dominant amino acid profiles of ileusine (1.46%, w/w), glutamate (1.37%), methionine (0.82%), and aspartic acid (0.72%). All seasoning formulations of flavored mushroom and mandai cempedak powder have a moisture content of 8.4–10.9%, total protein 7.0–9.0%, soluble protein 2.4–3.5%, ash content 4.5–19.2%, fat content 2.3–4.5%, carbohydrates 62.7–79.4%, and the solubility is 31.0–89.4%. The dominant volatile compounds in seasoning are heptanone, dodecoxyethanol, and etradecyloxyethanol with pleasant aroma profiles, pungent fruity, green, citrus, and herbal. In conclusion, mandai cempedak powder to be mixed with other abundant raw materials such as oyster mushroom (*Pleurotus ostreatus*) can be used as a typical Indonesian flavor ingredient with unique characteristics in terms of its amino acid content, volatile compounds, and essential oils.

## 1. Introduction

Mandai cempedak is a typical product from Kalimantan, and this product utilizes waste from the cempedak fruit (*Artocarpus champeden*). Mandai making is done by spontaneous fermentation and stored at room temperature. The

processing steps include peeling the fruit skin, removing the epidermis, and soaking it in salt water to preserve and soften the texture. The duration of immersion is from several hours to a month [1]. The process of making mandai cempedak by induction of lactic acid bacteria starter has received a patent number S00201708792.



Mandai cempedak can be used as a source of typical Indonesian flavor, as fruits with a strong and distinctive aroma. Mandai cempedak which has been fermented at 37°C for seven days has characteristics such as valeric acid (46.83% of the GCMS chromatogram area), lactic acid (8.17%), 1-hydroxy-2-propanone (7.86%), 3-isopropoxy-1, 1, 1, 7, 7, 7-hexamethyl-3,5,5-tris (trimethylsiloxy) tetrasiloxane (7.01%), and N-methyl-beta,3,4-tris (trimethylsiloxy) phenethylamine (6.86%). The typical mandai cempedak has been used in ice cream products [2]. One of the best drying results of fermented mandai cempedak is obtained at 45°C, with a total polyphenol content (TPC) of  $358.8 \pm 55.6$  mg gallic acid equivalent (GAE)  $\text{kg}^{-1}$  dry sample, total hydrolyzed tannin content (HTC) of  $143.8 \pm 9.3$  mg tannic acid equivalent (TAE)  $\text{kg}^{-1}$  dry sample, total flavonoid content (TFC) of  $17.5 \pm 1.3$  mg catechin equivalent (CAE)  $\text{kg}^{-1}$  dry sample, and antioxidant activity (IC<sub>50</sub>) 56.96 g/mL [1]. The taste of mandai cempedak as a plant-derived product fermented by lactic acid bacteria is preferred [1], similar to other fermented products [3]. Lactic acid bacteria as flavor enhancers and seasoning food products have been widely used [4–6].

Oyster mushroom is a popular product widely used as a snack, usually served in dry, crispy fried foods. Oyster mushrooms have a taste readily accepted due to the high content of free amino acids [7]. The composition of umami components detected in mushrooms consisted of 5'-nucleotides groups, namely, inosinic acid (IMP), adenylate monophosphate (AMP), guanylate monophosphate (GMP), xanthosine monophosphate (XMP), and free amino acid groups, namely: aspartic and glutamic acid. The components of 5'-nucleotides and free amino acids are what cause the acceptance of oyster mushrooms to be the best when compared to other mushrooms [8].

The potential of mandai cempedak powder to be mixed with other abundant raw materials such as oyster mushroom (*Pleurotus ostreatus*) as a flavor ingredient is an interesting thing to study. The production process of vegetable seasoning from mandai cempedak and oyster mushrooms has been registered as a patent (no. S00202007443). The success of seasoning products is determined by the ability to improve the taste. Therefore, this study aims to observe the panelist acceptance, proximate characteristics, amino acids, volatile compounds, and color profile on five mixed formulas of fermented cempedak (*Artocarpus champeden*) and oyster mushroom (*Pleurotus ostreatus*) seasoning.

## 2. Method

**2.1. Mandai Cempedak Powder.** The mandai cempedak fermentation process follows patent no S00201708792 regarding the suboptimal temperature slow fermentation process with starter culture for mandai cempedak production. Fermented mandai cempedak powder followed the previously published method [1]. The fermented mandai cempedak was separated from the liquid, and the solid was taken. The solid was dried at 55°C for 18 hours in a 300 W electric dryer.

**2.2. Flavored Mushroom Powder.** Fresh wet oyster mushrooms added with spices such as pepper (2.5%, w/w), shallot (10%, w/w), garlic (8%, w/w), sugar (2%, w/w), and salt (6%, w/w). Furthermore, the new oyster mushroom formula and seasonings mixture was dried at 55°C for 18 hours in a 300 W electric dryer. Mandai cempedak powder and mushroom and spice powder were mixed with specific formulations (6 combinations), as shown in Table 1. Details of the vegetable seasoning production process from mandai cempedak (*Artocarpus champeden*) and oyster mushroom (*Pleurotus ostreatus*) had been protected by patents in the territory of the Republic of Indonesia with registration number S00202007443.

**2.3. Hedonic and Hedonic Quality Tests.** There are 30 panelists, ranging in age from 18 to 40 years, with a minimum education of a bachelor's degree and having attended lectures on spice and seasoning technology. The term of Hedonic quality tests can be interchangeable with Acceptance quality tests and are carried out in a room designated for organoleptic tests. There is a separate tasting booth for each panelist. The table and partitions are white in color and are made of wood and have no odor. Room temperature ranges from 20 to 27°C with a humidity of 65–75%. The light source is a neutral LED lamp (3000°K). Tests were carried out simultaneously for six people. The panelist who carried out the test was in good health and gave a written statement to participate in the test. Testing time is around 10.00 and 16.00 Central Indonesia Time. The hedonic test uses 5 rating scales, namely, (5) very much like, (4) like, (3) somewhat like, (2) do not like, and (1) do not like it at all. The six formulas were tested for the quality of organoleptic acceptance consisting of taste, color, aroma, texture, and overall acceptance of the six treatments of the samples presented (Table 2). The control product used was 0.5 g of commercial mushroom seasoning dissolved in 750 mL of boiling water (100°C). This formula refers to the product usage rules listed on the packaging. Sample and control were presented by dissolving seasoning at 100°C and served at 40°C. Then, as much as 30 mL of each sample was given to the panelists according to the minimum number of servings for organoleptic testing [9].

The assessment results obtained from all panelists were then analyzed by the nonparametric ANOVA method using the Kruskal–Wallis method with GraphPad Prism software version 8.0. If there is a significant difference at 5%, the differences between formulas are analyzed further with Dunn's Test.

**2.4. Proximate, Dissolved Protein, and Solubility Analysis.** For samples of all treatments except control mandai cempedak powder 100% (sample F), solubility, water content, ash, protein, and fat were analyzed using the Sudarmadji method [10]. Carbohydrate content is calculated based on the difference between water, ash, protein, and fat content. The dissolved protein test was analyzed by the Rohman and Sumantri [11] method.

TABLE 1: Composition of flavored mushroom powder and mandai cempedak powder.

Code	Flavored mushroom powder (%)	Mandai cempedak powder (%)
A	40	60
B	70	30
C	30	70
D	50	50
E	60	40
F*	Mandai cempedak powder (100%)	
G	Commercial mushroom powder (100%)	

\*Sample F is only used as a comparison for sensory tests and will not be continued with further tests.

**2.5. Amino Acid Analysis.** Amino acid analysis (AAA) was performed using the standard fluorescence orthophthalaldehyde (OPA) method from the Laboratory Unit for Testing, Calibration and Certification Services, Bogor Agricultural University, procedure number IK.LP-04.7-LT-1.0. Conditions for HPLC (Shimadzu) were as follows: Thermo Scientific ODS-2 Hypersil column, buffers A and B, the gradient flow rate of mobile phase at 1 mL/min, and fluorescence detector (Shimadzu). Buffer A consisted of Na-acetate (pH 6.5; 0.02% w/v), Na-EDTA (0.005% w/v), methanol (9.00% v/v), and tetrahydrofuran (THF) (1, 50% v/v) dissolved in 1 liter of ultrapure water (Merck-Millipore). This buffer was filtered through 0.45 m Millipore paper and used for five days at room temperature ( $28 \pm 2^\circ\text{C}$ ), stored in dark bottles, and filled with He or Nitrogen gas. Buffer B consists of 95% methanol and ultrapure water (Merck-Millipore). 0.45-micron Millipore paper was used for filtration.

**2.6. Volatile Component Analysis (GCMS).** Seasoning powder analysis with GCMS was carried out using the modified method of Misnawi and Ariza [12]. Identification and determination of the volatile component content obtained using the GCMS instrument with the stages of work including (1) extraction with SPME (solid phase microextraction), (2) sample injection into the GCMS device, and (3) qualitative determination of volatile components.

The volatile compound extraction phase with SPME (solid phase microextraction) begins with the sample weighing process. Seasoning powder weighed as much as 5 g placed in a vial with a capacity of 40 ml. Next, the vial containing the powder was heated with a water bath at  $60^\circ\text{C}$ . During the heating process in a water bath, the volatile components of the powder were extracted with SPME. The absorber used was polydimethylsiloxane/divinylbenzene (PDMS/DVB) polymer at 1 cm in length (Supelco, USA).

Analysis of volatile component composition by GCMS: the GCMS instrument used is the GCMS-QP2010 Plus Shimadzu which is equipped with a split-split less injector which is set at  $260^\circ\text{C}$ . The MS detector temperature was set at  $200^\circ\text{C}$ . The column used is Rtx-50 with an inner diameter of 0.25 mm, a length of 30 m, and a thickness of 0.25 m. The detector temperature was programmed at an initial temperature of  $60^\circ\text{C}$  for 3 minutes, and then the temperature was increased to  $220^\circ\text{C}$  for 20 minutes at a rate of  $5^\circ\text{C}/\text{minute}$ .

Helium was used as the carrier gas at a rate of 3 mL/min. Samples of 1L were injected by the split less method. Sampling time is 1.00 min with flow control in the pressure mode. The pressure used is 38.9 kPa with a total flow of 37.5 mL/min and a column flow of 0.78 mL/min. The linear velocity was measured at 32.2 cm/sec, the purge flow was measured at 3.0 mL/min, and the split ratio was set at  $-1.0$ . The analysis was carried out at the UPT Bioscience Laboratory, Jember State Polytechnic, Jember, East Java. The peaks on chromatogram were identified using Shimadzu Mass Spectral Libraries and Databases.

**2.7. Color Analysis.** For samples, all treatments except control of 100% mandai cempedak powder (sample F) were carried out using the Chromameter CR-400 instrument at the food technology laboratory of Gadjah Mada University Yogyakarta.  $L^*$ ,  $a^*$ , and  $b^*$  values determine color coordinates in the CIELAB color space system.

### 3. Results and Discussion

**3.1. Acceptance/Hedonic Analysis.** Table 3 describes the acceptability (hedonic) analysis results for the six seasoning formulas derived from a mixture of mushroom-spice powder and mandai powder in terms of taste, color, aroma, texture, and overall acceptability parameters. In general, the aroma and texture of all samples were not significantly different compared to control references (samples F and G). However, in terms of taste acceptance, the seasoning sample with a composition of 70% flavored mushroom powder and 30% mandai cempedak powder (B) showed an acceptance closer to the control of commercial mushroom powder. Of course, this is because sample B has the highest content of the flavored mushroom powder. On the other hand, on the color parameter, the seasoning sample with a composition of 30% mushroom spice powder and 70% mandai cempedak powder (C) had a different reception when compared to control references (sample F and G). At the drying time, mandai cempedak powder will have a pale color, presumably because the color is influenced by water content. The phenomenon of discoloration in the drying process of foodstuffs has also been reported in garlic powder [13].

Overall, the panelists assessed that the seasoning sample with a composition of 40% flavored mushroom powder and 60% mandai cempedak powder (A) and the seasoning sample with a composition of 50% flavored mushroom powder and 50% mandai cempedak powder (D) were significantly different when compared to control references (samples F and G). Therefore, the difference in acceptance between the components of the assessment parameters does not seem to be a consideration for overall approval. Still, the panelists are likely to focus more on the hedonic quality than on the product's hedonic rating only. Therefore, it is suspected that the panelists emphasized the hedonic quality aspect, which is cognitively more valuable when compared to the general acceptance of likes and dislikes [14]. Furthermore, the psychochemical characteristics produced in each formula, including soluble protein and fat (Figure 1),

TABLE 2: Hedonic quality scale.

Scale	Savory taste	Browning color	Mandai cempedak-specific odor	Fineness/roughness texture
5	Very savory	White-pale	Highly sour cempedak fruit	Very smooth
4	Savory	Light brown	Sour cempedak fruit	Fine smooth
3	A bit savory	Brown	Slightly sour cempedak fruit	A bit smooth
2	Not savory	Dark brown	Less sour cempedak presence	Rough
1	Not very savory	Very dark	Cempedak presence not detected	Very rough

TABLE 3: The acceptability analysis for the six seasoning formulas.

Sample	Taste	Color	Odor	Texture	Overall
A	2.7 ± 1.0a	3.6 ± 0.6a	3.5 ± 0.8a	3.5 ± 0.8a	3.0 ± 0.8a
B	3.4 ± 1.0ab	3.9 ± 0.5a	3.6 ± 0.7a	3.9 ± 0.6a	3.7 ± 1.0b
C	3.0 ± 1.0a	3.2 ± 0.8b	3.2 ± 0.8a	3.6 ± 0.8a	3.2 ± 0.9b
D	2.7 ± 0.7a	3.4 ± 0.8a	3.1 ± 0.8a	3.5 ± 0.9a	3.0 ± 0.9a
E	3.1 ± 0.7a	3.6 ± 0.7a	3.3 ± 0.8a	3.6 ± 0.9a	3.1 ± 0.7b
F	3.1 ± 0.8a	3.6 ± 0.8a	3.2 ± 0.9a	3.3 ± 1.0a	3.5 ± 1.1b
G	3.6 ± 0.9b	3.8 ± 0.6a	3.5 ± 0.9a	3.7 ± 0.7a	3.6 ± 0.9b

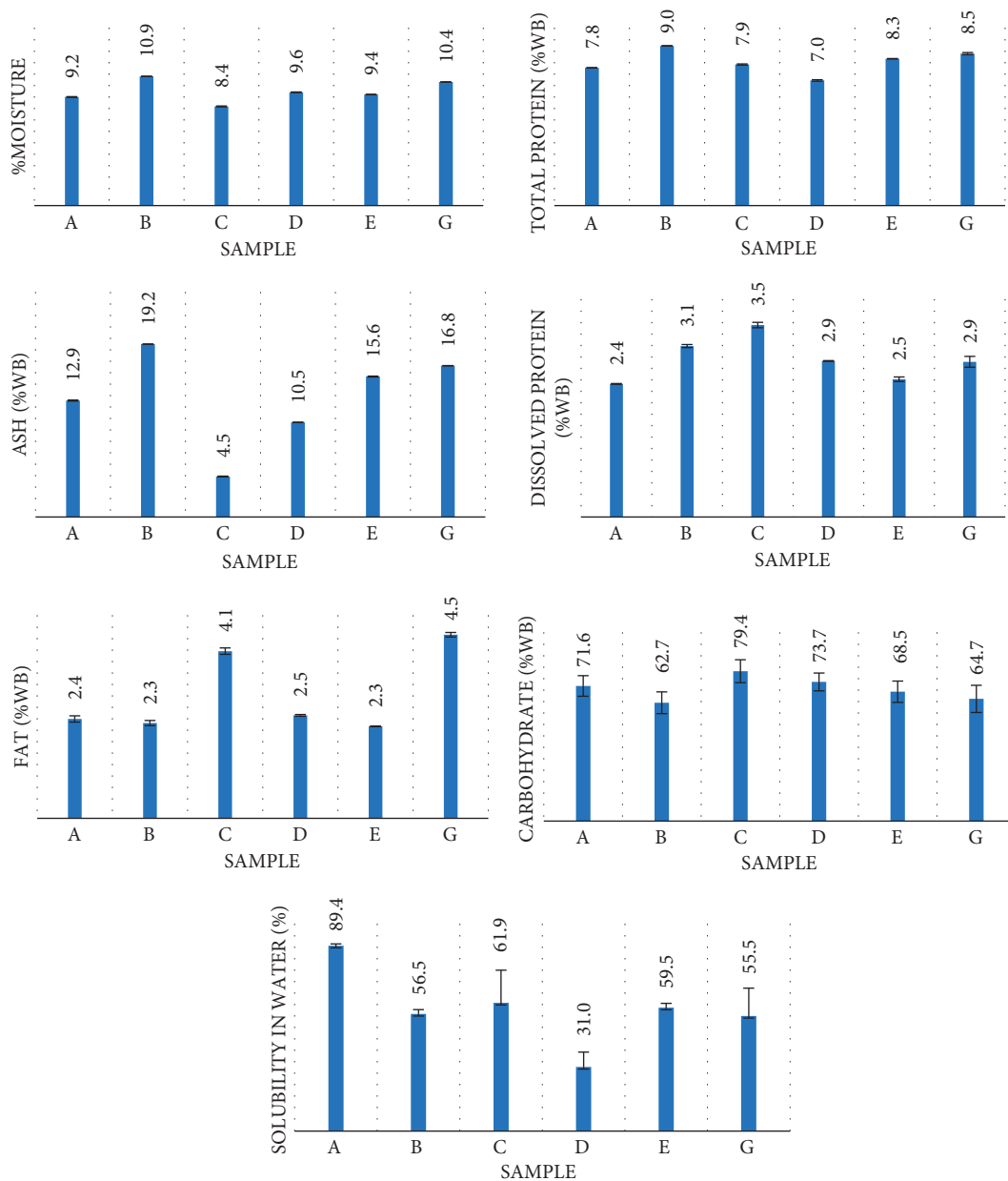


FIGURE 1: Results of the proximate analysis, soluble protein, and water solubility.

are thought to influence the likes and dislikes of a product [15].

Values are presented in average  $\pm$  standard deviation. Different letter after the values indicates the respective values are significantly different ( $p < 0.05$ ) in comparison to control references (samples F and G).

**3.2. Hedonic Quality Analysis.** Hedonic quality analysis was carried out on taste parameters with an umami scale of very unsavory to very savory, color parameters with a dark scale due to browning to pale white, aroma parameters with a ranking of very unscented to very fragrant, and texture parameters with a very coarse scale leading to very smooth. After going through the nonparametric ANOVA test, the aroma parameters were not significantly different for all samples (Table 4).

The highest savory taste was found in commercial mushroom powder (sample G). Furthermore, the seasoning sample with a composition of 70% flavored mushroom powder and 30% mandai cempedak powder (B) and a sample with a composition of 60% flavored mushroom powder and 40% mandai cempedak powder (E) were not statistically different ( $p < 0.05$ ) when compared with control references (samples F and G). The combination of compositions in the range of 60–70% flavored mushroom powder and 30–40% mandai cempedak powder is a balanced composition in terms of the umami quality of the seasoning products produced. The composition plays an essential role in determining the taste of the final product, especially in seasoning, as has been observed in similar products [16], sea grape protein hydrolysate sauce [17], and dried *Suillus granulatus* products [18].

The panelists can significantly distinguish the two reference controls from the texture and color parameters (F and G). Flavored mushrooms play an important role in determining texture and color. The texture tendency of the combination composition of 50–70% flavored mushroom powder and 30–50% mandai cempedak powder (B, C, D, and E) is closer to the texture of commercial mushroom powder (G). Due to the presence of spices such as pepper and shallots, the seasoning color tends to be dark, with a score of  $2.5 \pm 1.2$  (dark brown) to  $3.4 \pm 1.0$  (pale brown). For texture, mixing mandai cempedak powder with mushroom spice powder increased the acceptability observed in the control of mandai cempedak powder, namely,  $1.7 \pm 1.0$  (tends to be coarse) to a range of  $3.6 \pm 0.9$  to  $3.9 \pm 0.6$  (tends to be rough and fine). Brown color is an indicator of the Maillard reaction in food raw materials. The stronger the browning reaction caused by heating, the darker the resulting color. However, in the browning reaction of some products, such as *Takifugu obscurus* by-products hydrolysates [19], the product's taste is more acceptable to the panelists as the degree of browning increases to a certain extent. The drying process, heat treatment, enzymatic hydrolysis, and frying will change the taste of the food. Amino acid umami imagers are generally primary residues of peptides that have the N-terminus position. Peptides have umami imagers with double or

triple sequences because the heating process can amplify the umami taste [18].

Values are presented in average  $\pm$  standard deviation. A different letter after the values indicates the respective value is significantly different ( $p < 0.05$ ) in comparison to control references (samples F and G).

**3.3. Proximate Analysis, Soluble Protein, and Solubility.** Proximate analysis of seasoning of flavored mushroom powder and mandai cempedak powder was carried out to observe changes in composition due to formulation. For example, the seasoning sample with a composition of 70% flavored mushroom powder and 30% mandai cempedak powder (B) and a seasoning sample with a composition of 30% flavored mushroom powder and 70% mandai cempedak powder (C) turned out to contain dissolved protein, total protein, ash, fat, and carbohydrates were significantly different (Figure 1). Furthermore, the seasoning sample with a composition of 40% mushroom spice powder and 60% mandai cempedak powder (A) and the seasoning sample with a composition of 60% flavored mushroom powder and 40% mandai cempedak powder (E) also had significantly different proximate content and solubility. Likewise, the seasoning sample with a composition of 60% flavored mushroom powder and 40% mandai cempedak powder (D) was significantly different from all other samples tested. From Figure 1, it can be concluded that the 10% difference in each composition of the flavored mushroom powder and mandai cempedak powder will influence the proximate levels of the resulting seasoning.

**3.4. Amino Acid Analysis.** Table 5 presents the results of the amino acid analysis of (i) mandai cempedak powder, (ii) unflavored mushroom powder, (iii) flavored mushroom powder, and (iv) sample (E) 50% flavored mushroom powder and 50% mandai cempedak powder obtained with the chromatographic method. These data show that pure mushroom powder (ii) has more than double the total amino acid composition than mandai cempedak powder (i). The largest different compositions are in the amino acids leucine, glutamate, isoleucine, aspartic acid, alanine, and phenylalanine. Amino acids related to umami taste are aspartic acid and glutamate.

The addition of spices increased the amino acids valine from 0.68 to 0.95% and aspartic acid by about 0.16%, and to a lesser extent, threonine, serine, and methionine (Table 5). The composition of the spices used was pepper (2.5%, w/w), shallot (10%, w/w), and garlic (8%, w/w). Glutamic acid, aspartic acid, leucine, proline, and alanine are dominant amino acids in pepper (*Piper nigrum*) powder [20]. Shallots (*Allium cepa*) have dominant amino acids: arginine, glutamate, aspartic acid, threonine, leucine, and valine [21]. The predominant amino acid contents of garlic (*Allium sativum*) are proline, glutamate, phenylalanine, valine, and asparagine, in addition to alliin and methiin degradation products [22]. The addition of valine from the composition of the spice ingredients is obtained from shallots and garlic. Aspartic acid in flavored mushroom powder (iii) is obtained

TABLE 4: Results of hedonic quality analysis.

Sample	Savory Taste	Browning Color	Mandai cempedak-specific odor	Fineness/roughness texture
A	2.8 ± 0.8a	2.5 ± 0.9a	3.2 ± 0.8a	3.8 ± 0.7a
B	3.2 ± 0.9b	3.4 ± 1.0c	3.3 ± 0.9a	3.6 ± 0.9ac
C	2.8 ± 0.9a	2.7 ± 1.2a	3.2 ± 0.9a	3.9 ± 0.6ac
D	2.7 ± 0.8a	2.5 ± 1.2a	3.4 ± 0.9a	3.8 ± 0.7ac

TABLE 5: Amino acid composition of flavored mushroom powder and mandai cempedak powder.

Amino acid (% w/w)	(i) Mandai cempedak powder	(ii) Unflavored mushroom powder	(iii) Flavored mushroom powder	(iv) Sample (E) 50% flavored mushroom powder and 50% mandai cempedak powder
Aspartic acid	0.55	1.12	1.28	0.72
Threonine	0.27	0.59	0.68	0.44
Serine	0.3	0.59	0.67	0.46
Glutamate	0.97	2.07	2.15	1.37
Glycine	0.31	0.62	0.63	0.43
Alanine	0.36	0.92	0.88	0.56
Valine	0.4	0.68	0.95	0.04
Methionine	0.03	0.19	0.21	0.82

from pepper and shallot. Threonine is mainly sourced from onions.

In the sample of 50% mushroom spice powder and 50% mandai cempedak powder, the most significant compositions of amino acids were ileusine (1.46%, w/w), glutamate (1.37%), methionine (0.82%), aspartic acid (0.72%), and then the other amino acids (Table 5). This shows that the resulting seasoning will enhance savory flavors [23]. The total amino acids for these products are 9.08% or less when compared to unseasoned mushroom powder.

**3.5. Volatile Component Analysis (GCMS).** The composition of volatile compounds from samples (i) mandai cempedak powder, (ii) mushroom powder without spices, (iii) mushroom powder, and (iv) samples (E) 50% flavored mushroom powder and 50% mandai cempedak powder were presented chromatographically on Figure 2, and the results of identification with the Mass Spectro (Shimadzu) databank are presented in Table 6. Several compounds that dominate when viewed from the % area for mandai cempedak powder are (1) 1-hexanol, 2-ethyl-(cas)2-ethyl hexanol (6% area), (2) 1-dodecanol (cas) n-dodecanol (6.89% area), (3) oxirane, [(dodecyloxy)methyl]-(cas) lauryl glycidyl ether (8.85% area), (4) morpholine, 4-octadecyl-(7.41% area), (5) 9-octadecenoic acid (z)-(cas) oleic acid (14.12% area), and (6) furo [3,4-d]-1,3,2-dioxaborole, 2-ethyltetrahydro-cis-(cas) (6.26% area). Halim et al. [24] have analyzed the aromatic components of tropical fruits such as jackfruit (*Artocarpus heterophyllus*). The aromatic components of the fruit are characterized as decanoic acid, 1-decene, methyl salicylate, and stearyl alcohol. Meanwhile, hexanol, dodecanol, oxirane, morpholine, and octadecenoic acid are characteristics of fermented and powdered mandai cempedak.

Some of the compounds identified for the mushroom powder samples without spices were (1) 1-hexacosanol (cas) hexacosanol-1 (10.97% area), (2) 2-heptanol, 5-ethyl-(cas) 5-ethyl-2-heptanol (8.29% area), (3) 6-methyl-5-hepten-2-one

(15.51% area), and (4) octadecanoic acid (cas) stearic acid (5.81% area). Tagkouli et al. [25] and Selli et al. [26] identified aromatic compounds in fresh *Pleurotus ostreatus* mushrooms into groups of (1) eight carbon atoms compounds, (2) alcohols, (3) aldehydes, (4) fatty acids (FAME methyl esters), (5) toluene, and (6) ketones. The powdering process causes the volatile components of oyster mushroom powder to be dominated by alcohol, furan, and fatty acids and their derivatives.

Gas chromatography can be used to detect compounds that affect the olfactory, as in previous studies [27]. The validity of the test results from the GCMS is influenced by several things, mainly, the calibration of the tool, the accuracy of the test method, and the preparation of materials [28]. Judging from the results obtained in the tested samples (Table 6), the groups of compounds that appeared were mostly ethanol, furans, esters, ethers, fatty acids, and volatile acids. The flavored mushroom powder sample had several compounds identified as (1) 1-allyl-cyclopropane carboxylic acid (10.78% area), (2) 2,6-dihydro-2h-pyran-2-one (5.76% area), (3) 1-dodecanol (cas) n-dodecanol (8.51% area), (4) ethanol, 2-(dodecyloxy)-(cas) dodecoxyethanol (8.34% area), (5) Hexadecanoic acid (cas) palmitic acid (6.16% area), and (6) 3',4'-dihydro-2'-(morpholin-4-Yl) (7.68% area). Some compounds with significant area on the GCMS chromatogram for samples (E) 50% flavored mushroom powder and 50% mandai cempedak powder were (1) 6-methyl-5-hepten-2-one (8.26% area), (2) ethanol, 2-(dodecyloxy)-(cas) dodecoxyethanol (14.01% area), and (3) ethanol, 2-(tetradecyloxy)-(cas) 2-tetradecyloxyethanol (6.99% area).

**3.6. Color Analysis.** The color mapping of a product sample referring to the CIELAB color space is identified by three parameters:  $L^*$ ,  $a^*$ , and  $b^*$ . The  $L^*$  represents the brightness from dark (black) to light (white), starting from zero (dark) to 100 (light). In contrast,  $a^*$  is the range with the identification of green (negative  $a^*$ ) to red (positive  $a^*$ ) and the  $b^*$

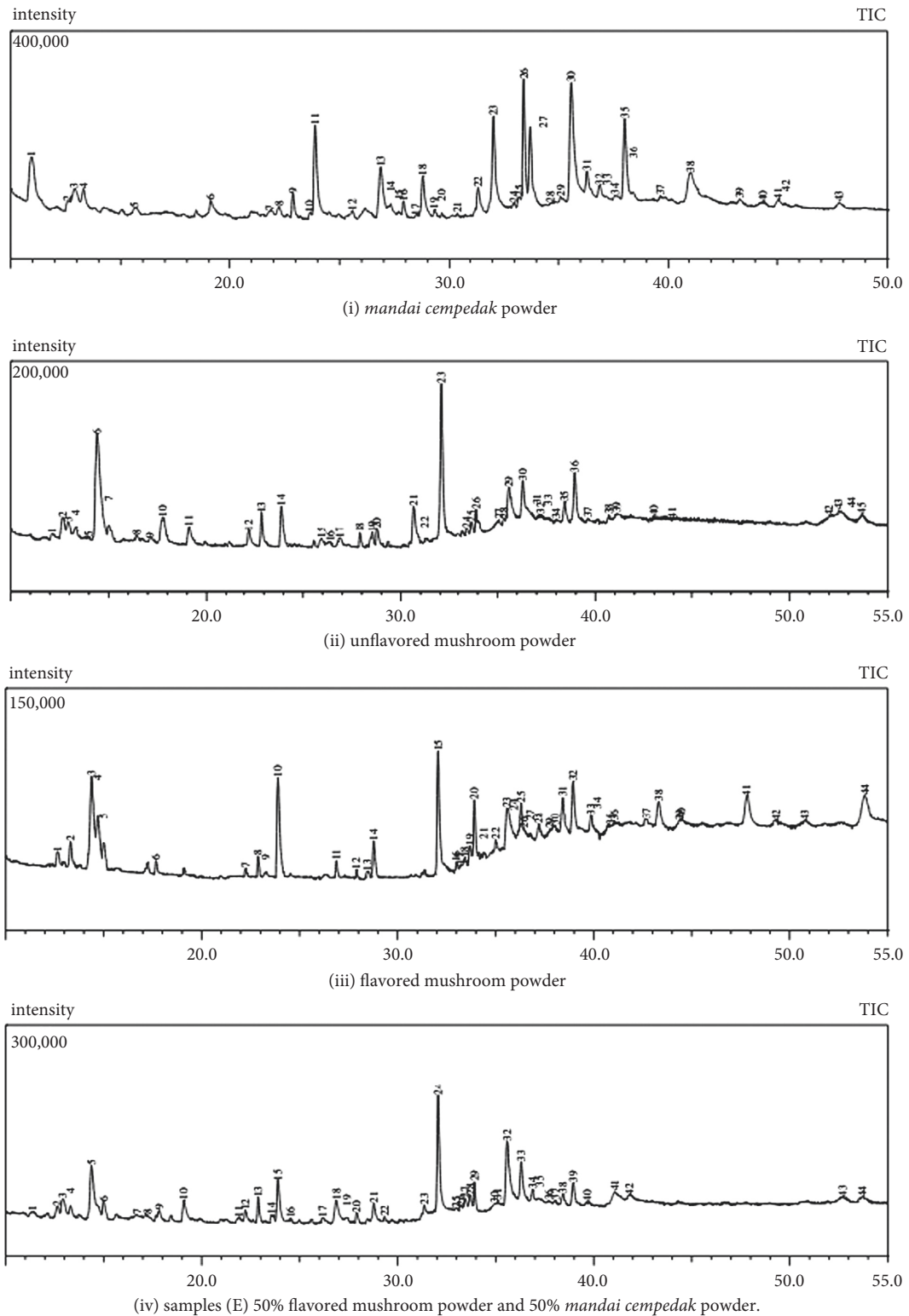


FIGURE 2: Chromatogram of GCMS.

axis is the range with the identification of blue (negative  $b^*$ ) to yellow (positive  $b^*$ ) [29]. All formulations had a color tendency similar to that of commercial mushroom powder control referring to the data presented in Table 7, namely, with brightness ranging from 65.68 to 67.06 (tends to be pale), positive  $a^*$  chromatic (tends to red), and positive  $b^*$

chromatic with larger values (tends to strengthen to yellow). The  $a^*$  color chromatic range for all samples and controls of commercial mushroom powders was 4.53–5.83 and  $b^*$  21.46–22.46. From this data, it can be concluded that the color tendency of the formulation is slightly reddish yellow with a paleness level of around 66–67%.

TABLE 6: Results of GCMS identification of the content of volatile compounds.

(i) Mandai cempedak powder		(ii) Unflavored mushroom powder		(iii) Flavored mushroom powder		(iv) Sample (E) 50% flavored mushroom powder and 50% mandai cempedak powder	
Compound name	% Area	Compound name	% Area	Compound name	% Area	Compound name	% Area
1-Hexanol, 2-ethyl- (cas) 2-ethylhexanol	6.48	Beta,d-xylopyranose tetrabenzoate	0.66	Ethanol, 2- (2-ethoxyethoxy)- (cas) 2- (2-ethoxyethoxy) ethanol	1.26	4-Heptanol (cas) dipropylcarbinol	0.75
Ethane, 1,1'-oxybis [2-ethoxy- (cas) bis (2-ethoxyethyl) ether	0.81	Ethane, 1,1'-oxybis [2-ethoxy- (cas) bis (2-ethoxyethyl) ether	2.53	1-Octanol (cas) octilin	1.80	Ethane, 1,1'-oxybis [2-ethoxy- (cas) bis (2-ethoxyethyl) ether	1.28
Ethanol, 2,2'-oxybis- (cas) diethylene glycol	2.79	Butanoic acid, 4-chloro	2.08	1-Allyl-cyclopropanecarboxylic acid	10.78	Butanoic acid, 4-chloro	2.52
1-Decanol (cas) decyl alcohol	1.83	1-Pentanol, 3-methyl- (cas) 3-methyl-1-pentanol	1.50	2,6-Dihydro-2h-pyran-2-one	5.76	1-Hexanol, 3-methyl- (cas) 3-methyl-1-hexanol	1.28
Butanoic acid, butyl ester (cas) n-butyl n-butyrate	0.64	Ethanedial, monohydrate, dimer (cas) glyoxal monohydrate dimer	0.51	2,5-Furandione (cas) maleic anhydride	2.29	6-Methyl-5-hepten-2-one	8.26
1-Heptanol, 6-methyl- (cas) 6-methyl-1-heptanol	1.17	6-Methyl-5-hepten-2-one	15.51	3-Oxo-alpha-ionone	0.69	2-Propanoic acid, 3-[(phenylmethyl) sulfonyl]-, methyl ester, (z)	1.75
Heptanoic acid (cas) heptoic acid	0.59	2,5-Furandione (cas) maleic anhydride	1.83	[3r- (3.alpha.,3a.alpha.,5as,7a.alpha.,11a.beta.,11b.alpha.)]- (+)-1,3,3a,6,7,8,9,10,11,11a,11b-Dodecahydro-3-hydroxy-8,8,11a-trimethyl-2h-cyclobuta [j] phenanthren-3-carboxylic acid methyl ester	0.49	2-Furan methanol, tetrahydro- (cas) tetrahydrofurfuryl alcohol	0.74
1-Pentanol, 5-cyclopropyliden-	0.76	2H-Pyran, 2-butoxytetrahydro- (cas) n-butyl tetrahydropyranyl ether	0.47	Bis-[3-oxo-6'-diethylamino-spiro (phthalan-1,9'-xanth-2-yl)] sulphide	1.15	Phenylactic acid benzyl ester	0.94
2-Propenamide, 2-methyl-n-phenyl-	1.38	4-Benzylloxy-1-bromobutane	0.46	Acetonyl decyl ether	0.43	2 (3H)-Furanone, dihydro-4-methyl- (cas) lactone 3-methylbutyric acid	1.35
Decanoic acid, 2-hydroxy- (cas) 2-hydroxy decanoic acid	0.32	Guanidine, methylhydrochloride (cas) n-methylguanidine hydrochloride	3.41	1-Dodecanol (cas) n-dodecanol	8.51	Oxetane, 2-propyl- (cas) 2-n-propyl-oxetan	2.50
1-Dodecanol (cas) n-dodecanol	6.89	Oxetane, 2-propyl- (cas) 2-n-propyl-oxetan	1.98	1-Tetradecanol (cas) alfol 14	0.88	Rs-2,3-hexanediol	0.65
2-Propyldecan-1-ol	0.36	Beta-myrcene	1.25	2-Nonen-1-ol	0.43	Cyclohexylidene triflate	1.31
Hexadecanoic acid (cas) palmitic acid	5.11	2-Propenamide, 2-methyl-n-phenyl-	2.21	6.Beta-acetoxy-3.alpha-angeloyloxy-1,10.beta-epoxyfuranolremophulan	0.64	Decane, 1-chloro- (cas) 1-chlorodecane	1.76
Tridecane, 4-cyclohexyl	1.61	1-Dodecanol (cas) n-dodecanol	3.30	1-Heptadecene (cas) hexahydroaplotaene	2.68	1- (1,3-Dimethylcyclohex-2-enyl) propan-2-one	0.85
1,3-Dimethyl-1,3-disseptidin-2,4-dione	0.39	Azetidine, 1-nitroso- (cas) nitrosoazetidine	0.84	Ethanol, 2- (dodecyloxy)- (cas) dodecoxyethanol	8.34	1-Undecanol (cas) n-undecanol	4.17

TABLE 6: Continued.

(i) Mandai cempedak powder		(ii) Unflavored mushroom powder		(iii) Flavored mushroom powder		(iv) Sample (E) 50% flavored mushroom powder and 50% mandai cempedak powder	
Compound name	% Area	Compound name	% Area	Compound name	% Area	Compound name	% Area
2-Propenamide, 2-methyl-n-phenyl	0.88	2H-Pyran-3,4-dihydro-2-carboxamide	0.65	Butane, 2,2-dimethyl- (cas)	0.61	10-Oxoundecyl acetate	0.52
1-Propyl-1-[(tert-butyl)dimethylsilyl]oxy]perfloroheptene	0.20	Tridecanoic acid (cas) tridecyclic acid	0.88	Methyl 2-azidobenzoate	0.43	3-Chloro-2-methyl-1-propanol	0.78
1-Tridecanol (cas) n-tridecanol	3.55	Bis-[3-oxo-6'-diethylamino-spiro (phthalan)-1,9'-xanth-2'-yl]sulphide	0.79	1- (3- (Morpholin-4-yl) propyl)cyclopentanol	0.83	Hexadecanoic acid (cas) palmitic acid	3.42
Oxirane, 2,3-diethyl- (cas)	0.45	2H-Pyran-2-one, tetrahydro-6-pentyl- (cas)	1.16	N,n-dimethyl-heptadecylamine	1.42	3-Hydroxy-4,4-dimethyldihydro (2-13c)furan-2-one	0.68
3,4-epoxyhexane	0.22	1-Heptadecanol (cas) n-heptadecanol	1.39	Nonanoic acid, 7-methyl-, methyl ester (cas)	4.39	Bis-[3-oxo-6'-diethylamino-spiro (phthalan)-1,9'-xanth-2'-yl]sulphide	0.84
Cyclohexane, (1,1-dimethylethyl)- (cas) tert-butylcyclohexane	0.14	Acetamide, n- (2-phenylethyl)- (cas) n-(2-phenylethyl) acetamide	3.84	(+)-Dehydrocamphor	0.43	1-Hexadecanol (cas) cetal	2.22
Di-lauryl thio-di-propionate	2.34	7-Alpha-methacryloyloxy-or-tiglinoyloxy-9-beta-methacryloyloxy-or-tiglinoyloxy-1-oxo-alpha	0.42	Dodecane, 1,1'-oxybis- (cas)	1.12	2-Hexylallyl alcohol	0.58
Oxirane, [ (dodecyloxy)methyl]- (cas) lauryl glycidyl ether	8.85	1-Hexacosanol (cas) hexacosanol-1	10.97	Hexadecanoic acid (cas) palmitic acid	6.16	Butane, 2-chloro-2-methyl- (cas) tert-amyl chloride	1.74
Ethanedione, diphenyl- (cas) benzil	0.85	1- (3- (Morpholin-4-yl) propyl) cyclopentanol	0.51	3-Methyldioxopiperazine	0.69	Ethanol, 2- (dodecyloxy)- (cas) dodecoxyethanol	14.01
1-Undecene, 9-methyl- (cas)	0.78	2-Propenamide, n-[2- (dimethylamino) ethyl]-	0.88	2,3,6,7-Tetramethyl-10- (4-methylphenylsulfonyloxy)-1,4,4.alpha.,5,8,8a.beta.,9.beta.,10.alpha.,10a.alpha.-decahydroanthracen-9-ol	3.63	N-methyl-n-nitro-o-benzoylhydroxylamine	0.72
Morpholine, 4-octadecyl-	7.41	Nonanoic acid, 7-methyl-, methyl ester (cas)	2.03	Pulegone	0.97	1h-1,2,4-Triazole, 1-methyl- (cas)	0.67
Furo [3,4-d]-1,3,2-dioxaborole, 2-ethyltetrahydro-, cis- (cas)	6.26	9-Octadecenoic acid (z)- (cas) oleic acid	1.34	1,6-Dioxaspiro [4.4] non-3-ene	0.42	4-Methylpent-3-en-2-ol	1.45



TABLE 6: Continued.

(i) Mandai cempedak powder		(ii) Unflavored mushroom powder		(iii) Flavored mushroom powder		(iv) Sample (E) 50% flavored mushroom powder and 50% mandai cempedak powder	
Compound name	% Area	Compound name	% Area	Compound name	% Area	Compound name	% Area
2h-Pyran-2-methanol, tetrahydro- (cas) 2-methanol tetrahydropyran	0.46	Bicyclo (3,3,1) nonan-1-ol	0.71	Docosane (cas) n-docosane	1.55	1-Hydroxycyclohexanecarboxylic acid tert-butyl-amide	1.50
Ethyl tridecanoate	0.82	Octadecanoic acid (cas) stearic acid	5.81	2-Ethyl-5-methylfuran	0.40	Heptadecanoic acid, methyl ester (cas) methyl heptadecanoate	1.72
9-Octadecenoic acid (z)-oleic acid	14.12	2-Heptanol, 5-ethyl- (cas) 5-ethyl-2-heptanol	8.29	Pentanal, 2,3-dimethyl- (cas) 2,3-dimethylpentanal	1.18	1-Fluoro-2,2,4,4-tetramethyl-3-pentanone	0.81
1-Docosanol (cas) behenic alcohol	3.53	(3r*,4r*)-3,4-Dimethyl-1-butyn-4-ol	0.79	10-Undecenoic acid, methyl ester (cas) methyl 10-undecenoate	3.64	Hydrazinedicarboxaldehyde (cas) 1,2-diformylhydrazine	1.11
1,14-Tetradecanediol (cas) tetra decamethylene glycol	1.83	6- (Allyloxy) hexane-1,2-diol	1.43	9-Octadecyne (cas)	3.94	9-Octadecenoic acid (z)- (cas) oleic acid	10.24
Butanoic acid, 3-methyl-, 3-methylbutyl ester (cas) apple oil	0.44	2-Pyrazoline, 1-butyl-5-methyl- (cas) 5-methyl-1-n-butyl-delta[2]-pyrazoline	1.14	Diethyl (decyloxy)-borane	2.13	Ethanol, 2- (tetradecyloxy)- (cas) 2-tetradecyloxyethanol	6.99
5-Undecene, 3-methyl-, (e)- (cas)	0.92	Morpholine, 4-octadecyl	0.90	Methyl 3- [ (tetrahydropranyloxy) but-2-enoate	0.44	2-Cyanato methyl cyclohexane	2.25
Morpholine, 4-octadecyl-	6.49	Methylester of 3-cyclohexyl-propionic acid	2.20	1,3-Dioxolane, 2- (1,1-dimethylethyl)- (cas) 2- <i>t</i> -butyl-1,3-dioxolane	0.44	5-Oxo-tetrahydro-furan-2-carboxylic acid	2.18
Nonanoic acid, 7-methyl-, methyl ester (cas) methyl 7-methylnonanoate	0.65	Bombykol	4.92	1-Methyl-cis-2- (n, n-dimethylaminomethyl-d2) isopropylidencyclopentane	0.96	2,3,13-Trioxabicyclo [8.2.1] tridecane	1.13
Silane, chloro (1,1-dimethylethyl) dimethyl-	0.56	Propane, 2-chloro-2-methyl- (cas) tert-butyl chloride	0.59	5-Iminopyrrolidine-2-carbonitrile	0.49	2-Thiazolamine (cas) abadol	0.81
9-Octadecenoic acid (z)-oleic acid	4.45	4-Methylchloride-hex-4-ene-1-ol	0.47	3',4'-Dihydro-2'- (morpholin-4-yl)-5',7'-dinitrospiro [cyclopentane-1,3'-quinazoline]	3.00	Methylester of 3-cyclohexyl-propionic acid	1.63
Nonane, 3-methyl-5-propyl- (cas)	0.49	Cyclohexanepropanoic acid (cas) 3-cyclohexylpropionic acid	1.27	Octanal, 7-methoxy-3,7-dimethyl- (cas) methoxycitronellal	0.62	Cyclooctene, 3-methyl-	2.88
Laurinsaeure, hex-3-enylester	0.63	1-Vinyl-1-cyclopropyl methyl ether	0.43	1,3-Dioxolane, 2-pentadecyl- (cas) 2-pentadecyl-1,3-dioxolane	0.61	Propane, 1- (ethenyl-2-methyl- (cas) isobutyl vinyl ether	0.78
Morpholine, 4-octadecyl-	0.69	1-Thymine-2-deoxy-.beta.-d-ribofuranos-5-yl butanoate	0.49	Heptadecane, 2,6,10,15-tetramethyl- (cas) 2,6,10,15-tetramethylheptadecane	4.67	Hexadecanoic acid (cas) palmitic acid	3.09
Spiropentane-1,3-dicarboxaldehyde	0.13	Citronellyl isobutyrate	2.30	1,3-Dioxolane, 2-pentadecyl- (cas) 2-pentadecyl-1,3-dioxolane	0.65	Cyclohexanethanol (cas) 2-cyclohexylethanol	1.63

TABLE 6: Continued.

(i) Mandai cempedak powder		(ii) Unflavored mushroom powder		(iii) Flavored mushroom powder		(iv) Sample (E) 50% flavored mushroom powder and 50% mandai cempedak powder	
Compound name	% Area	Compound name	% Area	Compound name	% Area	Compound name	% Area
Heptadecane, 2,6,10,15-tetramethyl- (cas)	0.73	Bicyclo [2.2.2] octan-1-ol (cas)	2.44	3-Dodecanol, 3,7,11-trimethyl- (cas)	0.40	2,3,4-Trimethyl-1-pentanol	1.79
2,6,10,15-tetramethylheptadecane		(cas) 1-hydroxybicyclo [2.2.2] octane		3',4'-Dihydro-2'- (morpholin-4-Yl)-5',7'-dinitrospiro [cyclopentane-1,3'-Quinazoline]	7.68	Tricosane, 2-methyl- (CAS)	1.70
		2-[[5-Methyl-1- (1-methylethenyl)-5-hexenyloxy] methyl]furan	0.57			methy]tricosane	
		2H-Pyran-2-methanol, tetrahydro- (cas)	1.87				
		2-methanol tetrahydropyran					

TABLE 7: Results of color analysis.

Code	Sample (flavored mushroom powder: mandai cempedak powder, %)	$L^*$	$a^*$	$b^*$
A	40:60	66.28	5.83	21.46
B	70:30	66.8	5.82	21.48

#### 4. Conclusion

Hedonic quality assessment on seasoning samples of flavored mushroom powder and mandai cempedak powder plays a more critical role in accepting the final product. Seasoning samples with a composition of 60–70% flavored mushroom powder and 30–40% mandai powder had a savory taste which was statistically ( $p < 0.05$ ) not significantly different from the control of commercial mushroom powder. All seasoning formulations of flavored mushroom and mandai cempedak powder have a moisture content of 8.4–10.9%, total protein 7.0–9.0%, soluble protein 2.4–3.5%, ash content 4.5–19.2%, fat content 2.3–4.5%, carbohydrates 62.7–79.4%, and the solubility is 31.0–89.4%. Samples of 50% mushroom spice powder and 50% mandai cempedak powder had the dominant amino acid profiles of ileusine (1.46%, w/w), glutamate (1.37%), methionine (0.82%), and aspartic acid (0.72%), as well as volatile compounds. In addition, the formula had dominant heptanone, dodecoxyethanol, and etradecyloxyethanol with a pleasant aroma profile, pungent fruity, green, citrus, and herbal. The color tendency of the entire formulation is slightly reddish yellow with a paleness level of about 66–67%.

#### Data Availability

The raw data for hedonic analysis and proximate analysis are provided at <https://doi.org/10.13140/RG.2.2.23808.51207>.

#### Conflicts of Interest

The authors declare that they have no conflicts of interest.

#### Acknowledgments

The authors thank the Faculty of Agriculture, Mulawarman University, for the research funding as stated in letter no. 89/SK/2020.

#### Supplementary Materials

The GCMS method, machine condition, chromatogram, and interpretation results are provided in the supplementary material: (i) mandai cempedak powder with file name: mandai.pdf; (ii) unflavored mushroom powder with file name: mushroom.pdf; (iii) flavored mushroom powder with file name: flavored mushroom.pdf; (iv) sample (E) 50% flavored mushroom powder and 50% mandai cempedak powder with file name: seasoning mandai-mushroom.pdf. s (Supplementary Materials)

#### References

- [1] A. Rahmadi, Y. Sabarina, and S. Agustin, "Different drying temperatures modulate chemical and antioxidant properties of mandai cempedak (*Artocarpus integer*)," *F1000Research*, vol. 7, p. 1706, 2018.
- [2] A. Rahmadi, F. A. R. Firdaus, and M. Marwati, "Karakterisasi sifat sensoris, proksimat, antioksidan, total BAL, dan uji pasar es krim berbahan puree dan bubuk mandai cempedak," 2018b, <http://litbang.kemenperin.go.id/jrti/article/view/4057/0>.
- [3] M. Tangyu, J. Muller, J. B. Christoph, and C. Wittmann, "Fermentation of plant-based milk alternatives for improved flavour and nutritional value," *Applied Microbiology and Biotechnology*, vol. 103, no. 23, pp. 9263–9275, 2019.
- [4] U. K. Akpi, C. I. Nnamchi, and J. O. Ugwuanyi, "Development of starter culture for the production of african condiments and seasoning agents," *Advances in Microbiology*, vol. 10, pp. 599–622, 2020.
- [5] A. Ricci, M. Cirlini, A. Guido et al., "From byproduct to resource: fermented apple pomace as beer flavoring," *Foods*, vol. 8, no. 8, p. 309, 2019.
- [6] S. Zhou, F. Ma, X. Zhang, and J. Zhang, "Carbohydrate changes during growth and fruiting in *Pleurotus ostreatus*," *Fungal Biology*, vol. 120, no. 6-7, pp. 852–861, 2016.
- [7] N. Widyastuti, "Processing of oyster mushroom as an alternative the needs of nutrition," *Jurnal Sains dan Teknologi Indonesia*, vol. 3, no. 15, pp. 1–7, 2013.
- [8] J.-L. Mau, "The umami taste of edible and medicinal mushrooms," *International Journal of Medicinal Mushrooms*, vol. 7, pp. 119–125, 2005.
- [9] B. M. Watts, G. L. Ylimaki, L. E. Jeffery, and L. G. Elias, *Basic Sensory Methods for Food Evaluation*, International Development Research Centre, Canada, 1989.
- [10] S. B. Sudarmadji, *Analisa Bahan Makanan Dan*, Liberty, Yogyakarta, Indonesia, 2007.
- [11] A. dan Rohman and Sumantri, *Analisis Makanan*, Universitas Gajah Mada, Yogyakarta Indonesia, 2007.
- [12] J. Misnawi and B. S. T. Ariza, "Use of gas chromatography-olfactometry in combination with solid phase micro extraction for Cocoa liquor aroma analysis," *International Food Research Journal*, vol. 18, pp. 829–835, 2011.
- [13] N. Utama-ang, T. Cheewinworasak, N. Simawonthamgul, and R. S. Samakradhamrongthai, "Effect of drying condition of thai garlic (*Allium Sativum L.*) on physicochemical and sensory properties," *International Food Research Journal*, vol. 25, no. 4, pp. 1365–1372, 2018.
- [14] B. Ciccantelli, T. Pribic, C. Malagelada, A. Accarino, and F. Azpiroz, "Relation between cognitive and hedonic responses to a meal," *Neuro-Gastroenterology and Motility*, vol. 29, no. 5, Article ID e13011, 2017.
- [15] C. V. Schmidt, L. Plankensteiner, P. Lionet Faxholm, K. Olsen, O. G. Mouritsen, and M. B. Frøst, "Physicochemical characterization of sous vide cooked squid (*Loligo forbesii* and *Loligo vulgaris*) and the relationship to selected sensory properties and hedonic response," *International Journal of Gastronomy and Food Science*, vol. 23, Article ID 100298, 2021.
- [16] L.-B. Sun, Z.-Y. Zhang, G. xin et al., "Advances in umami taste and aroma of edible mushrooms," *Trends in Food Science & Technology*, vol. 96, pp. 176–187, 2020.
- [17] M. N. Ghoyatul Amin, C. Rustyana, F. Rohim et al., "Optimization of sauce formulation from sea grape (*Caulerpa racemosa*) protein hydrolysate using response surface

- methodology,” *Journal of Applied Phycology*, vol. 33, pp. 1217–1227, 2021.
- [18] X. Zhao, Y. Wei, X. Gong, H. Xu, and G. Xin, “Evaluation of umami taste components of mushroom (*suillus granulatus*) of different grades prepared by different drying methods,” 2020, <https://www.sciencedirect.com/science/article/pii/S221345302030135X>.
- [19] N. Zhang, Y. Yang, W. Wang, Y. Fan, and Y. Liu, “A potential flavor seasoning from aquaculture by-products: an example of takifugu obscurus,” *Lebensmittel-Wissenschaft und -Technologie*, vol. 151, Article ID 112160, 2021.
- [20] H. Liu, J. Zheng, P. Liu, and F. Zeng, “Pulverizing processes affect the chemical quality and thermal property of black, white, and green pepper (*Piper nigrum* L.),” *Journal of Food Science & Technology*, vol. 55, no. 6, pp. 2130–2142, 2018.
- [21] Ž. Fredotović, B. Soldo, M. Šprung, Z. Marijanović, I. Jerković, and J. Puizina, “Comparison of organosulfur and amino acid composition between triploid onion *allium cornutum clementi ex visiani*, 1842, and common onion *Allium cepa* L., and evidences for antiproliferative activity of their extracts,” *Plants*, vol. 9, no. 1, p. 98, 2020.
- [22] J. Lee and J. M. Harnly, “Free amino acid and cysteine sulfoxide composition of 11 garlic (*allium sativum* L.) cultivars by gas chromatography with flame ionization and mass selective detection,” *Journal of Agricultural and Food Chemistry*, vol. 53, no. 23, pp. 9100–9104, 2005.
- [23] M. Dermiki, N. Phanphensophon, D. S. Mottram, and L. Methven, “Contributions of non-volatile and volatile compounds to the umami taste and overall flavour of shiitake mushroom extracts and their application as flavour enhancers in cooked minced meat,” *Food Chemistry*, vol. 141, no. 1, pp. 77–83, 2013.
- [24] H. R. Halim, D. P. Hapsari, J. Ahmad, A. W. Ritonga, A. Natawijaya, and R. Poerwanto, “Metabolomics dataset of underutilized Indonesian fruits; rambai (*baccaurea motleyana*), nangkadak (*artocarpus nangkadak*), rambutan (*nephelium lappaceum*) and sidempuan salak (*salacca sumatrana*) using GCMS and LCMS,” *Data in Brief*, vol. 23, 2019.
- [25] D. Tagkouli, G. Bekiaris, P. Stella et al., “Volatile profiling of *pleurotus eryngii* and *pleurotus ostreatus* cultivated on agricultural and agro-industrial by-products,” *Foods*, vol. 10, p. 1287, 2021.
- [26] S. Selli, G. Gamze, S. Onur, and K. Hasim, “Variations in the key aroma and phenolic compounds of champignon (*Agaricus bisporus*) and oyster mushrooms (*pleurotus ostreatus*) after two cooking treatments as elucidated by GC-MS-O and LC-DAD-ESI-MS/MS,” *Food Chemistry*, vol. 354, Article ID 129576, 2021.
- [27] B. Zellner, P. Dugo, G. Dugo, and L. Mondello, “Gas chromatography-olfactometry in food flavour analysis,” *Journal of Chromatography*, vol. 1186, no. 1-2, pp. 123–143, 2008.
- [28] K. C. Hernandez, É. A. Souza-Silva, C. F. Assumpção, C. A. Zini, and J. E. Zini, “Validation of an analytical method using HS-SPME-GC/MS-SIM to assess the exposure risk to carbonyl compounds and furan derivatives through beer consumption,” *Food Additives & Contaminants: Part A*, vol. 36, pp. 1808–1821, 2019.
- [29] K. L. Bao Chau, E. B. Dyer, J. L. Feig, A. L. Chien, and S. Del Bino, “Research techniques made simple: cutaneous colorimetry: a reliable technique for objective skin color measurement,” *Journal of Investigative Dermatology*, vol. 140, no. 1, pp. 3–12, 2020.

## Research Article

# Relationships between Shanghai Five Different Home-Brewed Wines Sensory Properties and Their Volatile Composition Assessed by GC-MS

Xin Dang <sup>1</sup>, Tao Feng <sup>2</sup>, LingYun Yao <sup>2</sup>, and Da Chen <sup>3</sup>

<sup>1</sup>School of Life Science and Technology, Xinjiang University, Urumqi, China

<sup>2</sup>School of Perfume and Aroma Technology, Shanghai Institute of Technology, Shanghai, China

<sup>3</sup>Department of Food Science and Technology, The Ohio State University, Columbus, OH, USA

Correspondence should be addressed to Tao Feng; [fengtao@sit.edu.cn](mailto:fengtao@sit.edu.cn)

Received 3 March 2022; Revised 27 April 2022; Accepted 17 May 2022; Published 2 June 2022

Academic Editor: Yuxia Fan

Copyright © 2022 Xin Dang et al. This is an open access article distributed under the Creative Commons Attribution License, which permits unrestricted use, distribution, and reproduction in any medium, provided the original work is properly cited.

In order to determine the key aroma components of home-brewed wines made from different local grapes in Shanghai. In the work, the identification and quantification of 63 aroma compounds of five home-brewed wines characterized by gas chromatography-mass spectrometry (GC-MS) combined with Headspace Solid-Phase Microextraction (HS-SPME). To study the possible correlation between the sensory attributions and 22 aroma compounds in Odor Activity Value (OAV) > 1 for five home-brewed wines, the Partial Least Squares Regression (PLSR) was a multivariate data analysis performed. Furthermore, to investigate the percentage of contribution of a particular aroma compound to its overall flavor, the relative odor contribution (ROC) and odor activity value of volatiles in home-brewed wines were conducted and performed. According to the comprehensive results, Summer Black Seedless grape (SBSG) and Black Beet grape (BBG) were the most appropriate varieties to be brewed wines for people in Shanghai or around it.

## 1. Introduction

Wine is the only alkaline alcoholic beverage rich in resveratrol, tannin, organic acids, sugars, amino acids, and other nutrients, with high nutritional health value, which is the loved by people in China and other countries. But the ordinary consumers feel that wine of more than one hundred yuan is too luxurious to offer, and suspect wine of more than ten yuan is likely sham product not to buy. Therefore, many home-brewed wines are very popular in China, and home-brewed wines in North America and Western Europe are not only very popular, but also very mature and successful industries [1]. The brewing process of home-brewed wine generally adopts crushing brewing method, including sterilization equipment, crushing grapes, alcoholic fermentation, lactic acid fermentation, and aging, respectively. These grape varieties and continuous processes have a positive impact on the formation of wine aroma. There are

subtle differences between many home-made wines made by different families.

The aroma characteristics of wine are an important index determining its quality and value [2]. The aroma composition of grape wine is the key elements of wine aroma characteristics, including esters, aldehydes, alcohols, lactones, phenols, ketones, acids, and terpenes. The volatile substances of grape wines are extremely [3] complex, so far, more than a thousand flavor compositions of grape wines have been detected. They are classified as primary, secondary, and tertiary aroma originated from grapes, wine fermentation, and the aging process. Aroma compounds including alcohols, esters, aldehydes, ketones, acids, and terpenes are frequently reported as the main contributors of pleasant wine aroma [4]. Detection and analysis of aroma characteristics of grape wines are very meaningful. Many volatiles characterization and detection in wines are usually performed by gas chromatography-mass spectrometry (GC-

MS) due to its highly effective and rapid [5–7]. Daniela Barbera et al. [8] used HS-SPME-GC-MS to detect and assay the 15 different Sicilian Muscat wines in different years effect on producing the aroma compounds especially four fundamental terpene alcohols (linalool, geraniol, nerol, and citronellol) as described by Lukić and Horvat [9]. To differentiate monovarietal wines made from native and introduced varieties in Istria (Croatia), samples of Malvazija istarska, Chardonnay, and Muscat yellow from two harvest years (2013 and 2014) were subjected to HS-SPME-GC/MS of volatile aroma compounds. Barata et al. [10] analyzed and identified the key aroma compounds of the monovarietal wines produced with the Portuguese red grape variety Trincadeira and in blends of Cabernet Sauvignon and sour rotten Trincadeira grapes, which are most likely associated with this disease (sour rot), have been studied by sensory analysis, gas chromatography-olfactometry (GC-O), and gas chromatography-mass spectrometry (GC-MS). Principal component analysis (PCA) and hierarchical cluster analysis (HCA) were selected to find the correlation of two or more quality indexes of wine and classify the parallel quality indexes to a class, which simplify quality index of wines. PCA and partial least squares regression (PLSR) were assayed to appraise the correlation between the aroma compounds' sensory properties in Spanish Albarino wines and chemical characteristics [11]. PCA, HCA, and PLSR were common and important chemical quantitative analysis, which have been applied to foods [12–14], Liu et al., 2010), nonfoods [3, 15], and other fields [16, 17]. Yu et al [18] evaluate the key aroma compounds in Chinese rice wine sensory attributes produced by different processing techniques, to analyze the aroma components using GC-MS, and finally to determine the key aroma compounds by GC-O and OAV measurement. The correlations between the key aroma compounds and the sensory attributes were calculated by PLSR.

Aroma is an important sensory characteristics of wine, which is complicated and not single. Although instrumental analysis such as GC-O [19, 20] plays a significant role in complex aroma of wine, the olfactory sensation is still needed to identify whether the wine can bring pleasure feeling and spiritual satisfaction to people. Hence, sensory analysis cannot all be replaced by any other advanced instruments. There were a phenomenon that the high-concentration volatile substance cannot be perceived by a trained sensory judge, but other low concentrations of sniffed aroma can be; why aroma compounds that are themselves above threshold (AT) are more easier to be smelled than sub-threshold (ST) substances [21]. Between the intricate matrix effects and oral human physiological effects, variables make a complex matter of wine aroma perception. Hence, Simonetta Capone et al. [22] quoted a parameter that was known as "odour activity value" (OAV), defined it as concentration/OTH ratio, which is commonly used to assess the contribution of each volatile compound detected by GC-MS to wine aroma. OTH is a logogram of the volatile compound odor threshold, which is defined as the lowest concentration that can be recognized by smelling [23]. Many researchers [24, 25] have estimated the OTHS of volatile compounds in synthetic wine. The aroma perception

in a sample cannot be related to OTHS but can be a positive correlation to OAV, and only volatile compounds with  $OAV \geq 1$  be perceived by trained sensory panels, and not all the volatiles present in wine [3, 26] using OAV to assess the contribution of individual chemical components in wine sample to wine aroma is useful and meaningful.

Studied on wines in the market [27–29] have been reported. For example, Sagratini et al. [30] studied and compared the volatile composition of Montepulciano monovarietal red wines from the Marche and Abruzzo regions of Italy by HS-SPME-GC-MS analysis, and a total of 50 aromatic compounds were having a characteristic flavor of jujube wine, such as 1 acid, 7 alcohol, 8 alkanes, 25 esters, 4 ketones, 3 phenols, and 2 others compounds, notably esters, and the volatile compounds of the highest values in the analysis of wines were consisting largely of ethyl esters which have C3–C8 straight chain fatty acid residues by Zhang reported [31]. Five premium red wines' aroma characterization have been studied by odor descriptive analysis, quantization of their volatile compounds been dealt with GC-MS, and odor interaction in wine volatiles showed aroma enhancers or aroma suppression by GC-O [32]. PCA assayed 17 volatile components with OAVs greater than 1 between Godello white wines, and PLSR analyzed the correlation between Godello white wines' sensory properties and their aromatic fingerprinting obtained by GC-MS [33]. And it turned out that the issue of wine in the market of aroma characterization depended on its aroma components, detected and quantized by GC-MS, and OAV of volatiles been estimated to analyze its contribution to wine aroma perception. Niu et al. [34] used a combination of GC-O, GC-MS, and OAVs to analyze the characteristic flavor components in Chinese liquors. Wang et al. [35] used physical and chemical analysis (HS-SPME-GC-MS, NMR), sensory evaluation, and multivariate analysis (PLSR) to study the relationship between aroma-phenolic reactions and perceived intensity of aroma attributes.

However, there is a little information about the correlation of sensory properties and volatile compositions identified by GC-MS regarding various home-brewed wines. In addition, no report about the sensory attributes of odor descriptors for home-brewed wines been described by the trained sensory judges and to identify key aroma compounds of home-brewed wines. The objectives of this study were the following: (a) to identify and quantify volatile compounds of the five home-brewed wines by HS-SPME combined with GC-MS. (b) To elucidate the correlation between sensory attributions and the aroma compounds in the five home-brewed wines by PLSR. (c) To analyze and compare the percentage of contribution of a particular compound in each wine to its overall aroma through its OAV combined ROC. A better comprehension of this knowledge will be significantly helpful for people in Shanghai or around it to find a good grape variable for brewing wine.

## 2. Materials and Methods

*2.1. Wine Samples and Materials.* The winemaking process of five home-brewed wines all adopted the home-brewed vinification method. The five grapes all were purchased from

TABLE 1: General analysis of the must and wine parameter.

<i>General analysis of the must</i>					
Parameter	DIG	SBSG	FCG	MG	BBG
Grape juice yield (%)	72.0	63.6	72.8	71.6	74.4
Total carbohydrate content (%)	12.0	11.2	12.2	11.6	10.8
<i>General analysis of the wine parameter</i>					
Parameter	DIW	SBSW	FCW	MW	BBW
pH	3.78	4.09	3.65	3.93	4.25
Alcoholic strength (%v/v)	13.40	12.50	13.60	12.90	12.20
Total acid	5.03	4.91	4.39	4.61	5.44

an identical vineyard in Shanghai, which were Muscat (MG), Black Beet (BBG), Summer Black Seedless (SBSG), Fuji cream (FCG), and Drunk the incense (DIG), respectively. The five home-brewed wines were, respectively, Muscat wine (MW), Black Beet wine (BBW), Summer Black Seedless wine (SBSW), Fuji cream wine (FCW), and Drunk the incense wine (DIW), ran as follows: an amount of 5 kg of each grape was crushed and pressed to obtain must with its skin and seed, and all were set in individual glass vessels. Alcoholic fermentation was conducted at temperature of 26~30°C for 7 days. During alcoholic fermentation, to mix must, skin, and seed with a long sterilized stick in case of *Saccharomyces cerevisiae* can not have enough fermentation, and to be monitored by measuring the temperature and density in each container on a daily basis. White granulated sugar, served as carbon source of *S.cerevisiae* in grapes' skin, was successively added 0.2 kg, 0.2 kg, and 0.1 kg in the first day, the third day, and the fifth day of alcoholic fermentation, respectively. After 7 days, each wine was clarified (natural clarification), filtered with 5 layers of gauze, and bottled to the new individual glass vessel with bibcock through siphonage.

The five musts (DIG, SBSG, FCG, MG, and BBG) been obtained to analyze grape juice yield, defined as must/grape ratio and its total carbohydrate content detected by polarimeter, showed in Table 1.

After 2 months of bottling, the five wines (DIW, SBSW, FCW, MW, and BBW) were obtained and subsequently analyzed for its pH by the five easy plus laboratory pH meter from Mettler-Toledo, its alcoholic strength and its total acid refers to "Analytical methods of wine and fruit wine" of the Chinese national standard (GB/T 15038-2006), which is showed in Table 1.

N-alkane standards (C7-C30) and 2-Octanol that be served as internal standard were purchased from Sigma-Aldrich Chemical Co.

**2.2. Sensory Analysis.** The sensory analysis of the home-brewed wines was performed in a sensory laboratory set in accordance with ISO 8589 (2007) so as to promote the tasters' task of identifying descriptors. A sensory panel consisted of nine members including six men and three women that had been trained according to ISO 13300-2 (2006). Five home-brewed wines (DIW, SBSW, FCW, MW, and BBW) were analyzed for sensory aroma quality in terms

of 11 descriptors (Table 2) according to ISO 11035 (1994) and GB/T 15038-2006.

A constant volume of 30 ml of each home-brewed wine was evaluated in a 215 ml wine-tasting glasses at 12°C according to ISO 3591 (1977). The sensory panel smelled five home-brewed wines presented in random order, noted the specific perceived descriptors and rated the intensity of each sensory attribute on a nine-point scale, where 0 indicated that the descriptor was not perceived, and values 1-9 that its intensity was from the lower to the higher. The average scores of odor descriptors based on the scores given by nine judges were provided as its sensory evaluation results (each repeated three times).

**2.3. Extraction of Home-Brewed Wine Volatiles.** The home-brewed wine volatiles were separated by adsorption on the extract fiber using 75 ul CAR/PDMS SPME (Shanghai Ann spectrum scientific instrument co., LTD), which performed the Headspace Solid-Phase Microextraction. Before the extraction, each home-brewed wine precisely been got 5 ml, to add directly 1 g NaCl and 5 ul of 2-octanol (262 mgL<sup>-1</sup> in absolute ethanol) to wine solution, and 2-octanol been viewed as internal standard to facilitate quantitative analysis of wine volatile compounds. The SPME filer been exposed to headspace for 30 min at 60°C, then the SPME fiber was introduced in the injector of the gas chromatography(GC) for desorption for 5 min at 250°C in the splitless mode.

**2.4. Gas Chromatography-Mass Spectrometry (GC-MS).** The home-brewed wine aroma compounds were separated and identified on a 7890 gas chromatography (GC) coupled to a 5973°C mass spectrometry (MS) (Agilent Technologies, USA). An HP-INNOWAX fused-silica capillary column (60 m × 0.25 mm ID, 0.25 film thickness) served as chromatographic column of wine volatiles separations. Helium, the carrier gas, had a flow rate of 1 ml/min in the constant flow mode. The sample injection was used in the splitless mode, and the injector temperature was set at 250°C. The oven temperature program was as follows: 40°C for 2 min, 5°C/min ramp to 230°C, and holding for 5 min. Temperature of the transfer line, the ion trap was manifold, and the quadrupole mass filter was set at 250°C, 230°C, and 150°C, respectively. The ion energy for electron impact (EI) was always 70 ev. The chromatograms of the five home-brewed wines volatiles were recorded by monitoring the total ion currents in 30-450 mass range, the samples were run in triplicate.

Identification of the home-brewed wines' aroma compounds was obtained through the following ways: comparing of the retention indices (RI) and the fragmentation patterns with those reported in the literature, or mass sepctrums in the Wiley 7 n, I Database (Hewlett-Packard, Palo Alto, CA) and Nist Database. The RI of wines' aroma compounds were calculated using a homologous series of n-alkanes (C7-C30) (concentration of 1000 mg/L in n-hexane) (Sigma-Aldrich, St. Louis, MO) under the same conditions. The RI of expression is as follows [36]:

TABLE 2: Odor descriptors for wines. The mean scores and definition of different descriptors.

Descriptor	DIW	SBSW	FCW	MW	BBW	Definition
Odour intensity	6.51 <sup>a</sup>	8.53 <sup>c</sup>	6.97 <sup>b</sup>	7.38 <sup>c</sup>	7.87 <sup>d</sup>	Overall odor strength
Pineapple	2.25 <sup>a</sup>	5.97 <sup>c</sup>	2.16 <sup>a</sup>	4.41 <sup>b</sup>	3.96 <sup>b</sup>	Perfumed
Citrus	0	0	0	0	4.62 <sup>b</sup>	Lemon
Grape	5.84 <sup>ab</sup>	6.25 <sup>b</sup>	5.35 <sup>a</sup>	7.17 <sup>c</sup>	6.86 <sup>c</sup>	Ripe grape
Alcohol	5.60 <sup>b</sup>	7.46 <sup>c</sup>	4.36 <sup>a</sup>	5.97 <sup>b</sup>	7.05 <sup>c</sup>	Napa
Cream	3.53 <sup>a</sup>	6.45 <sup>d</sup>	5.52 <sup>c</sup>	3.06 <sup>a</sup>	4.29 <sup>b</sup>	Butter fatty
Sweet	3.82 <sup>b</sup>	5.83 <sup>d</sup>	1.08 <sup>a</sup>	4.05 <sup>bc</sup>	4.25 <sup>c</sup>	Honey aroma
Phenolic	4.61 <sup>c</sup>	1.25 <sup>a</sup>	5.05 <sup>d</sup>	3.26 <sup>b</sup>	1.02 <sup>a</sup>	Clove curry
Floral	4.32 <sup>a</sup>	4.85 <sup>b</sup>	4.04 <sup>a</sup>	9.05 <sup>c</sup>	8.85 <sup>c</sup>	Rose, Violet flowers
Herbaceous	0	5.09 <sup>c</sup>	0.76 <sup>b</sup>	0	6.03 <sup>d</sup>	Green wood, freshly mown grass
Berry fruit	5.02 <sup>b</sup>	7.14 <sup>c</sup>	5.53 <sup>c</sup>	4.24 <sup>a</sup>	6.46 <sup>d</sup>	Tropical fruit
Undesirable flavor	5.27 <sup>c</sup>	0	4.36 <sup>b</sup>	0	0	Brett

(1)ND: Not detected. (2) \* Mean  $\pm$  SD Value in each row with different letters are significantly different ( $p < 0.05$ ).

$$RI(X) = 100 \times \left( \frac{\log(tx) - \log(tz)}{\log(tz + 1) - \log(tz)} \right) + z. \quad (1)$$

**2.5. Odor Activity Value (OAV) and Relative Odor Contribution (ROC).** To quantify the overall home-brewed wine aroma compounds identified by GC-MS through a comparison with the concentration of the internal standard (2-octanol), the wine aroma compounds' odor activity value were calculated by dividing each specific volatile' mean concentration by its recognition threshold concentration [22].

The values of OAV for aroma compounds which were presented OAV>1 in the five home-brewed wines are analyzed in Table 3. ROC was calculated by dividing the value of OAV for each individual compound by the sum of the OAV of compounds that showed OAV>1 (Table 4).

**2.6. Statistical Processing.** The sensory analysis of five home-brewed wines was carried out with the techniques of SAS V8 (SAS Institute Inc, Cary, NC, USA) with ANOVA. Duncan's multiple range tests were applied to ascertain a significant differences ( $p < 0.0001$ ) between the sensory attributions in the five home-brewed wines.

PLSR is a method for the correlation between sensory attributes and volatile compounds identified by GC-MS through Unscrambler version 9.7 (CAMO ASA, Oslo Norway). Our X-variables included the wines and Y variables were the odor descriptors by seven sensory panels (Figure 1). Figure 2 presented the correlation between the aroma compounds (OAV>1) in-X-variables and 11 odor descriptors in Y- variables.

### 3. Results and Discussion

**3.1. Volatile Compositions of Five Home-Brewed Wines.** Identification and quantification for aroma compounds of the five different species wines by GC-MS are showed in Table 2 and their RI calculated through the RI's expression. All the volatile compound concentrations' mean and standard deviation determined in triplication with SPME-GC-MS. Table 2 showed a total of 63 volatile compounds that were

identified. Volatiles in five wines basically were composed of seven groups: esters, alcohols, acids, aldehydes, volatile phenol, terpenes, and other. Aroma compounds' odour descriptor and odour threshold were reported in the literature showed in Table 2.

**3.2. Esters.** Esters comprised of important home-brewed aroma compounds in wine, which are associated with floral and fruity attributes [52]. Generally, wines contained a large number of different alcohols and acids, so esters formed by etherification of alcohols and acids followed by water molecule elimination. Table 2 shows 15 esters in the five wines. SBSW and BBW possessed the highest amount of total esters in comparison to other wines. Ethyl acetate gives pleasant pineapple aroma impact, and was the main contributor to this class of volatile compounds in home-brewed wines. SBSW presented the most content (31.676 mg/L) than MW (24.459 mg/L), FCW (20.463 mg/L), DIW (20.715 mg/L), and BBW (27.542 mg/L). The concentration of ethyl lactate with fruit and lactic aroma was higher in SBSW and MW (>1 mg/L) compared with DIW, FCW, and BBW (<1 mg/L). Ethyl octanoate (2.322 mg/L) and ethyl laurate (0.408 mg/L) were the highest in SBSW, while ethyl laurate was not found in FCW. Ethyl decanoate with pleasant grape fragrance was the lowest in SBSW (0.029 mg/L). Diethyl succinate with enjoyable fruit aroma was the main contributor to volatile compounds in Portugieser red wine and Kekfrankos red wine [53]; however, it was low among the wines (concentration between 0.116 and 0.322 mg/L). 2-Phenylethyl acetate with rose, honey, tobacco aroma, presented higher in FCW (0.633 mg/L), while in SBSW it was not found. Gamma-butyrolactone (1.029 mg/L, sweet), ethyl valerate (0.015 mg/L, yeast fruit), and isoamyl formate (8.486 mg/L, plum black currant ethereal vinous dry earthy fruit green) only appeared in BBW. Ethyl tetradecanoate (1.258 mg/L), and neryl acetate (1.029 mg/L, fruit) also only presented in SBSW.

**3.3. Alcohols.** As presented in Table 2, alcohols were detected in the five home-brewed wines and the total concentration of the alcohols ranged from 13.888 for FCW to 55.194 mg/L for SBSW. 1-Propanol with ripe fruit alcohol



TABLE 3: Volatile compounds of five home-brewed wines (mg/L, n = 3) identified by GC-MS.

Compound	RIcal <sup>a</sup>	ID <sup>b</sup>	Rirref	DIW <sup>h</sup>	SBSW <sup>h</sup>	FCW <sup>h</sup>	MW <sup>h</sup>	BBW <sup>h</sup>	Odour descriptor	Odour threshold(mg/L)
<b>Esters</b>										
Ethyl acetate	873	R	907 <sup>c</sup>	16.902 <sup>f</sup> ± 0.24 <sup>gh</sup>	25.052 ± 0.13 <sup>d</sup>	17.033 ± 0.02 <sup>b</sup>	20.990 ± 0.01 <sup>c</sup>	14.793 ± 0.18 <sup>a</sup>	pineapple <sup>i</sup> fruit <sup>i</sup>	12.27 <sup>p</sup>
Ethyl Lactate	1350	R	1358 <sup>c</sup>	0.928 ± 0.02 <sup>a</sup>	1.404 ± 0.01 <sup>c</sup>	0.931 ± 0.02 <sup>a</sup>	1.242 ± 0.01 <sup>b</sup>	0.906 ± 0.02 <sup>a</sup>	Pineapple-pear <sup>k</sup>	154 <sup>h</sup>
Ethyl octanoate	1434	R	1436 <sup>c</sup>	1.181 ± 1.02 <sup>b</sup>	2.322 ± 1.23 <sup>d</sup>	0.966 ± 0.28 <sup>a</sup>	1.581 ± 1.01 <sup>c</sup>	0.954 ± 0.28 <sup>a</sup>	Grape <sup>j</sup>	0.6 <sup>i</sup>
Ethyl decanoate	1630	R	1636 <sup>c</sup>	0.181 ± 0.13 <sup>b</sup>	0.029 ± 0.15 <sup>a</sup>	0.044 ± 0.02 <sup>a</sup>	0.181 ± 0.08 <sup>b</sup>	0.440 ± 0.15 <sup>c</sup>	Wine, fruit <sup>i</sup> Caramel, sweet <sup>i</sup>	0.023 <sup>r</sup> 200 <sup>q</sup>
Diethyl succinate	1693	R	1689 <sup>c</sup>	0.121 ± 0.02 <sup>a</sup>	0.116 ± 0.09 <sup>a</sup>	0.153 ± 0.09 <sup>b</sup>	0.121 ± 0.87 <sup>a</sup>	0.322 ± 0.28 <sup>c</sup>	Rose, honey, tobacco <sup>i</sup> Leaf <sup>i</sup>	0.25 <sup>s</sup> 0.4 <sup>t</sup>
$\gamma$ -butyrolactone	1643	R	1647 <sup>c</sup>	nd	Nd	nd	nd	1.029 ± 0.15 <sup>a</sup>		
2-Phenylethyl acetate	1832	R	1829 <sup>c</sup>	0.262 ± 0.19 <sup>a</sup>	Nd	0.633 ± 0.48 <sup>c</sup>	0.262 ± 0.12 <sup>a</sup>	0.393 ± 0.17 <sup>b</sup>		
Ethyl laurate	1845	R	1842 <sup>c</sup>	0.060 ± 0.04 <sup>a</sup>	0.408 ± 0.04 <sup>c</sup>	nd	0.041 ± 0.01 <sup>c</sup>	0.073 ± 0.01 <sup>b</sup>		
Diethyl phthalate	2295	M		0.040 ± 0.01 <sup>bc</sup>	0.029 ± 0.04 <sup>a</sup>	0.044 ± 0.01 <sup>c</sup>	0.042 ± 0.01 <sup>bc</sup>	0.029 ± 0.02 <sup>a</sup>	Odorless <sup>i</sup>	
Diisobutyl phthalate	2348	M		0.040 ± 0.01 <sup>b</sup>	0.029 ± 0.02 <sup>a</sup>	0.153 ± 0.08 <sup>c</sup>	0.041 ± 0.01 <sup>b</sup>	0.029 ± 0.02 <sup>a</sup>		
Ethyl Tetradecanoate	2031	R	2042 <sup>c</sup>	nd	1.258 ± 0.09 <sup>a</sup>	nd	nd	nd		
Neryl acetate	1718	R	1742 <sup>c</sup>	nd	1.029 ± 0.16 <sup>a</sup>	nd	nd	nd	Ether <sup>i</sup> Fruit <sup>i</sup> Wax <sup>i</sup>	0.18 <sup>r</sup> 0.88–905.4 <sup>u</sup> >2 <sup>v</sup>
Ethyl hexadecanoate	2262	R	2250 <sup>c</sup>	nd	Nd	nd	0.020 ± 0.01 <sup>a</sup>	0.073 ± 0.03 <sup>b</sup>	Yeast, fruit <sup>i</sup>	0.0015–0.005 <sup>r</sup>
Ethyl valerate	1152	R	1133 <sup>c</sup>	nd	Nd	nd	nd	0.015 ± 0.09 <sup>a</sup>		
Isoamyl formate	1195	M		nd	nd	nd	nd	8.486 ± 0.18 <sup>a</sup>	Plum black currant ethereal vinous dry earthy fruit green <sup>i</sup>	
Total esters				20.715 ± 1.68 <sup>a</sup>	31.676 ± 2.85 <sup>e</sup>	20.463 ± 3.97 <sup>a</sup>	24.459 ± 2.14 <sup>b</sup>	27.542 ± 1.58 <sup>bc</sup>		
<b>Alcohols</b>										
1-Propanol	1052	R	1037 <sup>c</sup>	4.676 ± 0.01 <sup>b</sup>	9.869 ± 0.04 <sup>d</sup>	1.201 ± 0.01 <sup>a</sup>	4.676 ± 0.06 <sup>b</sup>	4.745 ± 0.01 <sup>c</sup>	Alcohol, pungent <sup>i</sup>	0.9 <sup>v</sup>
2-Butyl alcohol	1036	R	1024 <sup>c</sup>	19.509 ± 0.79 <sup>b</sup>	25.239 ± 0.98 <sup>c</sup>	0	19.509 ± 0.58 <sup>b</sup>	16.346 ± 0.74 <sup>a</sup>	Wine <sup>i</sup>	
1-Butanol	1134	R	1158 <sup>d</sup>	0.181 ± 0.07 <sup>b</sup>	0.378 ± 0.09 <sup>d</sup>	0.131 ± 0.09 <sup>a</sup>	0.181 ± 0.07 <sup>b</sup>	0.306 ± 0.08 <sup>c</sup>	Medicine,	
Fruit <sup>i</sup>	4.33 <sup>r</sup>									
3-Methyl-1-butanol	1198	R	1205 <sup>c</sup>	9.029 ± 0.87 <sup>c</sup>	14.177 ± 0.98 <sup>d</sup>	7.183 ± 0.47 <sup>a</sup>	9.029 ± 0.67 <sup>c</sup>	8.544 ± 0.72 <sup>b</sup>	Whiskey, malt, burnt <sup>i</sup> fruit, onion <sup>i</sup>	1 <sup>r</sup> >100 <sup>r</sup>
2,3-Butanediol	1530	R	1583 <sup>c</sup>	2.499 ± 0.02 <sup>c</sup>	2.678 ± 0.04 <sup>d</sup>	2.336 ± 0.03 <sup>b</sup>	2.499 ± 0.04 <sup>c</sup>	1.121 ± 0.01 <sup>a</sup>		340 <sup>r</sup>
1,2-Propylene glycol	1565	M		0.081 ± 0.02 <sup>d</sup>	0.058 ± 0.01 <sup>c</sup>	0.022 ± 0.02 <sup>a</sup>	0.081 ± 0.02 <sup>d</sup>	0.029 ± 0.01 <sup>b</sup>	Odorless very slight alcoholic <sup>i</sup>	0.06 <sup>r</sup>
Phenylethyl alcohol	1921	R	1925 <sup>c</sup>	1.814 ± 0.12 <sup>b</sup>	1.633 ± 0.14 <sup>a</sup>	1.814 ± 0.02 <sup>b</sup>	3.603 ± 0.08 <sup>d</sup>	2.154 ± 0.30 <sup>c</sup>	Honey, spice, rose, lilac <sup>i</sup>	>20000 <sup>r</sup>
Glycerol	2112	M		0.202 ± 0.12 <sup>c</sup>	0.175 ± 0.11 <sup>a</sup>	nd	0.202 ± 0.24 <sup>ab</sup>	nd	Odorless <sup>i</sup>	
1-Hexanol	1353	R	1360 <sup>c</sup>	nd	0.175 ± 1.12 <sup>c</sup>	0.153 ± 0.12 <sup>b</sup>	nd	0.087 ± 0.03 <sup>a</sup>	Grass	
Resin,										
flower <sup>i</sup>	8 <sup>w</sup>									
Fenchyl alcohol	1591	M		nd	0.116 ± 0.06 <sup>a</sup>	nd	nd	nd	Camphor borneol pine woody dry sweet lemon <sup>i</sup>	2.25–10 <sup>r</sup>
Nerolidol	1846	M		nd	nd	nd	nd	2.558 ± 0.02 <sup>a</sup>	Floral green waxy citrus woody <sup>i</sup>	
Nerol	1779	R	1770 <sup>c</sup>	nd	0.696 ± 0.18 <sup>a</sup>	nd	nd	nd	Flower	
Grass <sup>i</sup> , sweet <sup>i</sup>	0.04 <sup>x</sup>									
Leaf alcohol	1368	R	1392 <sup>c</sup>	nd	nd	nd	nd	1.029 ± 0.42 <sup>a</sup>	Grass <sup>i</sup>	0.91 <sup>r</sup>
Alpha terpineol	1679	M		nd	nd	nd	nd	0.044 ± 0.08 <sup>a</sup>	Pine terpene lilac citrus woody floral <sup>i</sup>	5 <sup>r</sup>
Cedrol	2005	R	2100 <sup>c</sup>	0.040 ± 0.02 <sup>b</sup>	nd	nd	0.043 ± 0.02 <sup>b</sup>	0.029 ± 0.08 <sup>a</sup>	Cedarwood woody dry sweet soft <sup>i</sup>	
2-Propanol	1550	M		nd	nd	1.048 ± 0.02 <sup>a</sup>	nd	nd	Alcohol musty woody <sup>i</sup>	40–78 <sup>r</sup>
Total alcohols				38.030 ± 1.84 <sup>b</sup>	55.194 ± 0.81 <sup>c</sup>	13.888 ± 0.178 <sup>a</sup>	39.823 ± 1.78 <sup>bc</sup>	36.992 ± 2.50 <sup>b</sup>		
<b>Aldehydes</b>										
Acetaldehyde	717	R	724 <sup>c</sup>	1.653 ± 0.08 <sup>b</sup>	2.154 ± 0.06 <sup>c</sup>	3.231 ± 0.012 <sup>d</sup>	0.786 ± 0.01 <sup>a</sup>	1.063 ± 0.07 <sup>a</sup>	Pungent ethereal aldehydic fruity <sup>i</sup>	0.01 <sup>r</sup>
Furfural	1463	R	1455 <sup>c</sup>	0.081 ± 0.04 <sup>c</sup>	0.058 ± 0.001 <sup>b</sup>	nd	0.081 ± 0.04 <sup>c</sup>	0.029 ± 0.01 <sup>a</sup>	Sweet woody almond fragrant baked bread <sup>i</sup>	0.77 <sup>r</sup>
Benzaldehyde	1501	R	1495 <sup>c</sup>	0.061 ± 0.01 <sup>a</sup>	0.146 ± 0.012 <sup>b</sup>	0.131 ± 0.0025 <sup>b</sup>	0.065 ± 0.01 <sup>a</sup>	0.058 ± 0.02 <sup>a</sup>	Almond, burnt sugar <sup>i</sup>	2 <sup>r</sup>
Anisaldehyde dimethyl acetal	1728	M		nd	nd	0.246 ± 0.001 <sup>b</sup>	0.081 ± 0.01 <sup>a</sup>	0.277 ± 0.02 <sup>b</sup>	Mild floral Hawthorn, jasmine, lilac, elder flower <sup>i</sup>	
Total aldehydes				1.794 ± 0.13 <sup>b</sup>	2.358 ± 0.019 <sup>c</sup>	3.602 ± 0.0038 <sup>d</sup>	1.008 ± 0.07 <sup>a</sup>	1.427 ± 0.12 <sup>ab</sup>		
<b>Ketones</b>										
3-Hydroxy-2-butanone	1275	R	1287 <sup>c</sup>	2.036 ± 0.96 <sup>c</sup>	0.728 ± 0.002 <sup>b</sup>	3.397 ± 0.0028 <sup>d</sup>	2.036 ± 0.20 <sup>c</sup>	0.087 ± 0.01 <sup>a</sup>	Butter, cream <sup>i</sup>	0.8 <sup>r</sup>
1-Hydroxy-2-acetone	1288	M		0.042 ± 0.01 <sup>a</sup>	nd	nd	0.047 ± 0.01 <sup>a</sup>	nd	Pungent sweet caramellic ethereal <sup>i</sup>	0 <sup>r</sup>
1-Phenyl-2-acetone	1713	M		nd	0.403 ± 0.001 <sup>a</sup>	nd	nd	nd	Almond <sup>i</sup>	
$\beta$ -Ionone	1471	M		nd	nd	nd	nd	0.069 ± 0.02 <sup>a</sup>	Floral woody sweet fruity berry tropical beeswax <sup>i</sup>	0.00009 <sup>w</sup>
2-Octanone	1283	R	1285 <sup>c</sup>	nd	nd	nd	nd	0.029 ± 0.01 <sup>a</sup>	Earthy weedy natural woody herbal <sup>i</sup>	0.05 <sup>r</sup>
Iso E super				nd	0.323 ± 0.001 <sup>b</sup>	nd	nd	0.082 ± 0.02 <sup>a</sup>	Woody dry ambergris cedar old wood ketonic phenolic <sup>i</sup>	
Geranyl acetone	1838	R	1840 <sup>c</sup>	0.041 ± 0.01 <sup>b</sup>	nd	nd	0.218 ± 0.06 <sup>a</sup>	nd	Magnolia, green <sup>i</sup>	0.186 <sup>r</sup>
Total ketones				5.707 ± 1.24 <sup>b</sup>	6.17 ± 0.042 <sup>b</sup>	10.607 ± 0.0104 <sup>d</sup>	4.322 ± 0.41 <sup>ab</sup>	3.128 ± 0.3 <sup>a</sup>		

TABLE 3: Continued.

Compound	Rcal <sup>a</sup>	ID <sup>b</sup>	Rref	DIW <sup>h</sup>	SBSW <sup>h</sup>	FCW <sup>h</sup>	MW <sup>h</sup>	BBW <sup>h</sup>	Odour descriptor	Odour threshold(mg/L)
Acetic acid	1458	R	1450 <sup>c</sup>	1.915 ± 0.95 <sup>b</sup>	1.135 ± 0.68 <sup>b</sup>	17.183 ± 0.120 <sup>c</sup>	1.915 ± 0.83 <sup>b</sup>	0.466 ± 0.04 <sup>a</sup>	Sour <sup>i</sup>	25.59-26 <sup>f</sup>
Hexanoic acid	1863	R	1864 <sup>c</sup>	0.046 ± 0.01 <sup>b</sup>	0.029 ± 0.002 <sup>a</sup>	nd	0.049 ± 0.01 <sup>b</sup>	0.073 ± 0.02 <sup>c</sup>	Green <sup>m</sup>	0.42 <sup>w</sup>
Octanoic acid	2079	R	2083 <sup>c</sup>	0.161 ± 0.01 <sup>b</sup>	0.175 ± 0.004 <sup>c</sup>	0.109 ± 0.003 <sup>a</sup>	0.161 ± 0.01 <sup>b</sup>	0.116 ± 0.01 <sup>a</sup>	Candy,caramelized,perfumy,fruity,peachy,strawberry <sup>n</sup>	0.5 <sup>w</sup>
Decanoic Acid	2368	R	2361 <sup>c</sup>	0.081 ± 0.03 <sup>b</sup>	nd	nd	0.081 ± 0.03 <sup>b</sup>	0.058 ± 0.02 <sup>a</sup>	Rancid,	
fat <sup>1</sup>										
Dodecanoic acid	2516	R	2517 <sup>c</sup>	nd	0.146 ± 0.004 <sup>a</sup>	nd	nd	nd	Metal <sup>l</sup>	
Heptanoic acid	1836	M	nd	nd	nd	nd	0.047 ± 0.01 <sup>a</sup>	nd	Rancid sour cheesy sweat <sup>l</sup>	0.64-0.91 <sup>f</sup>
Propionic acid	1520	R	1523 <sup>c</sup>	nd	nd	0.066 ± 0.002 <sup>a</sup>	nd	nd	Pngent, rancid, soy <sup>l</sup>	8.1 <sup>y</sup>
Total acids				2.203 ± 1.00 <sup>b</sup>	1.485 ± 0.78 <sup>a</sup>	17.358 ± 0.125 <sup>c</sup>	2.253 ± 0.88 <sup>b</sup>	0.713 ± 0.09 <sup>a</sup>		
Phenols										
4-Ethylpheno	2194	R	2195 <sup>c</sup>	1.498 ± 0.014 <sup>c</sup>	nd	0.808 ± 0.014 <sup>b</sup>	0.065 ± 0.02 <sup>a</sup>	nd	Phenol, spice <sup>l</sup>	0.44 <sup>z</sup>
4-Ethylguaicol	2018	R	2031 <sup>c</sup>	0.784 ± 0.004 <sup>a</sup>	nd	0.635 ± 0.012 <sup>b</sup>	0.043 ± 0.001 <sup>a</sup>	nd	Spice, clove <sup>l</sup>	0.033 <sup>w</sup>
4-Vinylphenol	2425	R	2427 <sup>c</sup>	0.028 ± 0.001 <sup>a</sup>	0.084 ± 0.002 <sup>a</sup>	0.168 ± 0.004 <sup>b</sup>	0.126 ± 0.002 <sup>b</sup>	nd	Almond shell <sup>l</sup>	0.18 <sup>aa</sup>
4-Vinylguaicol	2202	R	2198 <sup>c</sup>	1.204 ± 0.012 <sup>b</sup>	nd	1.380 ± 0.009 <sup>b</sup>	0.184 ± 0.004 <sup>b</sup>	0.038 ± 0.01 <sup>a</sup>	Clove <sup>o</sup> ; clove, curry <sup>j</sup>	0.04 <sup>bb</sup>
2,4-Di-tert-pentylphenol	2106	M	nd	0.826 ± 0.028 <sup>b</sup>	0.932 ± 0.012 <sup>c</sup>	0.742 ± 0.018 <sup>b</sup>	0.826 ± 0.022 <sup>b</sup>	0.422 ± 0.09 <sup>a</sup>		
Total phenols				4.340 ± 0.059 <sup>c</sup>	1.016 ± 0.014 <sup>b</sup>	3.733 ± 0.057 <sup>c</sup>	1.244 ± 0.031 <sup>b</sup>	0.460 ± 0.10 <sup>a</sup>		
Terpenes										
Cedrene				nd	nd	nd	nd	0.044 ± 0.02 <sup>a</sup>	Cedarwood woody <sup>j</sup>	
2,6-Dimethyl-2,6-Octadiene	1541	M	nd	nd	0.116 ± 0.012 <sup>a</sup>	nd	nd	nd		
α-curcumene	1552	M	nd	nd	nd	nd	nd	0.058 ± 0.01 <sup>a</sup>		
1-Dodecene	1758	M	nd	nd	nd	nd	nd	0.087 ± 0.03 <sup>a</sup>		
Citronellol	1759	R	1762 <sup>c</sup>	0.042 ± 0.001 <sup>b</sup>	0.204 ± 0.012 <sup>c</sup>	0.047 ± 0.003 <sup>b</sup>	0.043 ± 0.001 <sup>b</sup>	0.029 ± 0.01 <sup>a</sup>	Rose <sup>l</sup>	
β-Guaiane	1827	R	1831 <sup>c</sup>	nd	nd	nd	nd	0.058 ± 0.01 <sup>a</sup>	Wood, spice <sup>l</sup>	
Total terpenes				0.042 ± 0.001 <sup>a</sup>	0.320 ± 0.024 <sup>c</sup>	0.047 ± 0.003 <sup>a</sup>	0.043 ± 0.001 <sup>a</sup>	0.276 ± 0.08 <sup>b</sup>		
Other										
Piperidine	1944	M	nd	nd	nd	nd	nd	0.015 ± 0.08 <sup>a</sup>	Heavy sweet floral animal <sup>l</sup>	D: 70.6 <sup>f</sup>
Tetradecane	1380	R	1400 <sup>c</sup>	nd	nd	nd	nd	0.044 ± 0.06 <sup>a</sup>	Alkane <sup>l</sup>	1 <sup>r</sup>
2-Methyltetrahydrothiophene	1788	M	nd	0.064 ± 0.02 <sup>b</sup>	nd	nd	0.060 ± 0.02 <sup>b</sup>	0.015 ± 0.01 <sup>a</sup>		
Total others				0.064 ± 0.02 <sup>a</sup>	0	0	0.060 ± 0.02 <sup>a</sup>	0.074 ± 0.15 <sup>b</sup>		

Values in each row with different letters are significantly different ( $p < 0.05$ ). Data are represented as the mean ± SD. nd: not found. (a) Linear retention index of unknown aroma compound on a HP-INNOWAX fused-silica capillary column ( $60 \times 0.25 \times \text{mm} \times 0.25 \mu\text{m}$ ) with a homologous series of n-alkanes (C7–C30). (b) Identification method is indicated as follows: M, mass spectrum and RI agree with of aroma compound conducted under similar GC-MS condition.; R, identification of retention index with literature data. (c) The referenced RI from the flavor net database (<https://www.flavornet.org>, accessed June 2007). (on C20 M stationary phase); in the literature. (d) The referenced RI from El-Sayed. (e) The referenced RI from Kondjayan and Berdague. (f) The means of aroma compounds of triplicates were calculated through an internal standard method (2-octanol). (g) Standard deviation of triplicates. (h) DIW, SBSW, FCW, MW, and BBW were abbreviation of Drunk the incense wine, Summer Black Seedless wine, Fuji cream wine, Muscat wine, and Black Beet wine, respectively. (i) Odour descriptor from <https://www.flavornet.org/flavornet.html>. (j) Odor descriptor from <https://www.thegoodscentscompany.com/index.html>. (k) Odor descriptor from [37]. (l) Odor descriptor from [38]; odor thresholds were determined in 14% ethanolic solution. (m) Odor descriptor from [39]. (n) Odor descriptor from [40]. (o) Odor descriptor from [41]. (p) Odor threshold from [42]. (q) Odor threshold from [43]. (i) Odor threshold from [38], odor thresholds were determined in 14% ethanolic solution. (r) Odor threshold from [shu]. (s) Odor threshold from [43], thresholds were calculated in a 12% water/ethanol mixture. (t) Odor threshold from [44]. (u) Odor threshold from [45]. (v) Odor threshold from [46]. (w) Odor threshold from [47]. (x) Odor threshold from [48]. (y) Odour threshold from [43], thresholds were calculated in wine. (z) Odor threshold from [49]. (aa) Odor threshold from [50]. (bb) Odor threshold from [51].

aroma had been reported in the literature [22], and was the highest in SBSW (9.869 mg/L), and the lowest in FCW (1.201 mg/L). The highest 2-butyl alcohol content was found in SBSW (25.239 mg/L, grape wine aroma), and about same amounts were found in DIW and MW, and was not found in FCW. 3-Methyl-1-butanol with banana fragrance [22] was a solvent [54] and had the highest content and was found in SBSW. Similar contents were found in the rest of wines. The concentration of phenylethyl alcohol with rose aroma was higher in MW and BBW compared with DIW, SBSW, and FCW. It has been found that fenchyl alcohol (0.116 mg/L) and nerol (0.696 mg/L) were present only in SBSW, nerolidol, leaf alcohol, and alpha terpineol only in BBW, and 2-propanol with pungent [55] aroma was only in FCW. These alcohols mainly were produced during the yeast metabolism which played an important role in the flavor for wines. In general, the alcohols were the largest group of the volatile compounds, accounting for more than half of the volatile constituents of the wines except FCW.

**3.4. Aldehydes and Ketones.** Four aldehydes were detected: acetaldehyde, furfural, benzaldehyde, and anisaldehyde dimethyl acetal. These compounds played an influence on the wines' flavor. The concentrations of the seven ketones identified in five home-brewed wines were shown in Table 2. 3-Hydroxy-2-butanone was responsible for butter and cream notes, which were markedly the most abundant higher ketones in all the five home-brewed wines. Further, it was found that 1-phenyl-2-acetone only was present in SBSW,  $\beta$ -ionone and 2-octanone only in BBW.

**3.5. Acids.** Seven different volatile acids were identified in five wines. Hexanoic acid, octanoic acid, and decanoic acid among others belong to the group of fatty acids, and were produced by the fermentation of ethanol and lactic acid [56]. Acids were responsible for fruity such as octanoic acid; cheese, and fatty such as decanoic acid; green such as hexanoic acid; and rancid, sour such as acetic acids. The suitable acid concentration of wines could contribute to a balanced aroma in wine [41], was welcome, and could inhibit the alcoholic fermentation [57].

**3.6. Phenol and Terpenes.** The structural properties and concentration of aroma and phenolic compounds are significant factors influencing the behavior of wine aroma release [58]. Five volatile phenols were identified in wines (Table 2). The highest phenol content was found first in the DIW, and second in FCW. 4-Vinylguaiacol with clove, spicy aroma was present in FCW (the highest 1.38 mg/L), which resulted from the decarboxylation of the nonflavonoid compound ferulic acid during fermentation [59]. However, 4-Vinylguaiacol could not have been detected in SBSW. 4-Ethylphenol and 4-ethylguaiacol, a certain concentration, were responsible for smoke, creosote, plastic, burnt plastic, cow dung flavor, and barnyard [60], and the former concentration was the highest first in DIW (1.498 mg/L), second in FCW (0.808 mg/L), the latter concentration also was the

highest in DIW (0.784 mg/L), second in FCW (0.635 mg/L), while both were not found in SBSW and BBW.

Other and important classes of aroma compounds were terpenes. Monoterpenes give wine distinctive floral aromas that represent the vinification character of wine grapes, adding complexity to the wine aroma [61]. As Table 2 shows that six terpenes were found in the five wines: cedrene, 2,6-dimethyl-2, 6-octadiene,  $\alpha$ -curcumene, 1-dodecene, citronellol, and  $\beta$ -guaiane. These volatiles all played a role in wines' aroma. Cedrene,  $\alpha$ -curcumene, 1-dodecene, and  $\beta$ -guaiane only were found in BBW, and 2,6-dimethyl-2,6-octadiene only was present in SBSW.

**3.6.1. Main Sensory Analysis.** The results of the sensory evaluation of five home-brewed wines were shown in Table 3. There were statistically significant differences for all the 11 odor descriptors ( $p < 0.0001$ ) used to describe the aroma feature of five home-brewed wines. ANOVA analysis indicated that SBSW shows the highest intensities of most of the odor descriptors, including odour intensity (8.53), pineapple (5.97), alcohol (7.46), cream (6.45), sweet (5.83), and berry fruit (7.14) comparing to the rest of wines. BBW with the highest of herbaceous (6.03) and only citrus (4.62) was shown in Table 3. Further, MW had the highest score in floral (rose 9.05) descriptor, which agreed well with the grape' flavor type.

The results for 11 odor descriptors used in the sensory analysis (Table 3) were analyzed in a partial least square regression (PLS). Figure 1 showed the relationships between sensory aroma descriptors and five home-brewed wines. A total of 50% of the explained variance shows small ellipses and 100% of the explained variance show in big ellipses. PLSR modeling between the matrices of five wines and 11 of odor descriptors provided a two-factor model explaining 50% of the variance in X (five wines) and 83% of that in Y (sensory attributes). DIW and FCW were similar with the phenolic and undesirable flavor (brett in Table 3), which are all located in the below left of PC1 that were positively correlated to phenolic and undesirable flavor. SBSW with rich flavors of cream, berry fruit, odor intensity, herbaceous, alcohols, sweet, and pineapple was shown in Figure 1 combined in Table 3. The only aroma of citrus was found in BBW, and it also had high sweet, pineapple, alcohols, odor intensity, herbaceous, grape, and floral aroma.

**3.7. Relationship among Sensory Attribute and Volatile Compounds with OVA > 1.** According to literature [22, 62, 63], odor activity value (OAV) had been extensively used to estimate aromatic compounds' sensory contribution to the overall aroma in wines and only the specific compound of OAV > 1 contribute to the wines' aroma [51]. In order to know those specific components in five home-brewed wines effect on its overall aroma and cite, OAV for volatiles were determined by GC-MS. A total of 22 of volatiles in wines (OAV > 1) contained four types of esters, alcohols, aldehydes, and phenols as shown in Table 4. The esters of nine were the main, and most compounds in 22 volatiles, specially, ethyl valerate (OAV = 10) has the highest

TABLE 4: OAV and ROC contents of volatile compounds in five home-brewed wines.

Cod-es	Compounds	OAV					ROC				
		DIW	SBSW	FCW	MW	BBW	DIW	SBSW	FCW	MW	BBW
C1	Ethyl acetate	1.380	2.040	1.390	1.710	1.210	0.005	0.007	0.003	0.01	0.001
C2	Ethyl octanoate	1.970	3.870	1.610	2.640	1.590	0.007	0.013	0.004	0.015	0.002
C3	Ethyl decanoate	7.870	1.260	1.910	7.870	1.901	0.028	0.004	0.004	0.045	0.002
C4	Gamma-butyrolactone	<1 <sup>a</sup>	<1	<1	<1	1.029	0	0	0	0	0.001
C5	2-Phenylethyl acetate	1.048	<1	2.532	1.048	1.572	0.004	0	0.006	0.006	0.002
C6	Ethyl laurate	<1	1.020	<1	<1	<1	0	0.003	0	0	0
C7	Ethyl tetradecanoate	<1	6.990	<1	<1	<1	0	0.023	0	0	0
C8	Neryl acetate	<1	1.170	<1	<1	<1	0	0.004	0	0	0
C9	Ethyl valerate	<1	<1	<1	<1	10.000	0	0	0	0	0.011
C10	1-Propanol	5.196	10.966	1.334	5.196	5.272	0.018	0.036	0.003	0.03	0.006
C11	3-Methyl-1-butanol	9.029	14.177	7.183	9.029	8.544	0.032	0.047	0.017	0.051	0.009
C12	Phenylethyl alcohol	30.230	27.170	30.230	60.050	35.900	0.107	0.09	0.07	0.342	0.038
C13	Nerolidol	<1	<1	<1	<1	1.137	0	0	0	0	0.001
C14	Nerol	<1	17.400	<1	<1	<1	0	0.058	0	0	0
C15	Leaf alcohol	<1	<1	<1	<1	1.131	0	0	0	0	0.001
C16	Acetaldehyde	165.300	215.400	323.100	78.600	106.300	0.587	0.715	0.753	0.447	0.113
C17	3-Hydroxy-2-butanone	2.545	<1	4.250	2.545	<1	0.009	0	0.01	0.014	0
C18	$\beta$ -Ionone	<1	<1	<1	<1	766.670	0	0	0	0	0.814
C19	Geranyl acetone	<1	<1	<1	1.172	<1	0	0	0	0.007	0
C20	4-Ethylpheno	3.405	<1	1.836	<1	<1	0.012	0	0.004	0	0
C21	4-Ethylguaicol	23.760	<1	19.240	1.212	<1	0.084	0	0.045	0.007	0
C22	4-Vinylguaicol	30.100	<1	34.500	4.600	<1	0.107	0	0.08	0.026	0
	Total	281.833	301.463	429.115	175.672	942.265	1	1	1	1	1

a. it showed OAV <1 or no found in five home-brewed wines.

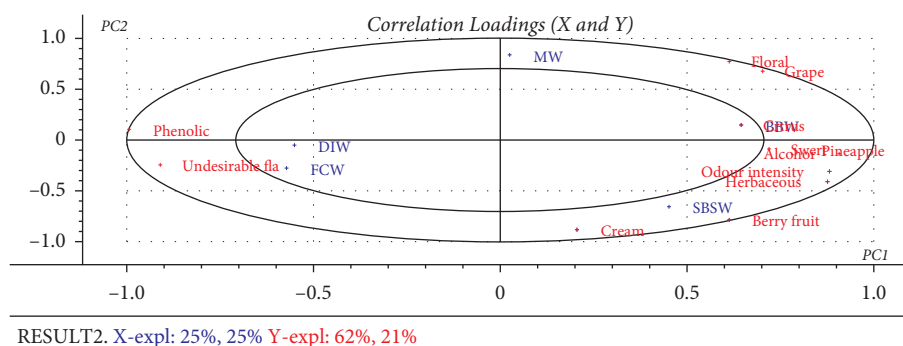


FIGURE 1: PLS regression map showing the five home-brewed wines correlated with 11 odor descriptors analyzed by seven sensory panels.

in the 9 kinds of esters that only were found in BBW, and not found in the rest of wines. While ethyl acetate (OAV = 2.04) and ethyl octanoate (OAV = 3.87) all were the highest in nine of esters for SBSW compared to DIW, FCW, MW, and BBW. Ethyl laurate, ethyl tetradecanoate, and neryl acetate in nine of the esters were only for SBSW and OVA of ethyl tetradecanoate that reached to 6.99, which ranked only second to ethyl valerate (OAV = 10) for BBW. Alcohols had 6 of 22 in total volatile (OAV > 1), account for a high proportion. 1-Propanol and 3-methyl-1-butanol were rich alcohols in wines reported in literature [32]. Showed the highest OAV values for SBSW, and nerol only existed in SBSW and its OAV value was very high (OAV = 17.4). While BBW had also two alcohols compounds: nerolidol (OAV = 1.137), leaf alcohol (OAV = 1.131), which were not determined in the rest of wines. Phenylethyl alcohol with rose aroma was the highest OVA values (OAV = 60.5) presented in MW, which

agreed well with the red grape wines' flavor type [64, 65].  $\beta$ -Ionone was the highest OVA value (OAV = 766.67) of 22 volatiles only occurred in BBW (Table 4).

To study the relationships between odor descriptors and aroma compounds only OAV > 1 detected by GC-MS was used, and partial least square regression (PLSR) was performed. A total of 11 of odor descriptors are shown in Table 3 and regarded as X variable, and 22 (C1-C22) of aroma compounds are shown in Table 4 and acted as Y variable as shown in Figure 2. PLSR modeling between the matrices of 22 of volatiles and 11 of odor descriptors provided a two-factor model explaining 76% of the variance in X (sensory attributes) and 93% of that in Y (volatiles of OVA > 1). As shown in Figure 2(b), x axis was mainly described by the odor descriptors showing a contrast between cream, sweet, pineapple, herbaceous, alcohols, floral, grape, and citrus aroma on the positive dimension and

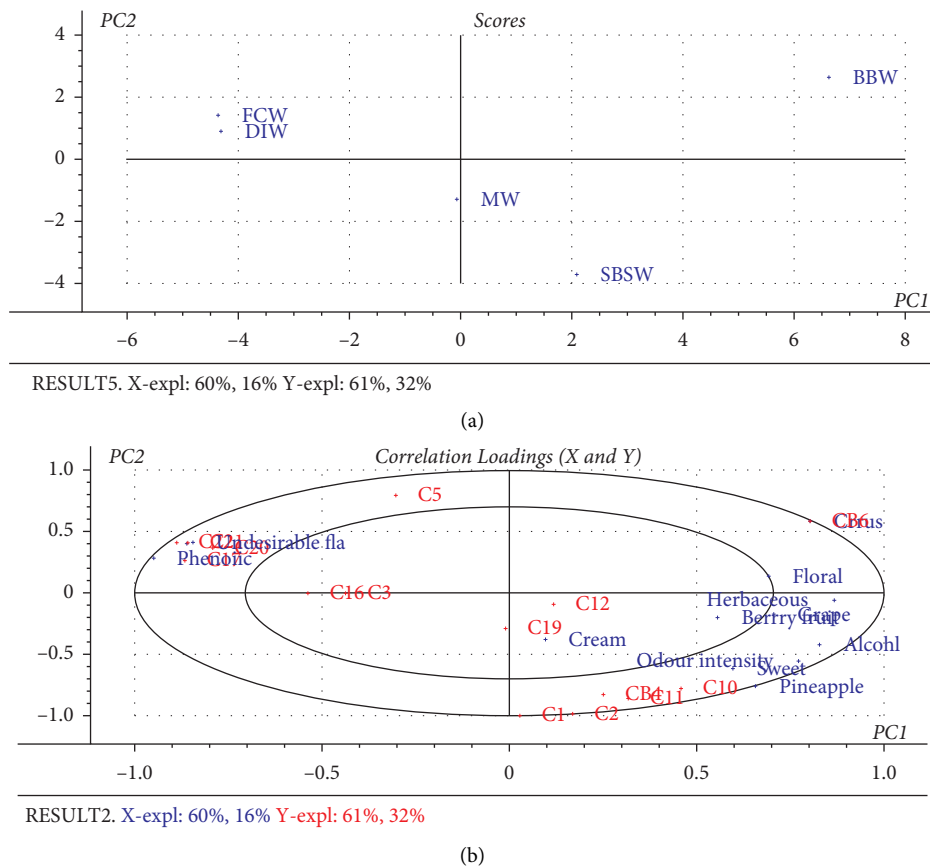


FIGURE 2: scores plot for five home-brewed wines (a). Correlation between loadings plots of X-variables for 22 volatiles compounds (OAV>1 Table 4) and Y-variables for the 11 odor descriptors (Table 3) (b).

phenolic and undesirable flavor aroma on the negative dimension. Obviously, the phenolic is located in the upper left of PC1 of Figure 2(b) and was mainly explained by positive contributions of not only 4-vinylguaiacol (C22) but also 4-ethylguaiacol (C21). Undesirable flavor near phenolic was significantly and positively correlated to 4-ethylphenol together with 4-ethylguaiacol, in a certain concentration, which both could be responsible for off-odor such as brett flavor, plastic burning taste [66, 67]. In the upper rightmost of PC1 of Figure 2(b), citrus and floral aroma correlated with  $\beta$ -ionone (C18), together with nerolidol (C13), which was in agreement with the results of GC-MS data and presented only in BBW (Figure 2(a)). Alcohol flavor accounted for a proportion in overall aroma of wines, which presented a negative correlation to 2-phenylethyl acetate. In the positive PC1 and negative PC2 in Figure 2(a) included only SBSW, which was strongly characterized by pineapple, sweet, herbaceous, and berry fruit and with the following volatiles compounds: ethyl acetate, ethyl octanoate, 1-propanol, 3-methyl-1-butanol, and nerol. Hence, PLSR can present an obvious and successful relationship of positive and negative correlations between odor descriptors and aroma compounds only OAV>1 detected by GC-MS.

To further judge the contribution of each individual compound in each wine to its overall aroma, the relative

odor contribution (ROC) was performed. Only 12 of 22 volatiles (OAV>1) was found in DIW, and the ROC of its 4-vinylguaiacol and phenylethyl alcohol were similarly highest, 4-ethylguaiacol with could off-odor was presented the second high percentage of its total ROC (Table 4). Hence, DIW might be not favorite by sensory panels. Although only 11 volatiles (OAV>1) was presented in SBSW, acetaldehyde with fruity aroma presented the highest of contribution to SBSW and its ROC reached 0.715, and phenylethyl alcohol (ROC = 0.09) was characterized for agreeable flavors, which accounted for the great proportion in its total ROC. The particular nerol (ROC = 0.058) in SBSW also gave a great contribution to SBSW aroma. Acetaldehyde (ROC = 0.753) occupied the highest percentage of FIW's ROC, but 4-ethylguaiacol in FIW also accounted for the third high percentage of total ROC for FIW. Phenylethyl alcohol (ROC = 0.342) and acetaldehyde (ROC = 0.447) were similar percentage of contribution to MW, ethyl decanoate and 3-methyl-1-butanol also took a great proportion in the total flavor for MW. BBW had 14 volatiles compounds with near unity or higher OAVs, which was the maximum type of compounds compared to the four rest of wines.  $\beta$ -Ionone (ROC = 0.814) was the obvious and particular volatile, which presented the most high proportion of contribution and only was found in BBW. Ethyl valerate only in BBW also provided an extent contribution to it. Therefore, ROC was successfully

able to analyze the percentage of contribution of a particular aroma compound to overall flavor of wines.

#### 4. Conclusions

The aroma volatile compounds of the five home-brewed wines were obtained by GC-MS combined with HS-SPME. Volatiles in five wines basically were composed of seven groups: esters, alcohols, acids, aldehydes, volatile phenol, terpenes, and other. ANOVA analysis indicated that SBSW showed the highest intensities of most of the odor descriptors, PLSR was successfully able to detect positive and negative correlations between odor descriptors and the OAV compounds that showed OAV with higher. It was successful to further judge contribution of each individual compound in each wine to its overall aroma through OVA combined with ROC. ROC results revealed that the following volatiles: ethyl acetate, ethyl octanoate, ethyl decanoate, ethyl laurate, ethyl tetradecanoate, neryl acetate, 1-propanol, 3-methyl-1-butanol, phenylethyl alcohol, nerol, and acetaldehyde, which showed the common contribution to favorite flavors for SBSW. ROC and OAV results showed that ethyl valerate, nerolidol, and  $\beta$ -ionone were particular components in BBW, especially,  $\beta$ -ionone gave its unique due to it is the most percentage of contribution in total ROC of BBW. What is more, grape juice yield of BBG was 77.4 as shown in Table 1, which was the highest maximum compared to the rest of grapes of variety. To conclude, BBG and SBSG are very appropriate to act as varieties of wines brewing for people in Shanghai and around it.

#### Data Availability

Some or all data, models, or code that support the findings of this study are available from the corresponding author upon reasonable request.

#### Conflicts of Interest

The authors declare that they have no conflicts of interest.

#### Acknowledgments

The research was supported by Key Projects of Technology Innovation of Shanghai Education Committee (12ZZ187), and The Experimental Facilities in School of Perfume and Aroma Technology, Shanghai Institute of Technology, Preparation of Natural Flavor by Multi-component solvent transfer extraction combined with rotating vertebral column technique, funded by Key Laboratory of Cigarette Flavoring Technology in Tobacco Industry, TX2018001.

#### References

- [1] Y. Dufour and P. Steane, "Building a good solid family wine business: casella Wines," *International Journal of Wine Business Research*, vol. 22, no. 2, pp. 122–132, 2010.
- [2] A. Lezaeta, E. Bordeu, E. Agosin, J. R. Pérez-Correa, and P. Varela, "White wines aroma recovery and enrichment: sensory-led aroma selection and consumer perception," *Food Research International*, vol. 108, pp. 595–603, 2018.
- [3] C. Gomez, P. Lagacherie, and G. Coulouma, "Continuum removal versus PLSR method for clay and calcium carbonate content estimation from laboratory and airborne hyperspectral measurements," *Geoderma*, vol. 148, no. 2, pp. 141–148, 2008.
- [4] M. A. Tetik, O. Sevindik, H. Kelebek, and S. Selli, "Screening of key odorants and anthocyanin compounds of cv. Okuzgozu (*Vitis vinifera* L.) red wines with a free run and pressed pomace using GC-MS-Olfactometry and LC-MS-MS," *Journal of Mass Spectrometry*, vol. 53, no. 5, pp. 444–454, 2018.
- [5] M. Dziadas and H. H. Jeleń, "Analysis of terpenes in white wines using SPE-SPME-GC/MS approach," *Analytica Chimica Acta*, vol. 677, no. 1, pp. 43–49, 2010.
- [6] A. Marquez, M. P. Serratosa, J. Merida, L. Zea, and L. Moyano, "Optimization and validation of an automated DHS-TD-GC-MS method for the determination of aromatic esters in sweet wines," *Talanta*, vol. 123, pp. 32–38, 2014.
- [7] A. C. Pereira, M. S. Reis, P. M. Saraiva, and J. C. Marques, "Madeira wine ageing prediction based on different analytical techniques: UV-vis, GC-MS, HPLC-DAD," *Chemometrics and Intelligent Laboratory Systems*, vol. 105, no. 1, pp. 43–55, 2011.
- [8] D. Barbera, G. Avellone, F. Filizzola, L. G. Monte, P. Catanzaro, and P. Agozzino, "Determination of terpene alcohols in Sicilian Muscat wines by HS-SPME-GC-MS," *Natural Product Research*, vol. 27, no. 6, pp. 541–547, 2013.
- [9] I. Lukic and I. Horvat, "Differentiation of commercial PDO wines produced in Istria (Croatia) according to variety and harvest year based on HS-SPME-GC/MS volatile aroma compounds profiling," *Food Technology and Biotechnology*, vol. 55, no. 1, 2017.
- [10] A. Barata, E. Campo, M. Malfeito-Ferreira, V. Loureiro, J. Cacho, and V. Ferreira, "Analytical and sensorial characterization of the aroma of wines produced with sour rotten grapes using GC-O and GC-MS: identification of key aroma compounds," *Journal of Agricultural and Food Chemistry*, vol. 59, no. 6, pp. 2543–2553, 2011.
- [11] M. Vilanova, Z. Genisheva, A. Masa, and J. M. Oliveira, "Correlation between volatile composition and sensory properties in Spanish Albariño wines," *Microchemical Journal*, vol. 95, no. 2, pp. 240–246, 2010.
- [12] E. Campo, V. Ferreira, A. Escudero, and J. Cacho, "Prediction of the wine sensory properties related to grape variety from dynamic-headspace gas Chromatography–Olfactometry data," *Journal of Agricultural and Food Chemistry*, vol. 53, no. 14, pp. 5682–5690, 2005.
- [13] H. Y. Yu, X. Y. Niu, H. J. Lin, Y. B. Ying, B. B. Li, and X. X. Pan, "A feasibility study on on-line determination of rice wine composition by Vis-NIR spectroscopy and least-squares support vector machines," *Food Chemistry*, vol. 113, no. 1, pp. 291–296, 2009.
- [14] H. Yu, Y. Zhou, X. Fu, L. Xie, and Y. Ying, "Discrimination between Chinese rice wines of different geographical origins by NIRS and AAS," *European Food Research and Technology*, vol. 225, pp. 313–320, 2007.
- [15] J. Farifteh, F. Van der Meer, C. Atzberger, and E. J. M. Carranza, "Quantitative analysis of salt-affected soil reflectance spectra: a comparison of two adaptive methods (PLSR and ANN)," *Remote Sensing of Environment*, vol. 110, no. 1, pp. 59–78, 2007.









- [16] S.-J. Chung, H. Heymann, and I. U. Grün, "Application of GPA and PLSR in correlating sensory and chemical data sets," *Food Quality and Preference*, vol. 14, pp. 485–495, 2003.
- [17] M. Zhang, H. Mu, G. Li, and Y. Ning, "Forecasting the transport energy demand based on PLSR method in China," *Energy*, vol. 34, no. 9, pp. 1396–1400, 2009.
- [18] H. Yu, T. Xie, J. Xie, L. Ai, and H. Tian, "Characterization of key aroma compounds in Chinese rice wine using gas chromatography-mass spectrometry and gas chromatography-olfactometry," *Food Chemistry*, vol. 293, pp. 8–14, 2019.
- [19] S. Capone, M. Tufariello, L. Francioso et al., "Aroma analysis by GC/MS and electronic nose dedicated to Negroamaro and Primitivo typical Italian Apulian wines," *Sensors and Actuators B: Chemical*, vol. 179, pp. 259–269, 2013a.
- [20] N. Lopez de Lerma, A. Bellincontro, F. Mencarelli, J. Moreno, and R. A. Peinado, "Use of electronic nose, validated by GC-MS, to establish the optimum off-vine dehydration time of wine grapes," *Food Chemistry*, vol. 130, no. 2, pp. 447–452, 2012.
- [21] I. L. Francis and J. L. Newton, "Determining wine aroma from compositional data," *Australian Journal of Grape and Wine Research*, vol. 11, no. 2, pp. 114–126, 2005.
- [22] S. Capone, M. Tufariello, and P. Siciliano, "Analytical characterisation of negroamaro red wines by "aroma wheels"," *Food Chemistry*, vol. 141, no. 3, pp. 2906–2915, 2013.
- [23] A. Janusz, D. L. Capone, C. J. Puglisi, M. V. Perkins, G. M. Elsey, and M. A. Sefton, "(E)-1-(2,3,6-Trimethylphenyl) buta-1,3-diene: a potent grape-derived odorant in wine," *Journal of Agricultural and Food Chemistry*, vol. 51, no. 26, pp. 7759–7763, 2003.
- [24] E. G. Garc A-Carpintero, E. S. Nchez-Palomo, G. M. A. Mez Gallego, and M. A. Gonz Lez-VI A, "Effect of cofermentation of grape varieties on aroma profiles of La Mancha red wines," *Journal of Food Science*, vol. 76, pp. C1169–C1180, 2011.
- [25] S. M. Rocha, F. Rodrigues, P. Coutinho, I. Delgado, and M. A. Coimbra, "Volatile composition of Baga red wine," *Analytica Chimica Acta*, vol. 513, no. 1, pp. 257–262, 2004.
- [26] M. Gil, J. M. Cabellos, T. Arroyo, and M. Prodanov, "Characterization of the volatile fraction of young wines from the Denomination of Origin "Vinos de Madrid" (Spain)," *Analytica Chimica Acta*, vol. 563, pp. 145–153, 2006.
- [27] A. C. Pereira, M. S. Reis, P. M. Saraiva, and J. C. Marques, "Aroma ageing trends in GC/MS profiles of liqueur wines," *Analytica Chimica Acta*, vol. 659, pp. 93–101, 2010.
- [28] S. Y. Sun, W. G. Jiang, and Y. P. Zhao, "Comparison of aromatic and phenolic compounds in cherry wines with different cherry cultivars by HS-SPME-GC-MS and HPLC," *International Journal of Food Science and Technology*, vol. 47, no. 1, pp. 100–106, 2012.
- [29] Z. Xiao, S. Liu, Y. Gu, N. Xu, Y. Shang, and J. Zhu, "Discrimination of cherry wines based on their sensory properties and aromatic fingerprinting using HS-SPME-GC-MS and multivariate analysis," *Journal of Food Science*, vol. 79, no. 3, pp. C284–C294, 2014a.
- [30] G. Sagratini, F. Maggi, G. Caprioli et al., "Comparative study of aroma profile and phenolic content of Montepulciano monovarietal red wines from the Marche and Abruzzo regions of Italy using HS-SPME-GC-MS and HPLC-MS," *Food Chemistry*, vol. 132, no. 3, pp. 1592–1599, 2012.
- [31] Z. Zhang, Y. Shu, G. Li et al., "Gc-ms analysis of characteristic aromatic compounds from jujube wine (LB396)," *The FASEB Journal*, vol. 28, Article ID LB396, 2014.
- [32] A. Escudero, E. Campo, L. Fariña, J. Cacho, and V. Ferreira, "Analytical characterization of the aroma of five premium red wines. Insights into the role of odor families and the concept of fruitiness of wines," *Journal of Agricultural and Food Chemistry*, vol. 55, no. 11, pp. 4501–4510, 2007.
- [33] M. Gonz Lez Álvarez, C. Gonz Lez-Barreiro, B. Cancho-Grande, and J. Simal-G Ndara, "Relationships between Godello white wine sensory properties and its aromatic fingerprinting obtained by GC-MS," *Food Chemistry*, vol. 129, pp. 890–898, 2011.
- [34] Y. Niu, Z. Yao, Q. Xiao, Z. Xiao, N. Ma, and J. Zhu, "Characterization of the key aroma compounds in different light aroma type Chinese liquors by GC-olfactometry, GC-FPD, quantitative measurements, and aroma recombination," *Food Chemistry*, vol. 233, pp. 204–215, 2017.
- [35] S. N. Wang, Q. T. Zhang, P. T. Zhao et al., "Investigating the effect of three phenolic fractions on the volatility of floral, fruity, and aged aromas by HS-SPME-GC-MS and NMR in model wine," *Food Chemistry X*, vol. 13, pp. 1575–2590, 2022.
- [36] Z. Xiao, D. Yu, Y. Niu et al., "Characterization of aroma compounds of Chinese famous liquors by gas chromatography-mass spectrometry and flash GC electronic-nose," *Journal of Chromatography B*, vol. 945–946, pp. 92–100, 2014.
- [37] H. Li, Y. S. Tao, H. Wang, and L. Zhang, "Impact odorants of chardonnay dry white wine from Changli Country (China)," *European Food Research and Technology*, vol. 227, 2008.
- [38] L. Moyano, L. Zea, J. Moreno, and M. Medina, "Analytical study of aromatic series in sherry wines subjected to biological aging," *Journal of Agricultural and Food Chemistry*, vol. 50, no. 25, pp. 7356–7361, 2002.
- [39] J. Cacho, "The perception of aromatic notes of wine and the effect of certain volatile molecules," *Minutes of the XVII Annual Congress of the ACE Vilanova del Valles*, 2006.
- [40] M. Cliff, D. Yuksel, B. Girard, and M. King, "Characterization of Canadian ice wines by sensory and compositional analyses," *American Journal of Enology and Viticulture*, vol. 53, pp. 46–53, 2002.
- [41] C. Flanzky, *Enología: Fundamentos Científicos Y Tecnológicos*, Mundi-Prensa Libros, 2003.
- [42] J. E. Amooore and E. Hautala, "Odor as an aid to chemical safety: odor thresholds compared with threshold limit values and volatilities for 214 industrial chemicals in air and water dilution," *Journal of Applied Toxicology*, vol. 3, no. 6, pp. 272–290, 1983.
- [43] H. Maarse, *Volatile Compounds in Foods and Beverages*, Marcel Dekker, New York, NY, USA, 1991.
- [44] H. Guth, "Identification of character impact odorants of different white wine varieties," *Journal of Agricultural and Food Chemistry*, vol. 45, no. 8, pp. 3022–3026, 1997.
- [45] C. Liu, Y. Cheng, H. Zhang, X. Deng, F. Chen, and J. Xu, "Volatile constituents of wild citrus Mangshanyegan (Citrus nobilis Lauriro) peel oil," *Journal of Agricultural and Food Chemistry*, vol. 60, no. 10, pp. 2617–2628, 2012.
- [46] F. Fazzalari, *Compilation of Odor and Taste Threshold Values Data*, ASTM, West Conshohocken, PA, USA, 1978.
- [47] V. Ferreira, R. Lpez, and J. F. Cacho, "Quantitative determination of the odorants of young red wines from different grape varieties," *Journal of the Science of Food and Agriculture*, vol. 80, no. 11, pp. 1659–1667, 2000.
- [48] P. Darriet, "The great diversity of aroma forms in grapes," *Vigne et Vin Publication Internationales-Matillac*, vol. 33, pp. 89–98, 1996.
- [49] R. López, M. Aznar, J. Cacho, and V. Ferreira, "Determination of minor and trace volatile compounds in wine by solid-phase extraction and gas chromatography with mass spectrometric

- detection," *Journal of Chromatography A*, vol. 966, pp. 167–177, 2002.
- [50] J. Boidron, P. Chatonnet, and M. Pons, "Influence du bois sur certaines substances odorantes des vins," *Knowledge of Vine and Wine*, vol. 22, 1988.
- [51] H. Guth, "Quantitation and sensory studies of character impact odorants of different white wine varieties," *Journal of Agricultural and Food Chemistry*, vol. 45, no. 8, pp. 3027–3032, 1997.
- [52] L. Huang, Y. Ma, X. Tian et al., "Chemosensory characteristics of regional Vidal icewines from China and Canada," *Food Chemistry*, vol. 261, pp. 66–74, 2018.
- [53] V. Ivanova, M. Stefova, B. Vojnoski et al., "Volatile composition of Macedonian and Hungarian wines assessed by GC/MS," *Food and Bioprocess Technology*, vol. 6, no. 6, pp. 1609–1617, 2013.
- [54] R. A. Peinado, J. A. Moreno, D. Muñoz, M. Medina, and J. Moreno, "Gas chromatographic quantification of major volatile compounds and polyols in wine by direct injection," *Journal of Agricultural and Food Chemistry*, vol. 52, no. 21, pp. 6389–6393, 2004.
- [55] M. Chastrette, D. Cretin, and E. El Aïdi, "Structure–Odor relationships: using neural networks in the estimation of camphoraceous or fruity odors and olfactory thresholds of aliphatic alcohols," *Journal of Chemical Information and Computer Sciences*, vol. 36, no. 1, pp. 108–113, 1996.
- [56] I. Mato, S. Suárez-Luque, and J. F. Huidobro, "A review of the analytical methods to determine organic acids in grape juices and wines," *Food Research International*, vol. 38, no. 10, pp. 1175–1188, 2005.
- [57] S. Lafon-Lafourcade, C. Geneix, and P. Ribéreau-Gayon, "Inhibition of alcoholic fermentation of grape must by fatty acids produced by yeasts and their elimination by yeast ghosts," *Applied and Environmental Microbiology*, vol. 47, no. 6, pp. 1246–1249, 1984.
- [58] E. Pittari, L. Moio, and P. Piombino, "Interactions between polyphenols and volatile compounds in wine: a literature review on physicochemical and sensory insights," *Applied Sciences*, vol. 11, no. 3, p. 1157, 2021.
- [59] P. Chatonnet, D. Dubourdieu, J. Boidron, and V. Lavigne, "Synthesis of volatile phenols by *Saccharomyces cerevisiae* in wines," *Journal of the Science of Food and Agriculture*, vol. 62, no. 2, pp. 191–202, 1993.
- [60] S. Galafassi, A. Merico, F. Pizza et al., "*Dekkera/Brettanomyces* yeasts for ethanol production from renewable sources under oxygen-limited and low-pH conditions," *Journal of Industrial Microbiology and Biotechnology*, vol. 38, no. 8, pp. 1079–1088, 2011.
- [61] A. Jeromel, A.-M. J. Korenika, and I. Tomaz, "An influence of different yeast species on wine aroma composition," *Fermented Beverages*, vol. 5, pp. 171–285, 2019.
- [62] B. Jiang and Z. Zhang, "Volatile compounds of young wines from Cabernet Sauvignon, Cabernet gernischt and Chardonnay varieties grown in the loess plateau region of China," *Molecules*, vol. 15, no. 12, pp. 9184–9196, 2010.
- [63] F. S. Juan, J. Cacho, V. Ferreira, and A. Escudero, "Aroma chemical composition of red wines from different price categories and its relationship to quality," *Journal of Agricultural and Food Chemistry*, vol. 60, no. 20, pp. 5045–5056, 2012.
- [64] R. Nogueroles-Pato, M. González-Álvarez, C. González-Barreiro, B. Cancho-Grande, and J. Simal-Gándara, "Evolution of the aromatic profile in Garnacha Tintorera grapes during raising and comparison with that of the naturally sweet wine obtained," *Food Chemistry*, vol. 139, pp. 1052–1061, 2013.
- [65] P. Snitkjær, J. Risbo, L. H. Skibsted et al., "Beef stock reduction with red wine - effects of preparation method and wine characteristics," *Food Chemistry*, vol. 126, no. 1, pp. 183–196, 2011.
- [66] P. Chatonnet, D. Dubourdieu, and J. Boidron, "The influence of *Brettanomyces/Dekkera* sp. yeasts and lactic acid bacteria on the ethylphenol content of red wines," *American Journal of Enology and Viticulture*, vol. 46, pp. 463–468, 1995.
- [67] R. Su Rez, J. Surez-Lepe, A. Morata, and F. Calder N, "The production of ethylphenols in wine by yeasts of the genera *Brettanomyces* and *Dekkera*: a review," *Food Chemistry*, vol. 102, pp. 10–21, 2007.



## Research Article

# Analysis of Volatile Components in *Tremella fuciformis* by Electronic Nose Combined with GC-MS

Lijun Fu <sup>1</sup>, Jing Tian <sup>2,3</sup>, Li Liu <sup>1</sup>, Yongzheng Ma <sup>1</sup>, Xiumin Zhang <sup>1</sup>,  
Changyang Ma <sup>3,4</sup>, Wenyi Kang <sup>2,3,4</sup> and Yong Sun <sup>1</sup>

<sup>1</sup>Beijing Academy of Food Sciences, Beijing 100050, China

<sup>2</sup>Kaifeng Key Laboratory of Functional Components in Health Food, Kaifeng 475004, China

<sup>3</sup>National R and D Center for Edible Fungus Processing Technology, Henan University, Kaifeng 475004, China

<sup>4</sup>Joint International Research Laboratory of Food and Medicine Resource Function, Kaifeng 475004, Henan Province, China

Correspondence should be addressed to Changyang Ma; [macaya1024@sina.com](mailto:macaya1024@sina.com), Wenyi Kang; [kangwenyi@hotmail.com](mailto:kangwenyi@hotmail.com), and Yong Sun; [sy183509@163.com](mailto:sy183509@163.com)

Received 7 March 2022; Accepted 11 April 2022; Published 27 April 2022

Academic Editor: Tao Feng

Copyright © 2022 Lijun Fu et al. This is an open access article distributed under the Creative Commons Attribution License, which permits unrestricted use, distribution, and reproduction in any medium, provided the original work is properly cited.

In order to quickly evaluate the quality of *Tremella fuciformis*, the volatile components of *T. fuciformis* from 4 provinces in China, including Hebei, Henan, Fujian, and Sichuan, were analyzed by electronic nose combined with gas chromatography-mass spectrometry (GC-MS), and the key aroma compounds were determined by relative odor activity value (ROAV). The results showed that the electronic nose combined with the principal component analysis method could distinguish the samples from four regions with good discrimination. At least 117 volatile components were detected in *T. fuciformis* by GC-MS and a total of 58, 59, 62, and 55 volatile components were identified from Hebei, Henan, Fujian, and Sichuan, respectively, of which there were 18 common components. The volatile components in *T. fuciformis* were mainly hydrocarbons, followed by aldehydes, acids, and esters, while acetic acid and hexanal were relatively rich in *T. fuciformis*. Based on the ROAV, 8 key components affecting the aroma of *T. fuciformis* strongly were found. Among them, hexanal, nonanal, and pentanal were the common components of *T. fuciformis*, while butyrolactone, 1-octen-3-ol, and 2-carene were the unique key aroma components of *T. fuciformis* in Hebei Province. Besides, octanal and butyrolactone were the special key components absent in the Sichuan and Henan samples, respectively.

## 1. Introduction

Edible fungi are rich in species and contain more nutrients, which have broad research prospects and potential application value in healthy food and medicine [1–3]. *Tremella fuciformis*, known as white fungus or snow fungus, mainly grows in the subtropical zone, as well as the tropical zone, temperate zone, and frigid zone [4]. As recording about a traditional and valuable edible fungus in China, *T. fuciformis* is rich in protein, amino acids, crude fiber, trace elements, and other nutrients and has the functions of nourishing body fluid and lungs, tonifying the brain and heart, moisturizing skin, antitumor, treating chronic bronchitis, and postpartum weakness [5–12].

Usually, consumers mainly use their own olfactory systems with less reliability and more subjectivity to evaluate the sensory quality of *T. fuciformis*. At present, GC-MS and other methods are often used to detect its volatile components [13], but the sensory evaluation is not subjective, with individual differences, abstraction, and other shortcomings. An electronic nose is often used to simulate the human olfactory system, with the characteristics of high automation, low operating cost, short detection time, and good repeatability. And, it can be directly applied to the rapid odor determination of most substances and has been widely applied in the field of internal quality detection of agricultural products [14]. The combined application of the electronic nose and GC-MS can well realize the

comprehensive analysis of volatile components in samples [15–17]. In this paper, electronic nose and GC-MS were used to detect and analyze the volatile components of *T. fuciformis* collected from four different regions, and the differences among the regions would be analyzed based on the compound content and ROAV value. The research on the volatile components of *T. fuciformis* could provide scientific and theoretical guidance for inspectors to analyze the quality and a reference for consumers to choose suitable products, benefiting the market of *T. fuciformis*.

## 2. Materials and Methods

### 2.1. Materials

**2.1.1. Instruments and Equipment.** Instruments and equipment used were as follows: SuperNose-14 electronic nose (ISENSO Inc., USA), HH-S4 digital thermostatic water bath (Kunlun Ultrasonic Instruments Co., Ltd, China), multi-function grinder (Yongkang Bo'ou Hardware Products Co., Ltd., China), GCMS-QP2010UL GC-MS (Shimadzu Inc., Japan), and AB135-S electronic balance (Sartorius Scientific Instruments (Beijing) Co., Ltd., China). The Unscrambler X 10.4 statistical analysis software (CAMO Inc., Norway).

**2.1.2. Samples.** The *T. fuciformis* was commercially available from Fujian, Henan, Sichuan, and Hubei provinces of China, the specific origin information of different batches of *T. fuciformis* is shown in Table 1. The research group only selected the samples from Hebei, Henan, Fujian, and Sichuan provinces because the output of *T. fuciformis* in these four provinces has a large yield and high quality. In the same province, we selected samples from different urban areas and different brands, which are representative. Among them, *T. fuciformis* from Gutian in Fujian is the most famous.

### 2.2. Experimental Methods

**2.2.1. Electronic Nose Detection.** The odor of *T. fuciformis* was determined by the modified method [18–21]. The powder of *T. fuciformis* (5.0 g) was put in the headspace bottle, and the injection needle was inserted into the headspace vial at room temperature.

**2.2.2. GC-MS Testing.** The volatile components of *T. fuciformis* [22–24] were determined by the GC-MS. The GC-MS condition was a DB-5MS capillary column (0.1  $\mu\text{m} \times 30.0 \text{ m} \times 250 \mu\text{m}$ ). The temperature of the program was as follows: the initial column temperature was 50°C and the temperature was raised to 180°C at the rate of 5°C/min, kept for 2 minutes, then was raised to 120°C at the rate of 8°C/min, kept for 2 minutes, and raised to 220°C at 5°C/min for 3 minutes. The total flow is 7.0 mL/min while the column flow is 1.00 mL/min. The temperature of the ion source of the mass spectrometer was set at 230°C and the interface temperature was 250°C. The MS scan range was 20~450  $m/z$ .

TABLE 1: Origin regions of *T. fuciformis*.

No.	City, province
1	Ningde, Fujian
2	Ningde, Fujian
3	Datian, Fujian
4	Ningde, Fujian
5	Ningde, Fujian
6	Gutian, Fujian
7	Ningde, Fujian
8	Ningde, Fujian
9	Datian, Fujian
10	Gutian, Fujian
11	Gutian, Fujian
12	Ningde, Fujian
13	Ningde, Fujian
14	Gutian, Fujian
15	Ningde, Fujian
16	Zhangzhou, Fujian
17	Ningde, Fujian
18	Ningde, Fujian
19	Putian, Fujian
20	Gutian, Fujian
21	Gutian, Fujian
22	Ningde, Fujian
23	Gutian, Fujian
24	Xiamen, Fujian
25	Ningde, Fujian
26	Putian, Fujian
27	Sanmenxia, Henan
28	Zhengzhou, Henan
29	Shangqiu, Henan
30	Xinxiang, Henan
31	Xinxiang, Henan
32	Luoyang, Henan
33	Longfeng, Henan
34	Longfeng, Henan
35	Xinxiang, Henan
36	Guangyuan, Sichuan
37	Guangyuan, Sichuan
38	Tongjiang, Sichuan
39	Qingchuan, Sichuan
40	Jianyang, Sichuan
41	Bazhong, Sichuan
42	Tongjiang, Sichuan
43	Cangzhou, Hebei
44	Hebei
45	Cangzhou, Hebei
46	Langfang, Hebei
47	Langfang, Hebei
48	Cangzhou, Hebei
49	Langfang, Hebei
50	Cangzhou, Hebei

**2.2.3. Identification of Compounds.** For the qualitative and quantitative analysis of volatile compounds, the National Institute of Standards and Technology (NIST) mass spectral library was used for compound identification (similarity between the peaks  $\geq 85\%$ ), and the peak area normalization method was adopted to calculate the relative content of each volatile component. The retention time and MS were used for qualitative analysis of volatile components in the samples.

**2.2.4. Evaluation of Volatile Aroma Substances.** The relative odor activity value (ROAV) was used to evaluate the contribution of volatile components to the total aroma of samples [25]. The ROAV calculation formula was as follows:

$$\text{ROAV}_i = \frac{C_{ri}}{C_{rstan}} \times \frac{T_{stan}}{T_i} \times 100. \quad (1)$$

$C_{ri}$ ,  $T_i$  were relative contents of volatile components/% and odor threshold/( $\mu\text{g}/\text{kg}$ );  $C_{rstan}$  and  $T_{stan}$  were the relative content/% and odor threshold/( $\mu\text{g}/\text{kg}$ ) of the components contributing most to the overall aroma of the sample, respectively.

### 3. Results and Discussion

#### 3.1. The Results of *T. fuciformis* from Different Regions Based on Electronic Nose

**3.1.1. PCA Analysis of *T. fuciformis*.** Principal component analysis (PCA) is a common method which could extract the characteristic information of samples from complicated information through reducing dimensions and data transformation without loss of original information. The factors with the large and leading contribution rates extracted from the electronic nose sensor data of *T. fuciformis* originating from four different regions (Figure 1) could inhibit the differences in the samples among different regions in the PCA distribution map [26, 27].

Note: “Fu, Si, Yu and Ji” represent “Fujian, Sichuan, Henan and Hebei,” respectively, and the numbers represent different sample batches.

In Figure 1, the cumulative variance contribution rate of PC-1 (80%) and PC-2 (9%) reached 89%, which indicated the two principal components could retain most of the information of these samples and was sufficient to analyze the similarity relationship between samples [28]. It could be seen that the spatial distribution of principal components of *T. fuciformis* samples was relatively scattered, and those from each origin region were relatively concentrated and separated. Therefore, the two principal components could distinguish the samples from the four regions well. The samples from Hebei and Henan Province were located in the upper right and lower right of Figure 1, respectively, while those from Fujian Province and Sichuan Province were located in the upper left and lower left, respectively. These results also confirmed the differences of *T. fuciformis* from different regions.

Note: “C” represents the gas sensor and numbers indicate the different sensor types.

**3.1.2. Loading Analysis of *T. fuciformis*.** Loading analysis is a similar method with PCA to extract the principal components from the origin data. However, the PCA algorithm is special for sample analysis, while loading analysis is for sensors of electronic noses. In this part, loading analysis was used to analyze the contribution of each sensor to the distinguishment of *T. fuciformis* (Figure 2) [26, 29]. It could be seen that  $C_1$ ,  $C_3$ ,  $C_4$ ,  $C_5$ ,  $C_6$ ,  $C_8$ , and  $C_9$  sensors

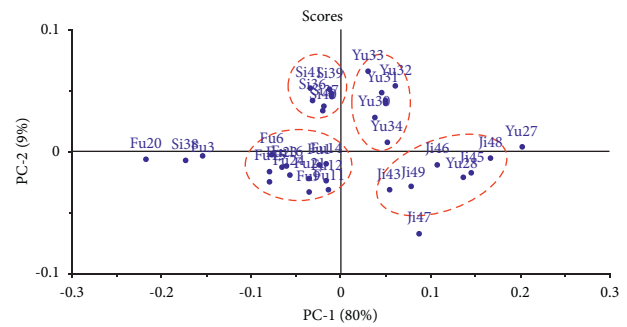


FIGURE 1: PCA result of *T. fuciformis* from different regions.

contributed a large proportion to the 1<sup>st</sup> principal component for the *T. fuciformis*.

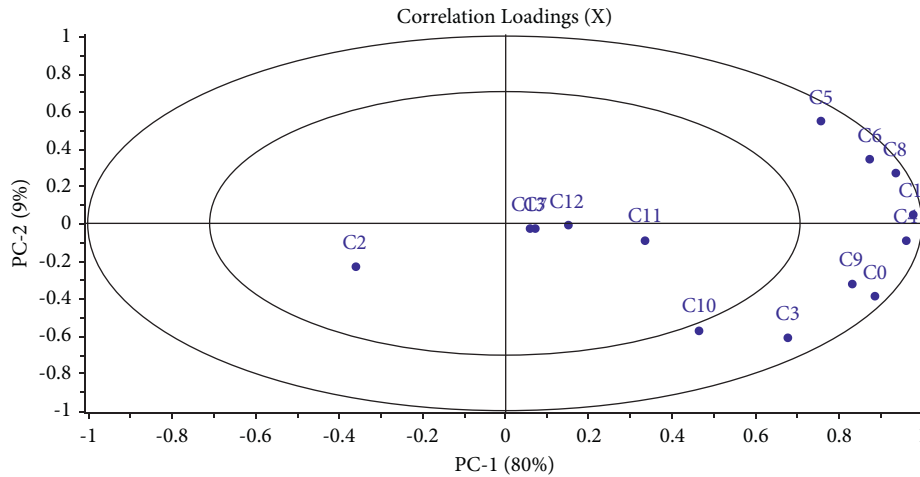
#### 3.2. GC-MS Results of *T. fuciformis*

**3.2.1. Components Analysis of *T. fuciformis*.** The volatile components of *T. fuciformis* from four regions were analyzed by GC-MS in Table 2.

A total of 117 volatile components, including 68 hydrocarbons, 12 esters, 10 alcohols, 10 aldehydes, 7 acids, and 10 other compounds, were detected from *T. fuciformis*. However, the relative contents of acids and aldehydes were the highest, which was consistent with Li Xiang’s research on *T. fuciformis* and bag cultivated *T. fuciformis* [13]. Moreover, 58, 59, 62, and 55 volatile components were detected from Hebei, Henan, Fujian, and Sichuan Provinces, respectively. Within them, there were a total number of 18 common components. However, a variety of volatile components were detected in *T. fuciformis* for the first time, such as eucalyptol, 2-butyl-1-octanol, 2-ethyl-1-pentanol, benzeneacetaldehyde, 4-methylvaleric acid, gamma-butyrolactone, n-hexyl formate, bute hydrocarbon, hydroxylamine, 2-carene have not been reported.

Among the 68 hydrocarbon compounds of *T. fuciformis*, most of them belonged to the saturated hydrocarbons, such as 5-methyltetradecane, bute hydrocarbon, 2, 6, 10, 14-tetramethylhexadecane, 4, 6-dimethyldodecane, and 2, 6, 10-trimethyldodecane. However, these compounds had generally low relative content in the samples with high threshold values, which contributed less to the overall odor of *T. fuciformis*. In contrast, unsaturated hydrocarbons such as (5E)-5-octadecene, camphene, and 2-carene contribute more for its relatively low thresholds [34]. Besides, no unique compounds with high relative content ( $\geq 1$ ) were found for the samples from different regions.

Esters are usually one type of compound with a fruit aroma and contribute to the overall aroma of *T. fuciformis* [35]. A total of 12 ester compounds were detected from *T. fuciformis*. Of them, butyrolactone (6.08%) and  $\gamma$ -butyrolactone (2.79%) were the top 2 esters of Hebei samples, while  $\gamma$ -butyrolactone, heptadecyl trifluoroacetate, and hydrazinecarboxylic acid, ethyl ester were the unique volatile constituents. For the Sichuan samples, the unique ester components included sulfurous acid, 2-ethylhexyl isobutyl ester, 2-ethylhexyl acrylate, hexatriacontyl

FIGURE 2: Loadings analysis of *T. fuciformis* from different regions.TABLE 2: Composition of volatile components of *T. fuciformis*.

Number	Compound name	Molecular formula	Relative content/%				RI value	Literature
			Hebei	Henan	Sichuan	Fujian		
<i>Alcohols</i>								
1	Pentyl alcohol	C <sub>5</sub> H <sub>12</sub> O	1.22	1.12	—	0.95	761	[30]
2	2-Ethyl-1-decanol	C <sub>12</sub> H <sub>26</sub> O	0.02	—	—	—	1393	
3	1-Hexanol	C <sub>6</sub> H <sub>14</sub> O	0.57	—	—	0.02	860	[20]
4	1-Octen-3-ol	C <sub>8</sub> H <sub>16</sub> O	0.38	—	—	—	969	[20]
5	Eucalyptol	C <sub>10</sub> H <sub>18</sub> O	5.00	—	—	—	1059	
6	Linalol	C <sub>10</sub> H <sub>18</sub> O	0.05	—	—	—	1082	[31]
7	Isotridecyl alcohol	C <sub>13</sub> H <sub>28</sub> O	0.01	—	—	—	1492	
8	2-Tetradecyloxyethanol	C <sub>16</sub> H <sub>34</sub> O <sub>2</sub>	—	0.01	0.03	—	1930	
9	2-Butyl-1-octanol	C <sub>12</sub> H <sub>26</sub> O	—	0.03	—	0.03	1393	
10	Isopentyl alcohol	C <sub>5</sub> H <sub>12</sub> O	—	—	—	0.21	697	[20]
<i>Aldehyde</i>								
11	Hexanal	C <sub>6</sub> H <sub>12</sub> O	27.35	25.21	23.60	21.60	806	[20]
12	Furfural	C <sub>5</sub> H <sub>4</sub> O <sub>2</sub>	0.01	0.17	—	0.02	831	
13	Heptanal	C <sub>7</sub> H <sub>14</sub> O	0.43	1.04	—	—	905	[20]
14	2-Furancarboxaldehyde, 5-methyl-	C <sub>6</sub> H <sub>6</sub> O <sub>2</sub>	—	0.08	—	—	920	
15	Octanal	C <sub>8</sub> H <sub>16</sub> O	1.03	0.04	—	0.04	1005	[30]
16	Benzeneacetaldehyde	C <sub>8</sub> H <sub>8</sub> O	0.82	0.01	—	—	1081	[20]
17	Nonanal	C <sub>9</sub> H <sub>18</sub> O	2.58	0.19	0.07	1.06	1104	[20]
18	Benzaldehyde	C <sub>7</sub> H <sub>6</sub> O	0.23	0.02	—	0.08	982	[20]
19	Pentanal	C <sub>5</sub> H <sub>10</sub> O	5.05	0.38	0.01	0.23	707	[20]
20	2-Ethyl-1-pentanol	C <sub>7</sub> H <sub>16</sub> O	—	—	—	0.03	896	
<i>Acids</i>								
21	Acetic acid	CH <sub>3</sub> COOH	35.36	49.42	39.92	40.85	576	[31]
22	4-Methylvaleric acid	C <sub>6</sub> H <sub>12</sub> O <sub>2</sub>	1.73	—	—	—	910	
23	Nonanoic acid	C <sub>9</sub> H <sub>18</sub> O <sub>2</sub>	0.40	—	—	—	1272	
24	Octanoic acid	C <sub>8</sub> H <sub>16</sub> O <sub>2</sub>	—	1.52	1.52	—	2069	[32]
25	Pentanoic acid	C <sub>5</sub> H <sub>10</sub> O <sub>2</sub>	—	0.21	—	—	1161	
26	Heptanoic acid	C <sub>7</sub> H <sub>14</sub> O <sub>2</sub>	—	2.01	1.33	—	1078	[30]
27	Hexanoic acid	C <sub>6</sub> H <sub>12</sub> O <sub>2</sub>	—	0.69	—	3.72	1856	[32]

TABLE 2: Continued.

Number	Compound name	Molecular formula	Relative content/%				RI value	Literature
			Hebei	Henan	Sichuan	Fujian		
<i>Esters</i>								
28	Butyrolactone	C <sub>4</sub> H <sub>6</sub> O <sub>2</sub>	6.08	—	1.06	0.11	825	
29	gamma-Butyrolactone	C <sub>5</sub> H <sub>8</sub> O <sub>2</sub>	2.79	—	—	—	886	
30	Heptadecyl trifluoroacetate	C <sub>19</sub> H <sub>35</sub> F <sub>3</sub> O <sub>2</sub>	0.52	—	—	—	1812	
31	Hydrazinecarboxylic acid, ethyl ester	C <sub>3</sub> H <sub>8</sub> N <sub>2</sub> O <sub>2</sub>	0.14	—	—	—	928	
32	Sulfurous acid, hexyl pentadecyl ester	C <sub>21</sub> H <sub>44</sub> O <sub>3</sub> S	—	0.42	—	0.18	2732	
33	n-Hexyl formate	C <sub>7</sub> H <sub>14</sub> O <sub>2</sub>	—	0.65	—	0.01	981	[20]
34	Docosyl pentafluoropropionate	C <sub>25</sub> H <sub>45</sub> F <sub>5</sub> O <sub>2</sub>	—	0.01	—	—	2369	
35	Sulfurous acid, 2-ethylhexyl isobutyl ester	C <sub>12</sub> H <sub>26</sub> O <sub>3</sub> S	—	—	0.02	—	1709	
36	2-Ethylhexyl acrylate	C <sub>11</sub> H <sub>20</sub> O <sub>2</sub>	—	—	0.01	—	1208	
37	Hexatriacontyl pentafluoropropionate	C <sub>39</sub> H <sub>73</sub> F <sub>5</sub> O <sub>2</sub>	—	—	0.02	—	3761	
38	Formic acid, ethenyl ester	C <sub>3</sub> H <sub>4</sub> O <sub>2</sub>	—	—	25.12	—	574	
39	1-Methyl-2-oxocyclohex-3-enecarboxylic acid, methyl ester	C <sub>9</sub> H <sub>12</sub> O <sub>3</sub>	—	—	—	0.01	1274	
<i>Hydrocarbons</i>								
40	2, 10-Trimethyldodecane	C <sub>15</sub> H <sub>32</sub>	—	0.01	0.01	0.02	1320	
41	Bute hydrocarbon	C <sub>19</sub> H <sub>40</sub>	—	0.72	—	0.03	1653	
42	3-Methylheptadecane	C <sub>18</sub> H <sub>38</sub>	—	0.02	—	—	1746	
43	3-Methylundecane	C <sub>12</sub> H <sub>26</sub>	0.03	0.02	0.04	0.03	1150	[33]
44	Dodecane	C <sub>12</sub> H <sub>26</sub>	0.15	0.09	0.10	0.30	1214	[30]
45	Tetradecane	C <sub>14</sub> H <sub>30</sub>	0.15	0.06	—	0.54	1413	[20]
46	4,6-Dimethyldodecane	C <sub>14</sub> H <sub>30</sub>	0.19	0.05	0.02	—	1285	
47	Dodecamethylcyclohexasiloxane	C <sub>12</sub> H <sub>36</sub> O <sub>6</sub> Si <sub>6</sub>	0.04	0.03	—	0.10	1240	
48	Heptadecane	C <sub>17</sub> H <sub>36</sub>	0.07	1.16	0.04	0.21	1711	
49	2,5-Dimethyltridecane	C <sub>15</sub> H <sub>32</sub>	—	0.01	0.02	0.02	1384	
50	6-Methyltridecane	C <sub>14</sub> H <sub>30</sub>	—	0.01	0.01	0.01	1349	
51	Octadecane	C <sub>18</sub> H <sub>38</sub>	0.02	0.29	0.03	0.07	1810	
52	10-Methylnonadecane	C <sub>20</sub> H <sub>42</sub>	—	0.01	—	—	1945	
53	Octacosane	C <sub>28</sub> H <sub>58</sub>	0.13	0.14	0.01	0.05	2804	
54	3,8-Dimethyldecane	C <sub>12</sub> H <sub>26</sub>	0.02	0.02	0.03	0.02	1086	
55	Camphene	C <sub>10</sub> H <sub>16</sub>	0.94	0.25	0.03	0.11	943	
56	Hexadecane	C <sub>16</sub> H <sub>34</sub>	0.37	0.29	0.09	0.33	1612	[20]
57	5-Methyltetradecane	C <sub>15</sub> H <sub>32</sub>	—	0.06	—	0.05	1448	
58	4-Methyltetradecane	C <sub>15</sub> H <sub>32</sub>	—	0.01	—	0.02	1448	
59	3-Methyltetradecane	C <sub>15</sub> H <sub>32</sub>	0.41	0.02	—	0.06	1448	
60	Eicosane	C <sub>20</sub> H <sub>42</sub>	0.55	0.14	0.06	0.19	2009	
61	Tetratriacontane	C <sub>34</sub> H <sub>70</sub>	0.12	0.03	—	0.01	3401	
62	4-Methylpentadecane	C <sub>16</sub> H <sub>34</sub>	0.02	0.36	—	0.08	1548	
63	2,6,10,15-Tetramethylheptadecane	C <sub>21</sub> H <sub>44</sub>	0.01	0.02	—	—	1852	
64	Nonadecane	C <sub>19</sub> H <sub>40</sub>	0.01	0.08	0.04	0.07	1910	
65	8-Hexylpentadecane	C <sub>21</sub> H <sub>44</sub>	—	0.01	0.01	0.07	2045	
66	2,2,4,6,6-Pentamethylheptane	C <sub>12</sub> H <sub>26</sub>	0.87	0.63	1.48	0.83	981	[20]
67	2,3-Dimethylundecane	C <sub>13</sub> H <sub>28</sub>	—	0.01	—	—	1185	
68	2-Bromo dodecane	C <sub>12</sub> H <sub>25</sub> Br	0.03	0.12	0.05	0.15	1446	
69	(9E)-9-octadecene	C <sub>18</sub> H <sub>36</sub>	—	0.01	—	—	1818	
70	Heptacosane	C <sub>27</sub> H <sub>56</sub>	—	0.01	—	—	2705	
71	2,6,10,14-Tetramethylhexadecane	C <sub>20</sub> H <sub>42</sub>	0.45	1.13	0.02	0.53	1753	
72	2,2,4,4,6,8-Heptamethylnonane	C <sub>16</sub> H <sub>34</sub>	—	0.02	—	—	1294	
73	Pentadecane	C <sub>15</sub> H <sub>32</sub>	—	0.32	0.01	—	1512	[30]
74	HMN	C <sub>16</sub> H <sub>34</sub>	0.04	—	0.03	—	1294	
75	Undecane	C <sub>11</sub> H <sub>24</sub>	0.02	—	0.04	—	1115	[20]
76	2,6,11-Trimethyldodecane	C <sub>15</sub> H <sub>32</sub>	0.02	—	0.01	—	1320	
77	11-Methyldodecane	C <sub>13</sub> H <sub>28</sub>	0.01	—	—	—	1249	
78	Heneicosane	C <sub>21</sub> H <sub>44</sub>	0.02	—	0.01	0.06	2109	
79	2-Carene	C <sub>10</sub> H <sub>16</sub>	0.01	—	—	—	948	
80	gamma-Terpinen	C <sub>10</sub> H <sub>16</sub>	0.21	—	—	—	998	
81	1-Tridecene	C <sub>13</sub> H <sub>26</sub>	1.01	—	0.02	—	1304	
82	5-Methyl-5-propylnonane	C <sub>13</sub> H <sub>28</sub>	0.02	—	0.01	—	1229	
83	2,5-Dimethyldecane	C <sub>12</sub> H <sub>26</sub>	0.03	—	0.01	—	1086	

TABLE 2: Continued.

Number	Compound name	Molecular formula	Relative content/%				RI value	Literature
			Hebei	Henan	Sichuan	Fujian		
84	2,4-Dimethyldecane	C <sub>12</sub> H <sub>26</sub>	0.01	—	—	—	1086	
85	Docosane	C <sub>22</sub> H <sub>46</sub>	0.01	—	0.03	—	2208	
86	Benzene, 1-methyl-2-(phenylmethyl)-	C <sub>14</sub> H <sub>14</sub>	—	—	0.02	—	1580	
87	1-Benzyl-3-methylbenzene	C <sub>14</sub> H <sub>14</sub>	—	—	0.02	—	1580	
88	Dotriacontane	C <sub>32</sub> H <sub>66</sub>	—	—	0.01	—	3202	
89	2,3,7-Trimethyldecane	C <sub>13</sub> H <sub>28</sub>	—	—	0.01	—	1121	
90	2,5-Dimethylundecane	C <sub>13</sub> H <sub>28</sub>	—	—	0.03	—	1185	
91	1-Sec-butyl-1-(2-methylbutyl)cyclopropane	C <sub>12</sub> H <sub>24</sub>	—	—	0.02	—	1062	
92	2,6,11,15-Tetramethylhexadecane	C <sub>20</sub> H <sub>42</sub>	—	—	0.01	0.02	1753	
93	4-Ethylundecane	C <sub>13</sub> H <sub>28</sub>	—	—	0.01	—	1249	
94	(5E)-5-octadecene	C <sub>18</sub> H <sub>36</sub>	—	—	0.01	0.01	1818	
95	3-Ethyl-3-methyldecane	C <sub>13</sub> H <sub>28</sub>	—	—	0.01	—	1229	
96	5-Isobutylnonane	C <sub>13</sub> H <sub>28</sub>	—	—	0.02	0.04	1185	
97	5-Butylnonane	C <sub>13</sub> H <sub>28</sub>	—	—	0.01	0.04	1249	
98	2,2-Dimethyldecane	C <sub>12</sub> H <sub>26</sub>	—	—	—	0.04	1130	
99	2-Methyltetradecane	C <sub>15</sub> H <sub>32</sub>	—	—	—	0.01	1448	
100	2-Methylhexadecane	C <sub>17</sub> H <sub>36</sub>	—	—	—	0.01	1647	
101	9-Methylnonadecane	C <sub>20</sub> H <sub>42</sub>	—	—	—	0.01	1945	
102	2-Methyl-6-propyldodecane	C <sub>16</sub> H <sub>34</sub>	—	—	—	0.01	1483	
103	Decamethylcyclopentasiloxane	C <sub>10</sub> H <sub>30</sub> O <sub>5</sub> Si <sub>5</sub>	—	—	—	0.01	1034	
104	Tetratetracontane	C <sub>44</sub> H <sub>90</sub>	—	—	—	0.02	4395	
105	2,2-Dimethylundecane	C <sub>13</sub> H <sub>28</sub>	—	—	—	0.27	1229	
106	4-Methyldodecane	C <sub>13</sub> H <sub>28</sub>	—	—	—	0.02	1249	
107	Undecylcyclohexane	C <sub>17</sub> H <sub>34</sub>	—	—	—	0.01	1775	
<i>Categories</i>								
108	Nickel tetracarbonyl	C <sub>4</sub> NiO <sub>4</sub>	0.09	2.20	0.16	0.29	—	
109	4,7-Dimethylbenzofuran	C <sub>10</sub> H <sub>10</sub> O	0.02	—	—	—	1244	
110	Hydroxylamine	H <sub>3</sub> NO	2.42	4.88	3.51	—	—	
111	4-Hexen-3-one	C <sub>6</sub> H <sub>10</sub> O	5.66	—	—	—	762	
112	2-Undecanone	C <sub>11</sub> H <sub>22</sub> O	—	0.16	—	—	1251	
113	Didecyl ether	C <sub>20</sub> H <sub>42</sub> O	—	0.07	—	0.03	2085	
114	Oxygen	O <sub>2</sub>	—	3.57	—	25.26	—	
115	Carbon monoxide	CO	—	—	0.06	0.10	—	
116	p-(1-Propenyl)anisole	C <sub>10</sub> H <sub>12</sub> O	—	—	0.01	—	1190	[30]
117	2-Cyclohexen-1-one	C <sub>6</sub> H <sub>8</sub> O	—	—	—	0.01	873	

Note. “—” means not detected. In Table 2, the constituents marked red were first detected from *T. fuciformis*.

pentafluoropropionate and formic acid, and ethenyl ester, of which the relative content of formic acid, ethenyl ester was as high as 25.12%. These unique components identified for corresponding regions would be used to distinguish the samples from this region from other regions.

Volatile acids are usually derived from the oxidation or biosynthesis of fatty acids [36, 37]. In this research, 7 kinds of acid compounds were detected in *T. fuciformis*. Acetic acid is a common acid with a fishy smell of oil [38] and exists in *T. fuciformis* at a high relative content (35.36%~49.42%). However, due to its high aroma threshold, it has little contribution to the overall odor of *T. fuciformis*.

Volatile alcohols in plants mainly come from the decomposition of secondary hydroperoxides of fatty acids and the reduction of sugars and amino acids [36]. Most alcohols are generally floral and fruity aromas [39]. According to the above GC-MS analysis results, 10 kinds of alcohol were detected, including 7 kinds in Hebei, 3 kinds in Henan, 4 kinds in Fujian, and 1 kind in Sichuan. Not only that, the

relative content of volatile alcohols was also high in the Hebei region. 2-ethyl-1-decanol, 1-octen-3-ol, eucalyptol, linalol, and isotridecyl alcohol were special to the samples of the Hebei region, while isopentyl alcohol to the samples in Fujian. These unique volatile components of different samples might be taken as a mark for the distinguishment of different regions.

Aldehyde compounds are mainly derived from fatty acid oxidation and amino acid metabolism [40], and their aroma thresholds are usually low. Therefore, it usually plays an important role in the overall aroma, although the content of aldehyde compounds is low [41]. There were 10 kinds of aldehydes in *T. fuciformis*, and 8 species were detected in Hebei province, nine in Henan province, seven in Fujian province, and three in Sichuan province. Among them, hexanal, nonanal, and pentanal were the common aldehyde volatile components of *T. fuciformis*, while 5-methyl-2-furancarboxaldehyde and 2-ethyl-1-pentanol were the unique aldehyde volatile components of Henan and Fujian provinces, respectively.

Besides, *T. fuciformis* also included phenols, ketones, furans, and so on. In addition, gases were detected in *T. fuciformis*. Because the whole detection environment was gaseous, the components in the air may have been detected in the sample, such as oxygen and carbon monoxide. But these gases are colorless and tasteless and did not affect the aroma quality of *T. fuciformis*. Among them, the detected ketones included 4-hexen-3-one, 2-undecanone, and 2-cyclohexen-1-one, and the relative content of 4-hexen-3-one, a unique component in Hebei samples, was relatively high. Nickel tetracarbonyl was the common component detected in all the 4 regions, while hydroxylamine was also detected in the samples from considerate regions except Fujian.

**3.2.2. Analysis of Volatile Components of *T. fuciformis* among Different Regions.** In Figure 3, there was no obvious difference in the types of volatile substances contained in *Tremella* among the 4 regions. The most abundant volatile component type was hydrocarbons, which were about 3 times as many as the other types. By comparing these substances among the samples from the 4 regions, it could be found that more types of hydrocarbons were detected in the *T. fuciformis* from Fujian, while more aldehyde types and acid types were detected in the Henan samples, more alcohol types from Hebei samples, and more ester from Sichuan samples.

In general, the relative contents of acid in the 4 regions (in Figure 4) were the highest of the detected volatile components, followed by aldehydes. However, the proportion varied from region to region. Also, it can be seen that the *T. fuciformis* from Henan owned more contents of acids while the Hebei samples had more aldehyde and Sichuan had more esters.

**3.3. ROAV Analysis of Key Aroma Compounds.** ROAV is used as one common index, which may range from 0 to 100 and reflects the aroma contribution degree of each volatile component. The higher the ROAV value of the compound, the greater the contribution of the compound to the overall odor of the sample [42–44]. By referring to the researched 29 compounds with the given aroma threshold values from relevant literature and combining, the corresponding ROAV analysis results were calculated and are shown in Table 3.

Overall, there were 8 compounds (ROAV  $\geq 1$ ) including 1-octen-3-ol, heptanal, octanal, nonanal, pentanal, hexanal, butyrolactone, and 2-carene, which were taken as the key aroma compounds of *T. fuciformis*. Among them, hexanal and nonanal were the common key aroma compounds and could be used as the characteristic identification components of *T. fuciformis*. As a basic product of the oxidative decomposition of linoleic acid, hexanal is a common volatile oil with the fragrance of green, grass, and fruit [51], contributing greater than the others to the overall aroma of *T. fuciformis*. Nonanal is also a common aroma compound with the fragrance of flowers, fat, and wax, and a low threshold value, and it offers people a pleasant feeling [52]. 1-Octene-3-ol, also known as agaritol with the aroma of fresh

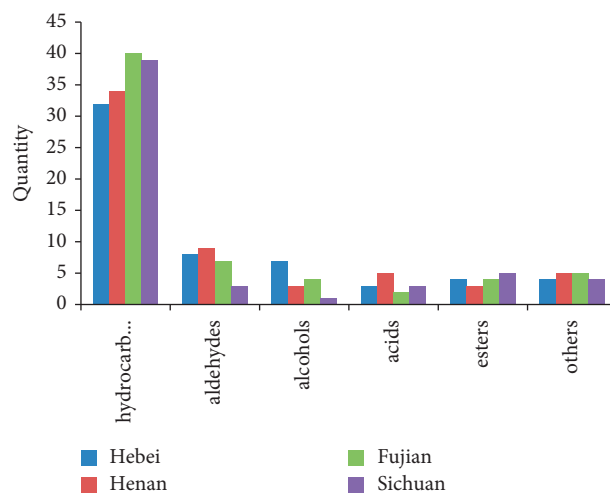


FIGURE 3: Volatile components types of *T. fuciformis* from different producing areas.

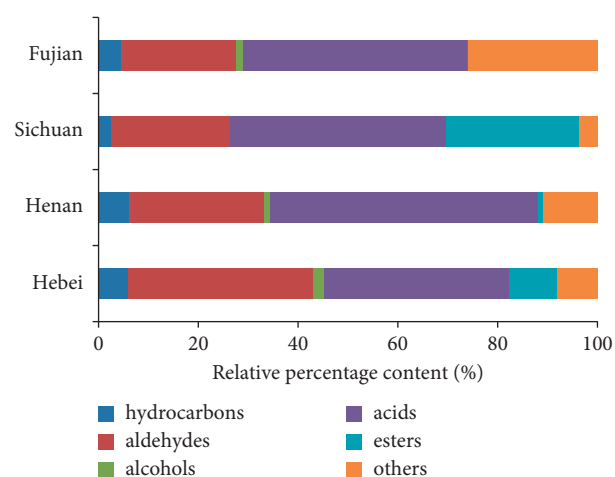


FIGURE 4: Relative contents of volatile compounds in *T. fuciformis*.

mushroom, licorice, and rose, was the unique key aroma compound of Hebei samples. This compound was mainly used as pharmaceutical raw materials and in aromatics [53]. Besides, butyrolactone generally has the fragrance characteristics of coconut or peach [40, 42], while heptanal has the odor of fat or fish [36]. These substances play an important role in the overall fragrance of *T. fuciformis*.

In Hebei *T. fuciformis*, all the 8 key aroma compounds were discovered, of which butyrolactone (ROAV = 100) is the compound with the highest ROAV, and it can be used as the aroma base of *T. fuciformis*, followed by hexanal, nonanal, octanal, 2-carene, 1-octen-3-ol, pentanal, and heptanal. But on the other hand, 1-octen-3-ol and 2-carene were the special compounds of these samples and could be used to distinguish the Hebei samples from the other 3 regions. The modified aroma compounds were eucalyptol, linalool, and  $\gamma$ -butyrolactone, which were also unique for Hebei samples. The potential aroma compound, nonanoic acid, was unique for the Hebei sample, while the other 3 compounds, acetic acid, dodecane, and hexadecane, were common for all the collected *T. fuciformis*.

TABLE 3: ROAV value of 29 components in *T. fuciformis* from different regions.

Number	Compound name	Aroma threshold ( $\mu\text{G/L}$ ) [31, 45–50]	ROAV			
			Hebei	Henan	Sichuan	Fujian
<i>Alcohols</i>						
1	1-Hexanol	250	<0.1	—	—	<0.1
2	1-Octen-3-ol	1	5.5	—	—	—
3	Eucalyptol	1.3	0.22	—	—	—
4	Linalol	1.5	0.48	—	—	—
5	Pentyl alcohol	4000	<0.1	<0.1	—	<0.1
6	Isopentyl alcohol	120	—	—	—	<0.1
<i>Aldehydes</i>						
7	Hexanal	4.5	87.97	100	100	100
8	Furfural	3000	<0.1	<0.1	—	—
9	Heptanal	3	2.07	6.19	—	—
10	Octanal	0.7	21.3	1.02	—	1.19
11	Benzeneacetaldehyde	4	<0.1	<0.1	—	—
12	Nonanal	1	37.34	3.39	1.33	22.08
13	Benzaldehyde	350	<0.1	<0.1	—	<0.1
14	Pentanal	20	3.65	0.34	<0.1	0.24
<i>Acids</i>						
15	Acetic acid	22000	<0.1	<0.1	<0.1	<0.1
16	Nonanoic acid	3000	<0.1	—	—	—
17	Octanoic acid	500	—	—	<0.1	—
18	Pentanoic acid	3000	—	—	—	—
19	Heptanoic acid	100	—	—	0.25	—
20	Hexanoic acid	3000	—	—	—	<0.1
<i>Esters</i>						
21	Butyrolactone	0.88	100	—	22.97	2.6
22	gamma-Butyrolactone	100	0.81	—	—	—
23	n-Hexyl formate	19800	—	<0.1	—	<0.1
<i>Hydrocarbons</i>						
24	Dodecane	2040	<0.1	<0.1	<0.1	<0.1
25	Tetradecane	1000	<0.1	<0.1	—	<0.1
26	Hexadecane	300	<0.1	<0.1	<0.1	<0.1
27	2-Carene	0.01	14.47	—	—	—
<i>Others</i>						
28	2-Undecanone	255	—	<0.1	—	—
29	p-(1-Propenyl)anisole	15	—	—	<0.1	—

Note. “—” means not detected.

The ROAV value of hexanal in the samples from Sichuan, Henan, and Hebei was 100, indicating that this component contributed the most to the aroma of tremella from these three regions. For the *T. fuciformis* of Henan province, there were 4 key aroma compounds, and hexanal was the highest, followed by heptanal, nonanal, and octanal. However, the samples from Henan province lacked butyrolactone, compared with the other three regions, so the compound could be used to distinguish other samples from Henan province. Pentanal and 2-undecanone were the modified and potential aroma compound in Henan province.

Three key volatile aroma compounds with threshold values were identified in Sichuan samples, which were hexanal, butyrolactone, and nonanal from high to low. Heptanoic acid was the modified aroma compound of *T. fuciformis*, while octanoic acid and p-(1-propenyl) anisole were the potential aroma compounds unique to Sichuan samples. On the other hand, octanal was a key aroma compound for the samples from Hebei, Henan, and Fujian, but not for the Sichuan samples.

Four kinds of key volatile aroma compounds detected in Fujian samples with the ROAV from high to low were hexanal, nonanal, octanal, and butyrolactone. The modified aroma compound was pentanal as well as Henan samples, and the potential aroma compounds special to Fujian samples were isopentyl alcohol and hexanoic acid.

#### 4. Conclusion

The difference between *T. fuciformis* from different regions existed, and the electronic nose is a good technology to distinguish *T. fuciformis* from different regions. During the determination, the sensors of C<sub>1</sub>, C<sub>3</sub>, C<sub>4</sub>, C<sub>5</sub>, C<sub>6</sub>, C<sub>8</sub>, and C<sub>9</sub> contributed much more to distinguish the overall odor of *T. fuciformis*. Electronic nose (PCA) combined with GC-MS (ROAV) suggested that the types and contents of volatile aldehydes might contribute significantly to the aroma degree of *T. fuciformis* from different regions. In the PCA results, the samples from Hebei and Henan were distributed on the right of the origin of coordinates. On the contrary, the



samples from Sichuan and Fujian were and distributed on the left. In ROAV, aldehydes from Hebei and Henan provinces had more kinds of aroma components, higher content, and higher aroma activity. 1-Octen-3-ol, heptanal, octanal, nonanal, pentanal, hexanal, butyrolactone, and 2-carene were the key aroma compounds contributing to the aroma of *T. fuciformis*. 1-Octen-3-ol, 2-carene, eucalyptol, linalool,  $\gamma$ -butyrolactone, and nonanoic acid were special to the Hebei samples, while octanoic acid and *p*-(1-propenyl) anisole were special to the Sichuan samples, as well as isopentyl alcohol and hexanoic acid were special to the Fujian samples. On the other hand, butyrolactone was the missing aroma compound for the Henan samples, while octanal was for the Sichuan samples [54].

### Data Availability

All the data used are included in this paper.

### Conflicts of Interest

The authors declare that there are no conflicts of interest.

### Acknowledgments

This work was supported by the National Key R&D Program of China (Project no. 2018YFD0400200), the Major Public Welfare Projects in Henan Province (201300110200), and the Key Project in Science and Technology Agency of Henan Province (212102110019).

### References

- [1] Z. Yin, Z. Liang, C. Li, J. Wang, C. Ma, and W. Kang, "Immunomodulatory effects of polysaccharides from edible fungus: a review," *Food Science and Human Wellness*, vol. 10, no. 4, pp. 393–400, 2021.
- [2] Z. Yin, D. Sun-Waterhouse, J. Wang, C. Ma, G. I. N. Waterhouse, and W. Kang, "Polysaccharides from edible fungi *Pleurotus* spp: advances and perspectives *pleurotus* spp: advances and perspectives," *Journal of Future Foods*, vol. 1, no. 2, pp. 128–140, 2021.
- [3] Y. Zhang, D. Wang, Y. Chen et al., "Healthy function and high valued utilization of edible fungi," *Food Science And Human Wellness*, vol. 10, no. 4, pp. 408–420, 2021.
- [4] T. Ma, L. Y. Zhang, Z. Lin et al., "Analysis and evaluation on main nutritional components in different tremella products," *Edible Fungi of China*, vol. 38, no. 11, pp. 57–60, 2019.
- [5] W. X. Liu, B. Du, W. D. Ma, and T. Sun, "Study and actualities of tremella fuciformis Standards in China," *Farm Products Processing*, vol. 02, 2015.
- [6] T. J. Barzee, L. Cao, Z. Pan, and R. Zhang, "Fungi for future foods," *Journal of Future Foods*, vol. 1, no. 1, pp. 25–37, 2021.
- [7] C. Xu, J. Y. Diao, and S. M. Wang, "Recent progress in pharmacological studies of polysaccharide from tremella fuciformis berk," *Pharmacy Today*, vol. 28, no. 03, pp. 207–210, 2018.
- [8] B. B. Li, H. Long, E. H. Wu et al., "Protective effects of polysaccharides extracted from tremella on cell membrane and sugar metabolism enzymes of freeze-dried *Lactobacillus plantarum*," *Modern Food Science and Technology*, vol. 37, no. 11, pp. 85–95, 2021.
- [9] L. G. Liu, S. J. Ma, P. Han, B. Che, L. Lin, and Z. Y. Du, "Optimization of extracting *Tremella fuciform* polysaccharide and its protection against SDS-induced damage of HaCaT cells," *Edible Fungi of China*, vol. 40, no. 1, pp. 97–102, 2021.
- [10] J. W. Wang, D. Q. Yin, X. Y. Li et al., "Preparation of quercetin microemulsion with *Tremella fuciformis* polysaccharide as emulsifier," *Chinese herbal medicine*, vol. 52, no. 02, pp. 378–385, 2021.
- [11] Y. H. Wang, Q. Wu, Y. L. Chi, K. Yao, and D. Y. Jia, "Properties of crude polysaccharides extracted from *Tremella fuciformis* by acid, alkali and enzyme-assisted methods," *Food Science and Technology*, vol. 44, no. 04, pp. 200–204, 2019.
- [12] M. Yang, Z. Zhang, Y. He, C. Li, J. Wang, and X. Ma, "Study on the structure characterization and moisturizing effect of *Tremella* polysaccharide fermented from GCMCC5.39," *Food Science and Human Wellness*, vol. 10, no. 4, pp. 471–479, 2021.
- [13] X. Li, H. Xu, J. Deng et al., "HS-SPME/GC-MS analysis on volatile components of *tilia tremella* with different cultivation methods," *Edible Fungi of China*, vol. 38, no. 01, pp. 45–50+63, 2019.
- [14] D. S. Zhu, X. F. Wu, L. N. Wang Lina et al., "Studies on volatile compounds of red sea bream at cold storage by electronic nose coupled with and HS-SPME/GC-MS," *Journal of Chinese Institute of Food Science and Technology*, vol. 16, no. 12, pp. 227–234, 2016.
- [15] H. M. Zhou, S. L. Zhang, Y. F. Hao et al., "Analysis of major flavor components of Tuotuo pork, a traditional meat product ill Liangshan, southwest China's Sichuan, by HS-SPME-GC-MS-O combined with electronic nose," *Food Science*, vol. 42, no. 2, pp. 218–226, 2021.
- [16] T. T. Zhang, X. L. Guo, and X. Y. Huang, "GC-MS analysis and antioxidant and antimicrobial properties of volatile oil from flos magnoliae," *Food Science*, vol. 37, no. 10, pp. 144–150, 2016.
- [17] X. W. Yan, Y. P. Zhong, S. S. Lu, and Q. X. Meng, "Pattern recognition analysis of tieguanyin oolong tea and ruanzhi oolong tea based on the volatile components and chemometrics methods," *Food Research and Development*, vol. 40, no. 20, pp. 155–163, 2019.
- [18] J. H. Lu, Y. L. Zhang, J. Liang, L. Zhang, and H. W. Zhang, "Effects of three drying processes on volatile substances and sensory characteristics in lentinus edodes," *Science and Technology of Food Industry*, vol. 40, no. 24, pp. 262–269, 2019.
- [19] L. J. Fu, G. Yang, L. Liu et al., "Analysis of volatile components of *auricularia auricula* from different origins by GC-MS combined with electronic nose," *Journal of Food Quality*, vol. 2020, Article ID 8858093, 9 pages, 2020.
- [20] Q. Ma, J. F. Bou, L. Fang et al., "Effect of drying method on volatile components of *Pleurotus eryngii* analyzed by combined use of GC-MS and electronic nose," *Food Science*, vol. 40, no. 14, pp. 276–282, 2019.
- [21] S. Y. Wang, F. Zhao, G. H. Rao et al., "Origin difference analysis of aroma components in jasmine tea based on electronic nose and ATD-GC-MS," *Science and Technology of Food Industry*, vol. 42, no. 15, pp. 234–239, 2021.
- [22] K. Lu, X. Y. Wang, X. J. sun et al., "Analysis of the volatile components of fermented hot pepper from different varieties grown in guizhou by electronic nose combined with SPME-GC-MS," *Food Science*, vol. 39, no. 04, pp. 199–205, 2018.
- [23] X. Fan and X. P. Cui, "Analysis of aroma compounds of different peach nesh types during postharvest storage by headspace s01id-phase microextraction combined wim gas

- chromatography-mass spectrometry and electronic nose," *Food Science*, vol. 42, no. 20, pp. 222–229, 2021.
- [24] C. Y. Liu, D. L. Fang, Y. H. Zhang, H. H. Zheng, Q. H. Hiu, and L. Y. Zhao, "Effect of cooking methods on volatile flavor compounds in lentinus edodes soups analyzed by electronic nose and SPME-GC-MS," *Science and Technology of Food Industry*, vol. 41, no. 20, pp. 6–11, 2020.
- [25] C. M. Yin, X. Z. Fan, Z. Fan, D. F. Shi, and H. Gao, "Analysis of volatile flavor compounds in different *Pleurotus* species using HSSPME-GC-MS," *Food Science*, vol. 39, no. 16, pp. 240–246, 2018.
- [26] Q. L. Xu, J. T. Guo, Z. J. Jiang et al., "Analysis and identification of aroma different habitats by HS-SPME-components of tartary buckwheat tea from GC-MS combined with electronic nose," *Food and Fermentation Industries*, vol. 43, no. 08, pp. 233–239, 2017.
- [27] W. Jiao, Y. Xu, H. Zhang et al., "Cheddar cheese with different ripening times: analysis of volatile aroma components and electronic nose discrimination," *Food Science*, vol. 41, no. 20, pp. 175–183, 2020.
- [28] Y. Liu, L. Q. Ge, and Y. X. Wang, "Analysis of volatile compounds and geographical origin discrimination of Lu mountain clouds-mist tea by principal components analysis," *Food Science*, vol. 38, no. 24, pp. 60–67, 2017.
- [29] C. K. Xia, Q. Q. Song, and C. W. Fang, "Distinguish moutan cortex from different producing areas based on electronic nose technology," *Chinese Journal of Modern Applied Pharmacy*, vol. 36, no. 21, pp. 2633–2637, 2019.
- [30] Y. P. Zhang, T. G. Liao, B. H. He, Y. W. Nui, J. C. Zhu, and M. F. Wang, "Identification of characteristic aroma compounds in prunes using gas chromatography-olfactometry, odor activity value and S-curve method," *Food Science*, vol. 41, no. 22, pp. 271–278, 2020.
- [31] H. Z. Cheng, Z. P. Cai, J. Wang et al., "Combined use of GC-MS, GC-O and electronic nose technology to evaluate the aroma characteristics of passion fruit wine," *Food Science*, vol. 42, no. 6, pp. 256–264, 2021.
- [32] C. Chen, Z. Liu, K. Huang, and H. X. Tian, "Effects of different processing methods on the flavor of dairy fan evaluated using GC-MS, GC-O and electronic nose," *Food Science*, vol. 42, no. 16, pp. 108–117, 2021.
- [33] X. Liu, B. D. Mu, M. Ju, G. H. Li, C. X. Piao, and M. X. Ciu, "Characterization of flavor components of dry-cured ham with different salt substitute formulations using solid phase microextraction-gas chromatography-mass spectrometry, electronic nose and electronic tongue," *Food Science*, vol. 43, no. 06, pp. 246–256, 2022.
- [34] Z. Q. Zhang, M. W. Zang, K. H. Zhang et al., "Effect of key processing steps on formation of volatile flavor components in steamed pork with rice," *Food Science*, vol. 40, no. 4, pp. 222–228, 2019.
- [35] L. Huang, Z. Sun, X. Q. Zeng, D. D. Pan, J. He, and J. L. Shen, "Effects of multi-ingredients for nitrite on the volatile flavor compounds in cured meat," *Journal of Chinese Institute of Food Science and Technology*, vol. 21, no. 03, pp. 324–333, 2021.
- [36] D. Melucci, A. Bendini, F. Tesini et al., "Rapid direct analysis to discriminate geographic origin of extra virgin olive oils by flash gas chromatography electronic nose and chemometrics," *Food Chemistry*, vol. 204, pp. 263–273, 2016.
- [37] L. Fu, Y. L. Liu, X. Q. Gao, B. J. Yang, and S. W. Song, "Analysis of volatile flavor compounds in different sterilization sauce beef with HSPME and GC-MS," *Modern Animal Husbandry*, vol. 4, no. 02, pp. 18–23, 2020.
- [38] H. Wang, Y. H. Zhao, and K. Yang, "Comparative analysis of volatile profiles in kernel oils of ten Korean pine (*Pinus koraiensis*) varieties by headspace solid phase microextraction-gas chromatography-mass spectrometry and electronic nose," *Food Science*, vol. 42, no. 18, pp. 178–184, 2021.
- [39] R. G. Jiang, Y. Huang, Y. L. Jin et al., "Analysis of characteristic aroma components of different grades of yellow tea," *Food Science*, vol. 42, no. 16, pp. 89–98, 2021.
- [40] T. T. Li, M. Z. Huang, W. Y. Tang, Q. Y. Li, and K. N. Kang, "Determination of volatile components in *Rosa roxburghii* Tratt juice and the analysis of its contribution for aroma," *Food and Fermentation Industries*, vol. 47, no. 04, pp. 237–246, 2021.
- [41] D. L. Li, Y. R. Weng, L. P. Du, C. Wang, L. J. Ma, and D. G. Xiao, "Detection of volatile compounds in different brands of Pu-erh tea using electronic nose and GC-MS," *Food and Fermentation Industries*, vol. 45, no. 03, pp. 237–245, 2019.
- [42] T. Wang, Y. N. Shi, X. Li, and A. X. Hang, "Analysis of the effect of curing time on the volatile flavor compounds of dahe black pig ham by SPME-GC-MS and ROAV," *Science and Technology of Food Industry*, vol. 42, no. 18, pp. 317–324, 2021.
- [43] Y. Zhang, S. Zhang, W. Fan, M. Duan, Y. Han, and H. Li, "Identification of volatile compounds and odour activity values in quinoa porridge by gas chromatography-mass spectrometry," *Journal of the Science of Food and Agriculture*, vol. 99, no. 8, pp. 3957–3966, 2019.
- [44] N. Zhao, X. Y. Wei, M. T. Fan et al., "Analysis of volatile components of kiwifruit wines made from different cultivars using solid phase microextraction-gas chromatography-mass spectrometry combined with electronic nose," *Food Science*, vol. 40, no. 22, pp. 249–255, 2019.
- [45] D. X. Liu, Z. H. Tian, Y. L. Zhao, C. Liu, and L. Yu, "Analysis and comparison of the volatile components in common buckwheat different parts with SPME-GC-MS," *The Food Industry*, vol. 42, no. 01, pp. 310–315, 2021.
- [46] M. Q. Fan, F. Yang, H. F. Jia, L. Xiao, and G. Q. He, "Effects of pixian douban and douchi on the volatile flavor compounds of fried pork with salted pepper based on GC-MS," *Science and Technology of Food Industry*, vol. 42, no. 13, pp. 274–283, 2021.
- [47] M. Q. Wang, Y. Zhu, Y. Zhang, J. Shi, Z. Lin, and H. P. Lu, "Analysis of volatile components and key aroma components of 'Qingxiang' green tea," *Food Science*, vol. 40, no. 22, pp. 219–228, 2019.
- [48] C. Schueuermann, C. C. Steel, J. W. Blackman et al., "A GC-MS untargeted metabolomics approach for the classification of chemical differences in grape juices based on fungal pathogen," *Food Chemistry*, vol. 270, pp. 375–384, 2019.
- [49] X. A. Chen, H. T. Cai, J. Y. Liu, N. Tang, S. X. Chen, and A. M. Zhou, "Analysis of volatile components in laoxianghuang during fermentation by electronic nose, GC-MS and GC-IMS," *Science and Technology of Food Industry*, vol. 42, no. 12, pp. 70–80, 2021.
- [50] Z. H. Han, S. Guo, T. Huang et al., "Difference analysis of volatile flavor metabolite in lactobacillus beverage fermented with complex probiotics," *Journal of Chinese Institute of Food Science and Technology*, vol. 21, no. 03, pp. 300–314, 2021.
- [51] H. W. Liu and M. L. Zhang, "Analysis of volatile components in sweet fermented oat produced by inoculated and natural

- fermentation,” *Food Science*, vol. 42, no. 20, pp. 203–207, 2021.
- [52] K. He, J. M. Yun, Y. Bi, R. Wang, Y. Q. Mao, and S. J. Wu, “Changes of volatile flavor components in *Hysizygnus marmoreus* packaged with nano-film during storage,” *Food Science*, vol. 42, no. 20, pp. 160–166, 2021.
- [53] Q. Lu, F. Liu, and J. Bao, “Volatile components of American silver carp analyzed by electronic nose and MMSE-GC-MS-O,” *Journal of Food Biochemistry*, vol. 43, no. 3, Article ID e13006, 2019.

## Research Article

# Response Surface Methodology for Optimization of L-Arabinose/Glycine Maillard Reaction through Microwave Heating

Qingru Xiang <sup>1</sup>, Tao Feng <sup>2</sup>, Qiang Su <sup>3</sup> and Lingyun Yao <sup>2</sup>

<sup>1</sup>School of Life Science and Technology, Xinjiang University, No. 777 Huarui Road, Ürümqi 830017, China

<sup>2</sup>School of Perfume and Aroma Technology, Shanghai Institute of Technology, No. 100 Haiquan Road, Shanghai 201418, China

<sup>3</sup>Yunnan Yangrui Technology Group Co., Ltd, No. 80 Chunman Avenue, Kunming 650217, China

Correspondence should be addressed to Tao Feng; [fengtao@sit.edu.cn](mailto:fengtao@sit.edu.cn)

Received 22 February 2022; Accepted 25 March 2022; Published 13 April 2022

Academic Editor: Wen yi Kang

Copyright © 2022 Qingru Xiang et al. This is an open access article distributed under the Creative Commons Attribution License, which permits unrestricted use, distribution, and reproduction in any medium, provided the original work is properly cited.

L-Arabinose is a low-calorie sweetener that inhibits sucrose absorption by inhibiting sucrase activity in the human intestinal tract. Response surface methodology (RSM) was applied to optimize the processing parameters of the L-arabinose/glycine Maillard reaction to improve the browning degree and antioxidant activity of Maillard reaction products (MRPs) through microwave heating. The effect of heating time, volume ratio of propylene glycol to double distilled water (ddH<sub>2</sub>O), and pH on MRPs was evaluated. A change in the volume ratio of propylene glycol to ddH<sub>2</sub>O, heating time, and pH was associated with a largely changed browning degree and reducing power of the MRPs. RSM predicted optimum conditions that under substrates of L-arabinose/glycine at a ratio of 2:1 (w/w) and concentration of 10% (w/v), a heating time of 7.44 min, volume ratio of propylene glycol to ddH<sub>2</sub>O 0.93, and pH 10.44 were optimum conditions for the Maillard reaction. The predicted data from the optimum reaction conditions coincided well with the experiment results. The main flavor of MRPs is roasted aroma, and the emulsifying ability of MRPs was 0.367 at 500 nm by microwave heating under the optimal Maillard reaction conditions. MRPs derived from L-arabinose and D-glucose had similar activities. However, a slightly greater activity was found with MRP derived from L-arabinose-glycine with a more volume. This study provided a new direction for the development of sweeteners in the future.

## 1. Introduction

The Maillard reaction is a series of complex reactions that occur between the free amino groups of amino acids, peptides or proteins, and carbonyl groups of sugar, especially reducing sugars, to produce the Maillard reaction products (MRPs) [1]. Under different reaction conditions, the reaction pathway and the mechanism will be greatly different, and most of the formed products have a specific flavor and color. MRPs contain volatile substances including low-molecular-weight hydrocarbons, alcohols, aldehydes, ketones, esters, ethers, and heterocyclic compounds, and some large-molecular-weight materials containing polyphenols, peptide polymers, melanoidins, and so on. Melanoidins (melanoidin) or melanoidins (melanoprotein) are brown part of the Maillard reaction in the ultimate stage polymer and copolymer containing nitrogen and are part of the brown macromolecular substances.

Melanoidins (melanoidin) or melanoidins (melano-protein) are the most common high-molecular-weight materials that are part of the brown macromolecular substances [2]. The time for the completion of a traditional Maillard reaction is generally some hours, but that could be reduced to 2–10 minutes if microwave heating is properly applied [3, 4]. Zhao et al. [5] studied the Maillard reactions of different neutral amino acids with glucose and fructose under microwave conditions and found that both acidic and alkaline amino acids had strong characteristics and strong flavor sensation.

The Maillard reaction in aqueous systems has been used in the manufacture of food pigments for a long time, and flavors and MRPs are needed in certain food products with a certain emulsification, such as instant coffee products. This study suggests the feasibility of obtaining new compounds with potentially desirable characteristics through the Maillard reaction in ethanolic systems. Further investigation

in this area is likely to be valuable. Z.-c. Tu et al. [6] described that the UV absorbance, browning intensity, and antioxidant activities as well as the emulsifying activity and emulsion stability of the Maillard reaction products (MRPs) were increased in accordance with the raise of microwave treatment power and time. The reaction time of microwave treatment is much shorter than those using traditional methods, suggesting that microwave irradiation is a novel and efficient approach to promote the Maillard reaction (MR).

The high-molecular-weight melanoidins prepared from glucose and different amino acids (asparagine, glycine, and arginine) have been found to possess a higher browning degree, reducing power, and antioxidant activity [7]. Yen and Tsai [8] evaluated the antioxidant activity of partially fractionated MRPs prepared by refluxing glucose and tryptophan at pH 11.0 and 100°C for 10 h, and the results showed that, compared with low-molecular-weight fractions, the high-molecular-weight fractions achieved a higher reducing power and antioxidant activity. Therefore, the preparation of high-molecular-weight MRPs might be an alternative method to develop valuable high antioxidant products.

Response surface methodology (RSM) is of considerable value for the improvement and optimization of complex processes that elucidate the causality between explanatory variables and response variables [9]. Furthermore, RSM is one of the best experiment design methods to reduce the number of experimental trials needed to evaluate multiple parameters and their interactions to provide sufficient information for statistically acceptable results [10, 11]. The objective of the present study is to optimize the Maillard reactions between L-arabinose and glycine using microwave heating to develop high antioxidant MRPs. The relationship between browning degree and reducing power of the MRPs will also be evaluated.

Microwave radiation uses a heating mechanism that rotates and vibrates the electric dipole of target molecules. The reaction time of microwave treatment is much shorter than those using traditional methods. This study applies the microwave heating energy to the L-arabinose and glycine in the mixed solvent propylene glycol and ddH<sub>2</sub>O. Short reaction time and less on the substrate concentration have better reducing power and emulsifying ability.

## 2. Materials and Methods

**2.1. Chemicals.** Glycine of food grade was purchased from Shanghai Weihong Bio-Sci and Tech Co., Ltd. (Shanghai, China) and L-arabinose from Jinan Shengquan Biotechnology Co., Ltd. (Jinan, China). All other chemicals were of analytical grade and purchased from Shanghai Chemical Reagent Co., Ltd. (Shanghai, China).

**2.2. Preparation of Maillard Reaction Products (MRPs).** Based on our preliminary experiments, a L-arabinose: glycine ratio of 2:1 (w/w) and substrate concentration of 10% (w/v) were used in the Maillard reaction. This reaction

model system has been reported by Peterson, Tong, Ho, and Welt [12] and modified in this study. Briefly, L-arabinose (2g) and glycine (1g) were dissolved in a certain amount of ddH<sub>2</sub>O and propanediol. The pH of the solution was adjusted with 5M NaOH and 1M HCl; 27 ml solutions were transferred to a 100 ml beaker and heated in a microwave oven with 500 W of power level (Galanz WD800 T model, 2450 MHz, 800 W, 305 mm × 508 mm × 395 mm, Shunde, China) for a certain time. After heating, samples were collected and placed in an ice bath to cool down to stop the reaction before they were stored at a 4°C fridge. These samples were referred to as MRPs.

**2.3. Determination of Browning Degree (BD).** Samples of 1.0 ml MRPs were diluted to 100-fold with the addition of ddH<sub>2</sub>O. The browning degree was determined by measuring the absorbance at 420 nm using a UV-Vis spectrophotometer [13, 14] (UV-2100 UNICO spectrophotometer, Jiangsu Scientific Instruments and Materials Co., LTD, Jiangsu, China).

**2.4. Experimental Design.** According to our prior experimental findings, the most influential factors on the BD and RP of MRPs are heating time (factor A: 5 min, 7 min, 9 min), volume ratio of propylene glycol to ddH<sub>2</sub>O (factor B: 0.5, 1, 1.5 v/v), and pH (factor C: pH 8, pH 10, pH 12). The effects of interactions of these three factors were also considered in the RSM experimental design.

The “Design-Expert” software (version 8.0.6, Stat-Ease, Inc., Minneapolis, USA) was used to generate the Box-Behnken experimental designs. The independent variables were heating time (A), volume ratio of propylene glycol to ddH<sub>2</sub>O (B), and pH (C). Each independent variable had coded levels of -1, 0, and 1 and was constructed based on a 3<sup>3</sup> factorial design. Five replications of the central points were run, leading to 17 sets of experiments, allowing each experimental response to be optimized. The experimental designs of the coded factors and actual levels of variables are shown in Table 1. The two responses (Y) were browning degree (Y<sub>1</sub>, A<sub>420nm</sub>) and reducing power (Y<sub>2</sub>, A<sub>700nm</sub>). The response functions Y<sub>1</sub> and Y<sub>2</sub> were related to the coded variables (A, B, C) by a second-degree polynomial equation using the method of least squares:

$$Y = a_0 + a_1A + a_2B + a_3C + a_4A^2 + a_5B^2 + a_6C^2 + a_7AB + a_8AC + a_9BC, \quad (1)$$

where Y is the response calculated by the model; A, B, and C are coded variables, corresponding to heating time, volume ratio of propylene glycol: ddH<sub>2</sub>O, and pH, respectively; a<sub>1</sub>, a<sub>2</sub>, and a<sub>3</sub> are the linear; a<sub>4</sub>, a<sub>5</sub>, and a<sub>6</sub> are the quadratic, and a<sub>7</sub>, a<sub>8</sub>, and a<sub>9</sub> are the cross-product effects of the A, B, and C factors on the response.

Analysis of variance (ANOVA) was performed. ANOVA tables were generated, and the effect and regression coefficients of individual linear, quadratic, and interaction terms were determined. The statistical significance of the regression coefficients was determined by using the F-test, and the

TABLE 1: Experiment design and results of RSM.

Run	A/Time(min)	B/Ratio	C/pH	BD/A <sub>420nm</sub> <sup>a</sup>	RP/A <sub>700nm</sub> <sup>b</sup>
1	-1	-1	0	0.112	0.032
2	0	0	0	0.369	0.238
3	0	0	0	0.387	0.255
4	-1	1	0	0.1	0.02
5	1	1	0	0.265	0.184
6	1	0	-1	0.254	0.159
7	0	1	1	0.343	0.221
8	0	-1	1	0.358	0.232
9	1	-1	0	0.307	0.195
10	0	0	0	0.383	0.254
11	-1	0	-1	0.087	0.011
12	0	-1	-1	0.289	0.196
13	1	0	1	0.376	0.247
14	0	0	0	0.38	0.25
15	0	1	-1	0.206	0.139
16	0	0	0	0.375	0.244
17	-1	0	1	0.15	0.064
R <sup>2</sup>				0.9967	0.9957
CV%				3.4	5.01

<sup>a</sup> BD, browning degree as absorbance of 420 nm; <sup>b</sup> RP, reducing power at an absorbance of 700 nm.

applicability of the model was checked with significant coefficients of determination ( $R^2$ ) and the coefficient of variation (CV) values. The optimal processing conditions were obtained by using graphical and numerical analysis based on the criterion of desirability.

**2.5. Qualitative Analysis of Volatiles Compounds MRPs by GC/MS.** A manual solid-phase microextraction (SPME) device and divinylbenzene/carbo-xen/polydimethylsiloxane (DVB/CAR/PDMS) fibres (100  $\mu$ m film thickness) were obtained from Supelco Co. (Bellefonte, PA, USA). The fibre was conditioned for 1 h at 270°C as recommended by the manufacturer. Five milliliter of MRPs was placed in a 10-ml vial closed by a PTFE/silicone septum (Supelco). Before the extraction process, a time of 30 min at 40°C was requested for headspace equilibration. After 1 h of fibre exposure in the sample headspace, the fibre was thermally desorbed in a gas chromatography (GC) injection port for 20 min. The injector was set at 250°C and operated in a splitless mode for 3 min. The GC/MS analyses were carried out using an Agilent 7890A gas chromatograph (NYSE: A, USA), equipped with an FID and coupled to a quadrupole Agilent 5975C Network mass selective detector (NYSE: A, USA). The gas chromatography was equipped with a fused silica capillary column HP-INNOWAX (PEG, 60 m  $\times$  0.32 mm i.d. film thickness = 0.25  $\mu$ m, NYSE: A, USA). The carrier gas was helium (head pressure for both columns = 25 psi); oven temperature was programmed from 60 °C (2 min) to 200°C at 2°C/min and then at 5°C/min to 230°C and held isothermal for 5 min. The FID temperature was set at 250°C, and the temperatures of the ion source and the transfer line were 170 and 280°C, respectively. Energy was set at 70 eV and mass range of 35 ~ 350 amu. Qualitative method is done by comparing the spectrum of the detected substance with the standard spectrum in the NIST 05al and Wiley 7n databases

(Agilent, USA). By comparing retention time with standard products, the results were compared with the retention index (RI) of standard substances, and those without standard substances were compared with RI in the reported literature.

**2.6. Determination of Reducing Power (RP).** The reducing power of the MRPs was determined according to the method previously reported [14, 15] with slight modification. Samples of 1 ml MRPs (100-fold dilution) were mixed with 1.0 ml of 0.2 M sodium phosphate buffer (pH 6.6) and 1.0 ml of 1% potassium ferricyanide ( $K_3Fe(CN)_6$ ) in a test tube and sealed. The reaction mixtures were incubated in a water bath at 50°C for 20 min, followed by rapid cooling to 25°C. The solution of 1.0 ml was further mixed with 1.0 ml ddH<sub>2</sub>O and 200  $\mu$ l 0.1% FeCl<sub>3</sub> (w/v), and the absorbance was read at 700 nm with a spectrophotometer. The reducing power of MRPs was expressed as absorbance ( $A_{700}$ ) using the mean values of three determinations.

**2.7. DPPH Radical Scavenging Activity of MRPs.** DPPH radical-scavenging activity of MRPs was determined according to the method of Yen and Hsieh [16] with a slight modification. An aliquot of 80  $\mu$ l MRP sample was diluted with 320  $\mu$ l of ddH<sub>2</sub>O and 2 ml of 0.12 mM DPPH in methanol was added. The solution was then mixed vigorously and allowed to stand at room temperature in the dark for 30 min. The absorbance of mixtures was measured at 517 nm on the UNICO UV-2100 spectrophotometer. The control was prepared in the same way, except that ddH<sub>2</sub>O was used instead of MRP samples. For the blank sample, the assay was conducted in the same way, but methanol was added instead of DPPH solution. The percentage of DPPH radical-scavenging activity is calculated as follows:

$$\text{radical scavenging activity (\%)} = \left( 1 - \left( \frac{A_{\text{sample}(517\text{nm})}}{A_{\text{control}(517\text{nm})}} \right) \right) \times 100 \quad (2)$$

**2.8. Determination of Emulsifying Ability of MRPs.** Emulsifying ability of MRPs was determined according to the method reported by Pearce and Kinsella [17] with minor modifications. Five milliliters of corn oil were added to 15 ml of MRPs solution (1 mg/ml, ddH<sub>2</sub>O) and homogenized (FA25 Model homogenizer, Fluko Equipment Shanghai Co., Ltd, China) at 13,000 rpm at 25°C for 1 min to form an emulsion. The emulsion of 5 ml was transferred into a test tube and diluted with 5 ml of 0.1% sodium dodecyl sulfate solution. The absorbance at 500 nm of the diluted emulsion was measured with the UNICO UV-2100 spectrophotometer against a blank (ddH<sub>2</sub>O). The data of emulsifying ability were expressed as absorbance units ( $A_{500}$ ) at 500 nm and were shown as mean values of the three determinations.

TABLE 2: Variance analysis of the browning degree experiment.

Variance	Sum of	df <sup>a</sup>	Mean	F-value	p value	
Source	Squares		Square		Prob > F	
Model	0.19	9	0.021	234.03	<0.0001	Significant
A <sup>b</sup>	0.071	1	0.071	787.45	<0.0001	
B	2.89E-03	1	2.89E-03	32.09	0.0008	
C	0.019	1	0.019	212.32	<0.0001	
AB	2.25E-04	1	2.25E-04	2.5	0.1579	
AC	8.70E-04	1	8.70E-04	9.67	0.0171	
BC	1.16E-03	1	1.16E-03	12.84	0.0089	
A <sup>2</sup>	0.074	1	0.074	821.59	<0.0001	
B <sup>2</sup>	0.011	1	0.011	118.24	<0.0001	
C <sup>2</sup>	3.67E-03	1	3.67E-03	40.78	0.0004	
Residual	6.30E-04	7	9.00E-05			Not significant
Lack of fit	4.33E-04	3	1.44E-04	2.94	0.1626	
Pure error	1.97E-04	4	4.92E-05			
Cor total	0.19	16				

<sup>a</sup>df is the degree of freedom; <sup>b</sup>A, reaction time; B, volume ratio of propylene glycol: distilled-deionized water; C, pH.

TABLE 3: Variance analysis of the reducing power experiment.

Variance	Sum of	df <sup>a</sup>	Mean	F-value	p value	
Source	Squares		Square		Prob > F	
Model	0.12	9	0.014	182.03	<0.0001	Significant
A <sup>b</sup>	0.054	1	0.054	720.17	<0.0001	
B	1.04E-03	1	1.04E-03	13.77	0.0075	
C	8.39E-03	1	8.39E-03	111.58	<0.0001	
AB	2.50E-07	1	2.50E-07	3.33E-03	0.9556	
AC	3.06E-04	1	3.06E-04	4.08	0.0833	
BC	5.29E-04	1	5.29E-04	7.04	0.0328	
A <sup>2</sup>	0.05	1	0.05	660.8	<0.0001	
B <sup>2</sup>	4.27E-03	1	4.27E-03	56.84	0.0001	
C <sup>2</sup>	1.58E-03	1	1.58E-03	20.98	0.0025	
Residual	5.26E-04	7	7.52E-05			Not significant
Lack of fit	3.21E-04	3	1.07E-04	2.09	0.2441	
Pure error	2.05E-04	4	5.12E-05			
Cor total	0.12	16				

<sup>a</sup>df is degrees of freedom. <sup>b</sup>A, reaction time; B, volume ratio of propylene glycol to distilled-deionized water; C, pH.

2.9. Data Processing. Data were processed using software such as SPSS 20.0 and Design-Expert 8.0.6.

### 3. Results and Discussion

3.1. Mathematic Model of Maillard Reaction. RSM experiments of L-arabinose/glycine were carried out in a random order. Values obtained from the Maillard reaction system are given in Table 1, while characteristics of the model for BD and RP are shown in Table 2 and 3, respectively. The ANOVA confirmed the adequacy of the statistical models since their Prob > F values were less than 0.05 and statistically significant at the 95% confidence level. The models presented high determination coefficients ( $R^2$ ) and low coefficients of variation (CV). These values are listed as follows:  $R^2 = 0.9967$  and  $CV\% = 3.4$  for BD;  $R^2 = 0.9957$  and  $CV\% = 5.01$  for RP. These results indicated a good precision and reliability for the experiment. The fitted model equations are as follows:

$$Y_1 = 0.38 + 0.082 \times A - 0.016 \times B + 0.045 \times C - 0.014 \times A \times B + 0.023 \times A \times C + 0.017 \times B \times C - 0.12 \times A^2 - 0.046 \times B^2 - 0.034 \times C^2, \quad (3)$$

$$Y_2 = 0.23 + 0.054 \times A + 0.022 \times B + 0.051 \times C - 0.023 \times A \times B + 0.046 \times A \times C - 0.03 \times B \times C - 0.081 \times A^2 - 0.016 \times B^2 - 0.080 \times C^2. \quad (4)$$

3.1.1. Optimization for Browning Degree. As shown in Table 2, the browning degree (BD) of MRPs was positively related to the linear effect of heating time (Time), volume ratio of propylene glycol to ddH<sub>2</sub>O (ratio), and pH (pH) ( $p < 0.05$ ). The interaction effects of heating time and

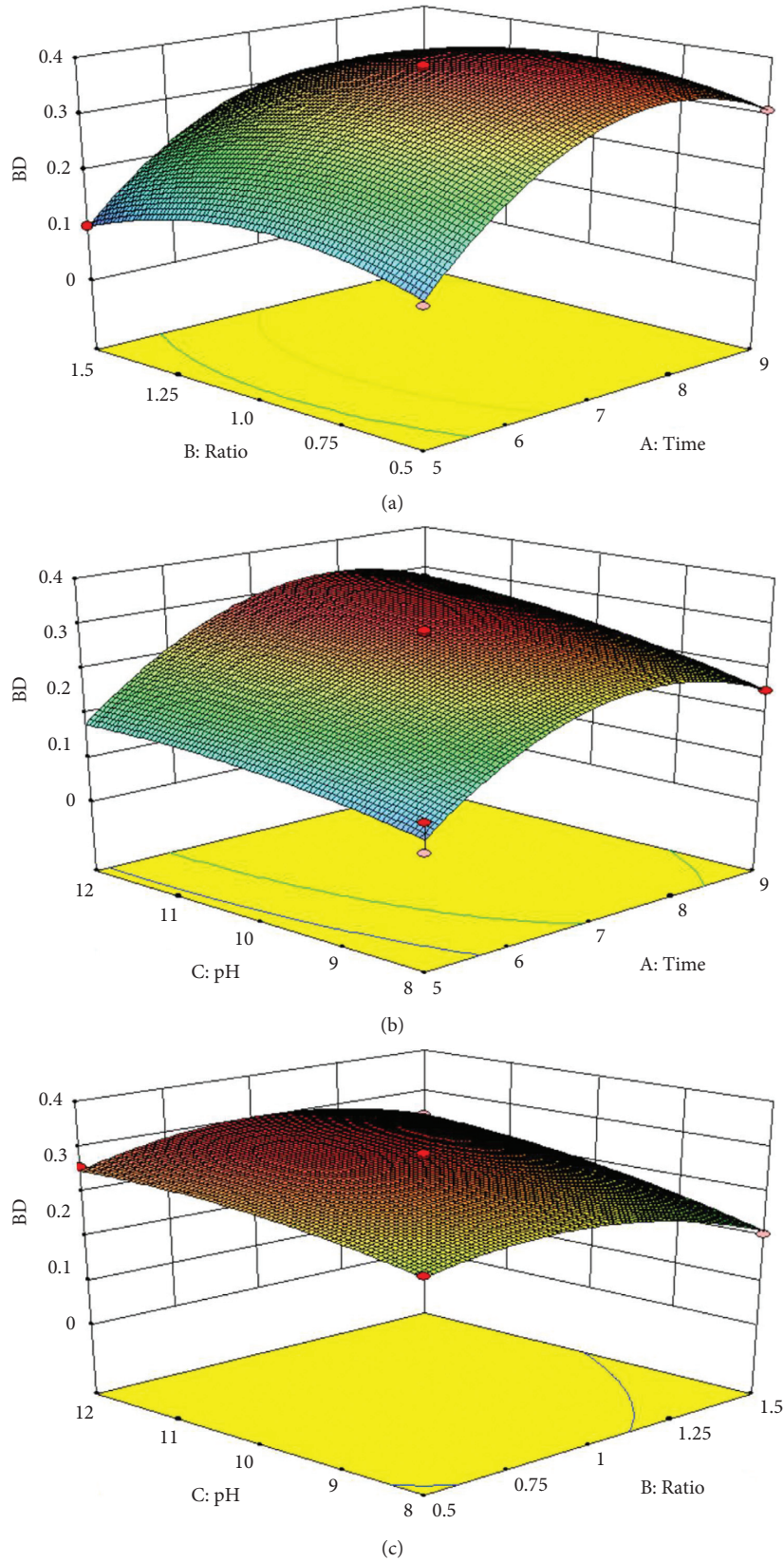


FIGURE 1: Three-dimensional figures of interactive effects of heating time (time), volume ratio of propylene glycol to ddH<sub>2</sub>O (ratio), and pH (pH) on browning degree (BD) of an L-arabinose/glycine Maillard reaction system.



volume ratio had a negative but not significant effect equation (3) on BD. However, the linear terms and quadratic terms of volume ratio have a significantly negative effect on BD.

Figure 1(a) shows the dependence of BD on the reaction factors of heating time (time) and the volume ratio of propylene glycol to ddH<sub>2</sub>O (Ratio) at a fixed pH. It is clear that at a constant pH value and heating time, BD increased slightly with the increase in the volume ratio. It was also observed that the BD increased quickly at the beginning of the experiment and then decreased slightly with the extending of heating time at a fixed volume ratio and pH (Figure 1(a)). The variation is curvilinear in nature.

The variation in the BD with heating time and pH at a constant volume ratio of propylene glycol to ddH<sub>2</sub>O is presented in Figure 1(b). It is evident that at a fixed volume ratio and pH, the BD increased rapidly with heating time at the first stage and then decreased slowly. At a fixed volume ratio and heating time, the BD increased with slow increment of pH but decreased slightly in later stages.

Figure 1(c) shows the effects of the pH value and the volume ratio of propylene glycol to ddH<sub>2</sub>O on BD at a fixed heating time. The BD increased slowly at the beginning and decreased slightly afterwards with an increased volume ratio at a constant pH and heating time. The same trend can be seen for the variable of pH at a fixed heating time and volume ratio.

The results indicated that the linear effects of pH value, volume ratio of propylene glycol to ddH<sub>2</sub>O, and heating time were dominant over the interaction terms. The interaction effects between heating time and volume ratio were not significant ( $p > 0.05$ ), but they slightly influenced the BD. The quadratic effects were significantly negative to the browning degree ( $p < 0.05$ ).

**3.1.2. Reducing Power.** The reducing power (RP) of the MRPs has a positive linear effect on the variation in heating time, volume ratio of propylene glycol to ddH<sub>2</sub>O, and pH, as shown in Table 3. The quadratic effects also have a significant effect on the RP of MRPs. The interaction terms of the variables of volume ratio and pH were found to have significant effects on RP.

Figure 2(a) presents the value of RP with the variation of heating time and the volume ratio of propylene glycol to ddH<sub>2</sub>O at a given pH. The RP value increased rapidly with the heating time at a given volume ratio and pH, while at a fixed volume ratio and heating time, the RP value slightly increased with increased pH values (Figure 2(b)). However, the RP value increased slightly at the beginning and decreased slowly with the variation in the volume ratio at a fixed heating time and pH (Figure 2(c)).

It has been widely recognized that melanoidins from Maillard reactions possess high reducing power [18, 19]. The present experimental results showed that the browning degree and reducing power of MRPs from the L-arabinose/glycine system have a good positive correlation with each other (higher browning degree and higher reducing power) and are consistent with the reported results of Yamaguchi, Koyama, and Fujimaki [7].

**3.1.3. Optimization and Experimental Validation.** The optimal processing parameters were obtained from SRM to the preparation of L-arabinose/glycine MRPs with high browning degree and reducing power. Browning degree can be optimized from the contour plot figures of Figure 1(a)–1(c). The pH region is in the range of 8–12, the volume ratio of propylene glycol to ddH<sub>2</sub>O is 0.5–1.5, and the heating time is 5–9 min. The model describing the optimum conditions for BD was as follows: a heating time of 7.44 min; a volume ratio of propylene glycol to ddH<sub>2</sub>O of 0.93; and a pH of 10.44. Reducing power can be optimized from contour plots of Figure 2(a)–2(c), and the model describing the optimal conditions for RP were the same to those of BD: a heating time of 7.44 min; a volume ratio of propylene glycol to ddH<sub>2</sub>O of 0.93; and a pH of 10.44. The highly coincident data also suggested that the BD and RP of the MRPs are positively correlated with each other. Therefore, the responses ( $Y_1$  and  $Y_2$ ) of the optimal conditions for both BD and RP could be expressed using the same model. The responses ( $Y_1$  and  $Y_2$ ) calculated from the final polynomial functions were a BD of 0.405 at 420 nm and a RP of 0.268 at 700 nm. The Maillard reaction conditions were experimentally validated, and the results were a BD of  $0.461 \pm 0.02$  at 420 nm and a RP of  $0.319 \pm 0.01$  at 700 nm. Based on the relative deviation values of BD (SD% = 3.96) and RP (SD% = 3.61), it could be tentatively concluded that the methodology employed for the optimization of the Maillard process conditions was satisfactory and that the surface responses obtained by the full experimental design were suitably validated.

**3.2. HS-SPME GC-MS Analysis Results of MRPs.** Table 4 shows the volatile chemicals of MRPs produced by microwave heating under the optimum Maillard reaction conditions obtained by the SRM design. The major compounds identified in the MRP sample were pyrazines (peak area = 21.27%), furans (peak area = 4.49%), alcohols (7.8%), pyrroles (peak area = 10.34%), acids (peak area = 12.88%), ketones (3.51%) and phenols (peak area = 16.97%). The types of pyrazines of the result are more than the ascorbic acid/glycine Maillard reaction [20]. And alkylated pyrazines are an important group of flavor compounds, which contribute substantially to the unique roasted aroma of various food products [21]. Pyrazines came from the Maillard reaction involving glycine [22]. Pyrroles were the key antioxidant activity compounds [23]. So the MRPs have the pyrazines characteristics of pyrazines flavor and fine antioxidant activity.

**3.3. Emulsifying Ability Analysis of MRPs.** The emulsifying ability of MRPs was 0.367 absorbance at 500 nm by microwave heating under the optimal Maillard reaction conditions, which was very close to the emulsifying ability of the casein-glucose Maillard reaction product (the emulsifying ability was 0.397 absorbance at 500 nm) reported by Gu, Abbas, and Zhang [24]. So the MRPs have a good emulsifying ability like the casein-glucose Maillard reaction product. We can also conclude that some hydrophilic and lipophilic substances must be formed by the reaction products. If it can

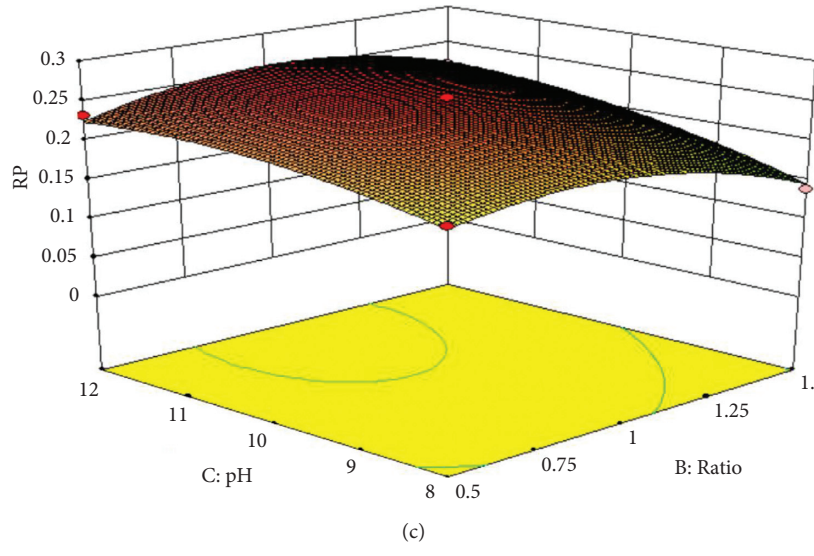
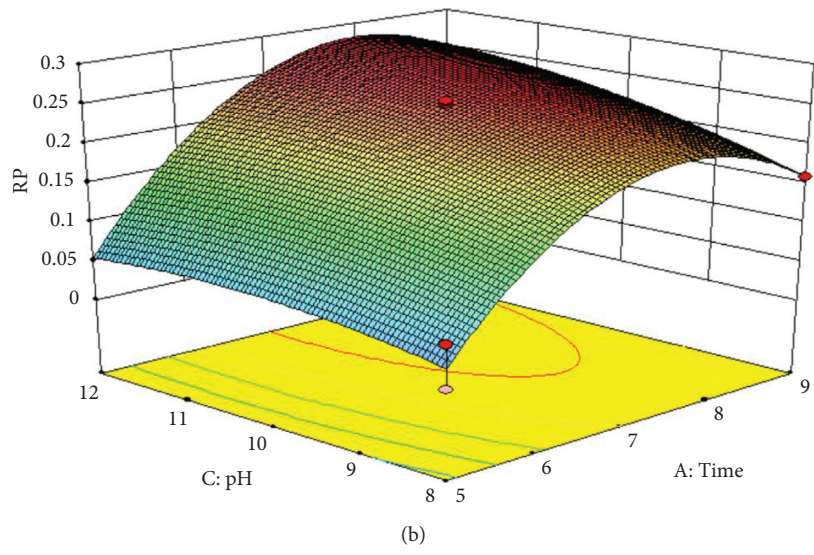
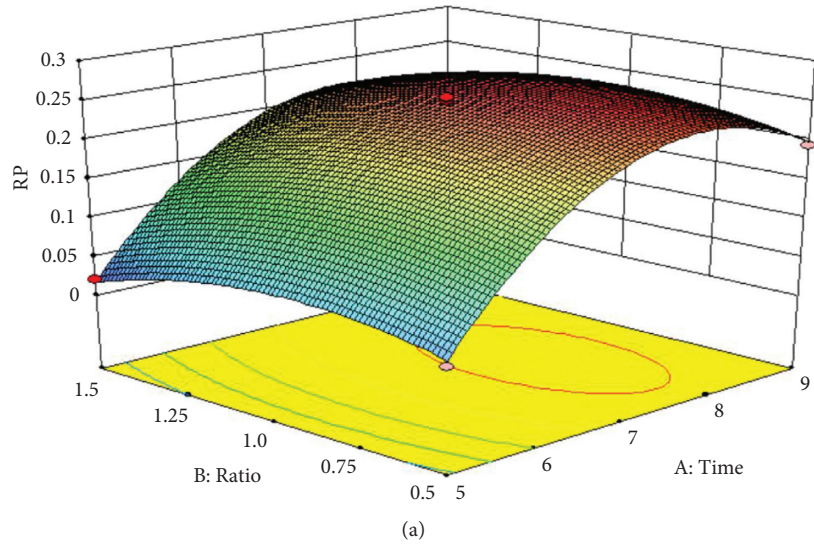


FIGURE 2: Three-dimensional figures of interactive effects of heating time (time), volume ratio of propylene glycol to ddH<sub>2</sub>O (ratio), and pH (pH) on reducing power (RP) of an L-arabinose/glycine Maillard reaction system.

TABLE 4: Volatile compounds identified in MRPs using HS-SPME.

Serial number	Compound name	Cas	Fragrance description	Peak area (%)	RI	
1	N-Methylpyrrole	96-54-8	Smoky, herbal	0.20	1145	1246
2	1-Pentanamine	17839-26-8	-	0.20	-	1301
3	2-Methyltetrahydrofuran-3-one	3188-00-9	Bread, butter	0.78	1270	1380
4	2-Pyridinamine	146580-32-7	-	0.20	-	1384
5	2-Methylpyrazine	109-08-0	Nutty, cocoa	0.20	1267	1385
6	Hydroxyacetone	116-09-6	Pungent, caramellic	3.32	1301	1422
7	2,5-Dimethylpyrazine	123-32-0	Cocoa, nuts	1.17	1328	1437
8	Pyrazine, 2,6-dimethyl-	108-50-9	Coffee buttermilk	0.78	1340	1444
9	2,3-Dimethyl pyrazine	5910-89-4	Peanut butter	1.17	1355	1461
10	2-Ethyl-6-methylpyrazine	13925-03-6	Roasted potato	0.39	1389	1497
11	2-Ethyl-5-methylpyrazine	13360-64-0	Coffee bean	0.39	1395	1503
12	2,3,5-Trimethylpyrazine	14667-55-1	Nutty, baked potato	5.85	1414	1517
13	DL-2-octanol	123-96-6	Fresh, woody herbal	0.20	-	1525
14	2-Propylpyrazine	18138-03-9	Green vegetable	0.20	1430	1528
15	2-Ethyl-3,6-dimethylpyrazine	27043-05-6	Burnt coffee	3.51	-	1555
16	Acetic acid	64-19-7	Sour vinegar	3.51	1473	1561
17	Pyrazine, 2-ethyl-3,5-dimethyl-	248-182-2	Burnt coffee	3.32	-	1571
18	2-Methyl-5-propylpyrazine	29461-03-8	-	0.98	-	1574
19	Pyrazine, 2-methyl-5-propyl-	2884-14-2	-	0.20	-	1587
20	Pyrazine, 3,5-diethyl-2-methyl-	18138-05-1	Nutty meaty	0.78	-	1602
21	3,5-Dimethyl-2-propylpyrazine	32350-16-6	Hazelnut	0.39	-	1644
22	Propanoic acid	79-09-4	Pungent acidic	0.39	1526	1647
23	2,3-Dimethyl-5-n-propylpyrazine	32262-98-9	-	0.59	-	1650
24	2,3,5-Trimethyl-6-propylpyrazine	92233-82-4	-	0.98	-	1678
25	1-Acetoxy-2-propanol	1331-12-0	-	7.02	-	1682
26	Ethyl digol	111-90-0	-	6.83	1628	1741
27	Isopropyl formate	625-55-8	Cocoa	0.59	-	1746
28	2-Allyl-5-methylpyrazine	55138-63-1	-	1.17	-	1768
29	Furfuryl alcohol	98-00-0	Caramel bread	2.15	1678	1771
30	(3,4-Dimethylphenyl) ethanone	3637-01-2	-	0.98	-	1802
31	2-Allyl-3-hydroxybenzaldehyde	79950-42-8	-	0.98	-	1868
32	1-Furfurylpyrrole	1438-94-4	Fruity coffee	9.17	1850	1939
33	2-Pentylfuran	3777-69-3	Fruity, beany	0.98	-	1980
34	2,6-Di-tert-butyl-4-methylphenol	128-37-0	Phenolic camphor	16.58	1920	2024
35	2-Butylfuran	4466-24-4	Mild fruity	0.59	-	2041
36	1-Dodecanol	112-53-8	Earthy, soapy	0.78	1973	2074
37	2-Acetyl pyrrole	1072-83-9	Musty nut skin	0.98	1960	2079
38	2-Pentadecanone	2345-28-0	Fresh jasmine	0.20	2031	2133
39	Isopropyl palmitate	142-91-6	Bland oily	1.76	-	2140
40	2,4-Di-tert-butylphenol	96-76-4	Phenolic	0.39	2315	2225
41	4-Hydroxy-4-methyl-2-pentanone	123-42-2	-	0.20	-	2273
42	Cyclohexadecane	295-65-8	-	1.76	-	2293
43	N-Hexadecanoic acid	57-10-3	Fatty	6.63	2931	2319
44	Dodecanoic acid	143-07-7	Bay oil	2.34	2503	2400

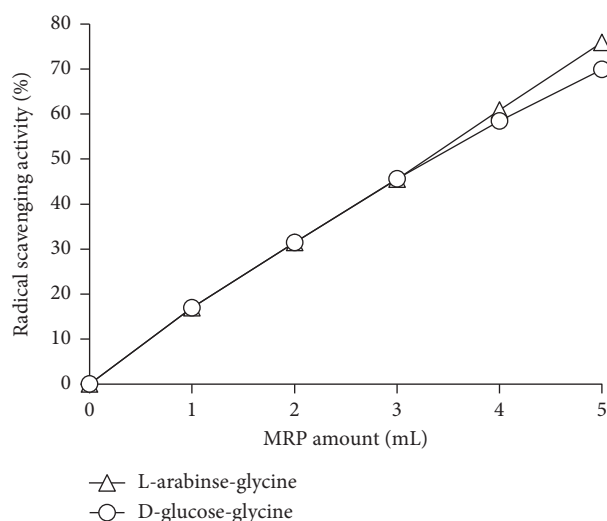


FIGURE 3: DPPH radical-scavenging activity of the Maillard reaction product (MRP) of an L-arabinese/glycine system.

be separated and identified, one may be able to get good emulsifier. MRPs have a more broad application area.

**3.4. Changes in DPPH Radical-Scavenging Activity.** The DPPH radical was scavenged by MRPs by the donation of hydrogen to form a stable DPPH-H molecule. And the color changed from purple to yellow by the acceptance of a hydrogen atom from MRPs, and it became a stable diamagnetic molecule [25]. As shown in Figure 3, it can be observed that DPPH radical-scavenging activity of the MRPs of L-arabinese-glycine and D-glucose-glycine is positively related to the linear effect of heating time (Time), volume ratio of propylene glycol to ddH<sub>2</sub>O (ratio), and initial pH (pH) ( $p < 0.05$ ). MRPs derived from L-arabinese and D-glucose had similar activities. However, a slightly greater activity was found with MRP derived from L-arabinese-glycine with more volume.

## 4. Conclusion

The response surface methodology has been demonstrated as a useful tool to optimize the reaction conditions of heating time, volume ratio of propylene glycol to ddH<sub>2</sub>O, and pH to improve the browning degree and reducing power in the L-arabinese/glycine Maillard reaction product. The coefficients of determinations and  $R^2$  values showed a good fit of the models with the experimental data at the 95% confidence level. The different conditions for Maillard reaction revealed that heating time had the significant effect on browning degree and reducing power using microwave heating, while the other two variables (volume ratio of propylene glycol to ddH<sub>2</sub>O and pH) had an optimum zone for emulsifying ability and DPPH scavenging ability. These results were well fitted with the experimental data, and the obtained models have the potential to be used to maximize the antioxidant activity of the Maillard reaction products.

The peak area of pyrazines is 21.27%, and alkylated pyrazines are the unique roasted aroma of various food products, so the main flavor of MRPs is roasted aroma. MRPs have better reducing power and emulsifying ability. The reaction time of microwave treatment is much shorter than those using traditional methods, so microwave irradiation is a highly efficient approach to promote MR and has huge potential in MR. This study provides a new direction for the development of sweet flavor.

## Data Availability

The data used to support the findings of this study are included within the article.

## Conflicts of Interest

The authors declare that they have no conflicts of interest.

## Acknowledgments

This study was financially supported by Scientific Innovation Key Project from Shanghai Education Committee12zz187.




## References

- [1] S. I. Martins, W. M. Jongen, and M. A. Van Boekel, "A review of Maillard reaction in food and implications to kinetic modelling [J]," *Trends in Food Science & Technology*, vol. 11, no. 9, pp. 364–373, 2000.
- [2] D. Mastrocola, M. Munari, M. Cioroi, and C. R. Lerici, "Interaction between Maillard reaction products and lipid oxidation in starch-based model systems," *Journal of the Science of Food and Agriculture*, vol. 80, no. 6, pp. 684–690, 2000.
- [3] A. M. Hamdani, I. A. Wani, N. A. Bhat, and R. A. Siddiqi, "Effect of guar gum conjugation on functional, antioxidant and antimicrobial activity of egg white lysozyme," *Food Chemistry*, vol. 240, no. 1, pp. 1201–1209, 2018.
- [4] I. G. Hwang, H. Y. Kim, K. S. Woo, J. Lee, and H. S. Jeong, "Biological activities of Maillard reaction products (MRPs) in a sugar-amino acid model system," *Food Chemistry*, vol. 126, no. 1, pp. 221–227, 2011.
- [5] L.-Q. Zhao, Q.-R. Peng, and R. Zhang, "Maillard reaction under microwave conditions [J]," *China Food Additives*, vol. 30, no. 04, pp. 55–64, 2019.
- [6] Z.-C. Tu, Y.-M. Hu, H. Wang, X.-Q. Huang, S.-Q. Xia, and P.-P. Niu, "Microwave heating enhances antioxidant and emulsifying activities of ovalbumin glycosylated with glucose in solid-state," *Journal of Food Science & Technology*, vol. 52, pp. 1453–1461, 2015.
- [7] Q. Li, Z. Yin, and H. Jing, "Physicochemical properties and antioxidant activity of three glucose-amino acid model maillard reaction products," *Journal of Chinese Institute of Food Science and Technology*, vol. 03, pp. 12–22, 2008.
- [8] G.-C. Yen and L.-C. Tsai, "Antimutagenicity of a partially fractionated Maillard reaction product," *Food Chemistry*, vol. 47, no. 1, pp. 11–15, 1993.
- [9] R. H. Myers, D. C. Montgomery, and C. M. Anderson-Cook, *Response Surface Methodology: Process and Product Optimization Using Designed Experiments [M]*, pp. 500–660, Wiley, 2009.

- [10] A. Simsek, E. S. Poyrazoglu, S. Karacan, and Y. Sedat Velioglu, "Response surface methodological study on HMF and fluorescent accumulation in red and white grape juices and concentrates," *Food Chemistry*, vol. 101, no. 3, pp. 987–994, 2007.
- [11] J. Lee, L. Ye, W. O. Landen, and R. R. Eitenmiller, "Optimization of an extraction procedure for the quantification of vitamin E in tomato and broccoli using response surface methodology," *Journal of Food Composition and Analysis*, vol. 13, no. 1, pp. 45–57, 2000.
- [12] B. I. Peterson, C.-H. Tong, C.-T. Ho, and B. A. Welt, "Effect of moisture content on Maillard browning kinetics of a model system during microwave heating," *Journal of Agricultural and Food Chemistry*, vol. 42, no. 9, pp. 1884–1887, 1994.
- [13] H. Jing and D. D. Kitts, "Redox-related cytotoxic responses to different casein glycation products in caco-2 and int-407 cells," *Journal of Agricultural and Food Chemistry*, vol. 52, no. 11, pp. 3577–3582, 2004.
- [14] S. He, Y. Chen, C. Brennan et al., "Antioxidative activity of oyster protein hydrolysates Maillard reaction products," *Food Sciences and Nutrition*, vol. 8, no. 7, pp. 3274–3286, 2020.
- [15] W. Lertittikul, S. Benjakul, and M. Tanaka, "Characteristics and antioxidative activity of Maillard reaction products from a porcine plasma protein-glucose model system as influenced by pH," *Food Chemistry*, vol. 100, no. 2, pp. 669–677, 2007.
- [16] G. C. Yen and P. P. Hsieh, "Antioxidative activity and scavenging effects on active oxygen of xylose-lysine maillard reaction products [J]," *Journal of the Science of Food and Agriculture*, vol. 67, no. 3, pp. 415–420, 2006.
- [17] K. N. Pearce and J. E. Kinsella, "Emulsifying properties of proteins: evaluation of a turbidimetric technique," *Journal of Agricultural and Food Chemistry*, vol. 26, no. 3, pp. 716–723, 1978.
- [18] L. Cai, D. Li, Z. Dong, A. Cao, H. Lin, and J. Li, "Change regularity of the characteristics of Maillard reaction products derived from xylose and Chinese shrimp waste hydrolysates," *Lebensmittel-Wissenschaft und -Technologie- Food Science and Technology*, vol. 65, pp. 908–916, 2016.
- [19] K. Yanagimoto, K.-G. Lee, H. Ochi, and T. Shibamoto, "Antioxidative activity of heterocyclic compounds formed in Maillard reaction products," in *International Congress Series* vol. 1245, pp. 335–340, Elsevier, 2002.
- [20] A. Adams and N. D. Kimpe, "Formation of pyrazines from ascorbic acid and amino acids under dry-roasting conditions," *Food Chemistry*, vol. 115, no. 4, pp. 1417–1423, 2009.
- [21] J. A. Maga, "Pyrazine update," *Food Reviews International*, vol. 8, no. 4, pp. 479–558, 1992.
- [22] Y.-G. Guan, B.-S. Zhang, S.-J. Yu et al., "Effects of ultrasound on a glycin-glucose model system-A means of promoting maillard reaction," *Food and Bioprocess Technology*, vol. 4, no. 8, pp. 1391–1398, 2011.
- [23] K. Yanagimoto, K.-G. Lee, H. Ochi, and T. Shibamoto, "Antioxidative activity of heterocyclic compounds found in coffee volatiles produced by maillard reaction," *Journal of Agricultural and Food Chemistry*, vol. 50, no. 19, pp. 5480–5484, 2002.
- [24] F.-I. Gu, S. Abbas, and X.-m. Zhang, "Optimization of Maillard reaction products from casein-glucose using response surface methodology," *Lebensmittel-Wissenschaft und -Technologie- Food Science and Technology*, vol. 42, no. 8, pp. 1374–1379, 2009.
- [25] S. Benjakul, W. Visessanguan, and V. Phongkanpai, "Antioxidative activity of caramelisation products and their preventive effect on lipid oxidation in fish mince [J]," *Food Chemistry*, vol. 90, no. 1, pp. 231–239, 2005.

## Research Article

# Comparison of the Nutritional and Taste Characteristics of 5 Edible Fungus Powders Based on the Composition of Hydrolyzed Amino Acids and Free Amino Acids

Jian Li,<sup>1,2</sup> Junmei Ma ,<sup>3,4,5</sup> Sufang Fan,<sup>3,4,5</sup> Shengquan Mi ,<sup>1</sup> and Yan Zhang <sup>3,4,5</sup>

<sup>1</sup>College of Applied Arts and Science, Beijing Union University, Beijing 100191, China

<sup>2</sup>School of Food and Biological Engineering, Hefei University of Technology, Hefei 230009, China

<sup>3</sup>Hebei Food Inspection and Research Institute, Hebei Food Safety Key Laboratory, Shijiazhuang 050091, China

<sup>4</sup>Key Laboratory of Special Food Supervision Technology for State Market Regulation, Shijiazhuang 050091, China

<sup>5</sup>Hebei Engineering Research Center for Special Food Safety and Health, Shijiazhuang 050091, China

Correspondence should be addressed to Shengquan Mi; [msq65@buu.edu.cn](mailto:msq65@buu.edu.cn) and Yan Zhang; [snowwinglv@126.com](mailto:snowwinglv@126.com)

Received 28 January 2022; Revised 22 February 2022; Accepted 2 March 2022; Published 7 April 2022

Academic Editor: Tao Feng

Copyright © 2022 Jian Li et al. This is an open access article distributed under the Creative Commons Attribution License, which permits unrestricted use, distribution, and reproduction in any medium, provided the original work is properly cited.

The nutritional characteristics and taste of some edible fungus powders were scientifically evaluated and compared. Five common edible fungus powders were used as test materials (*Agrocybe chaxinggu* edible fungus powder, *Pleurotus citrinopileatus* edible fungus powder, *Flammulina velutipes* edible fungus powder, *Lentinus edodes* edible fungus powder, and *Hericium erinaceus* edible fungus powder). The hydrolyzed amino acid and free amino acid content were measured by an automatic amino acid analyzer, and the ratios of hydrolyzed amino acid and free amino acid components and the taste characteristics of these eatables were systematically compared. The results showed that the total amount of hydrolyzed amino acids contained in the 5 edible fungus powders was between 2.583 and 14.656 g/100 g. The total amount of free amino acids contained in the 5 edible fungus powders was between 0.550 and 2.612 g/100 g. Comparative analysis of the mass fractions and composition of amino acids indicated that *Pleurotus citrinopileatus* edible fungus powder best met the ideal protein standard. The taste characteristics of protein were evaluated by calculating the taste active value (TAV) of taste-producing free amino acids. The most significant TAV values of the 5 edible fungus powders appeared in glutamic acid, and this amino acid is an umami amino acid. Principal component analysis (PCA) suggested that four principal components could reflect all the information on the free amino acids with a total cumulative variance contribution rate of 100%, and three principal components could reflect most of the information on the hydrolyzed amino acids with a total cumulative variance contribution rate of 99.143%, which could represent the main trends of free amino acids and hydrolyzed acids in edible fungus powder. The comprehensive evaluation model was established, and the comprehensive score indicated that *Agrocybe chaxinggu* edible fungus powder had the best comprehensive amino acid quality.

## 1. Introduction

Edible fungi are widely grown all over the world. There are at least 2,000 species of edible fungi in the world, of which about 200 are wild edible fungi [1]. China is the largest producer of edible fungi in the world, accounting for two-thirds of the world's production [2, 3]. Edible fungi are widely cultivated for their medicinal and nutritional value. Some edible fungi have been reported as therapeutic

foods, useful in preventing diseases such as hypertension, hypercholesterolemia, atherosclerosis, or cancer [4–7]. Edible fungi are valuable health foods, low in calories, lipids, and essential fatty acids, and high in vegetable proteins, minerals, and vitamins [8]. As a delicacy, edible fungi have unique umami, texture, and increasingly high-rated nutritive value. Umami is produced by glutamic acid, ribonucleotide and chemicals that make edible fungi tasty and are widely used in food preparation [2].

An amino acid is a biologically active substance that plays an important role in human metabolism. Its composition and content are important indicators for evaluating the nutritional value of edible fungi [9, 10]. Free amino acids (FAA), also known as nonprotein amino acids, are an important class of taste active ingredients [11], and their content and types are often used as important indicators for food nutritional value and taste and taste evaluation [12]. Some studies have shown that the main taste substances that have a significant impact on the taste of edible fungi are nucleotides, soluble sugars, organic acids, free amino acids, and other taste substances. Among them, free amino acids play an extremely important role in the presentation of the taste and deliciousness of edible fungi [13]. The typical umami taste of edible fungi is attributed to aspartic acid and glutamate [2]. Umami not only alleviates salty, sour or bitter tastes and improves the perception of sweetness, it also reduces the pungent meaty smell and the earthy taste [14, 15]. At present, the analytical methods for amino acids in edible fungi include ninhydrin colorimetry [16], high performance liquid chromatography [14, 17, 18], gas chromatography [19], gas chromatography-mass spectrometry [6, 20], nuclear magnetic resonance [21], amino acid analyzers [22–27], and high performance liquid chromatography-triple quadrupole mass spectrometry [28]. In the present study, the amino acid analyzer was used to analyze the nutritional characteristics of hydrolyzed amino acids and free amino acids of five common edible fungi powder, and their differences in nutritional and taste components were compared. The research results not only provide scientific data for revealing the nutritional value and taste characteristics of edible fungi, but also provide a scientific basis for guiding people to establish a scientific and healthy diet structure.

## 2. Materials and Methods

**2.1. Materials and Reagents.** Aspartic acid, threonine, serine, glutamic acid, glycine, alanine, valine, methionine, isoleucine, leucine, tyrosine, phenylalanine, lysine, histidine, arginine, and proline mixed standard solution were obtained from Wako Pure Chemical Industries, Ltd. (2.5  $\mu\text{mol/mL}$ , Tokyo, Japan). Water was purified using a Milli-Q-System (Millipore, Guyancourt, France). Ethanol was HPLC grade and was purchased from Merck (Darmstadt, Germany). Sodium citrate dihydrate, citric acid monohydrate, sodium chloride, sodium hydroxide, sodium borohydride, and hydrochloric acid were premium grade pure and were purchased from Beijing Chemical Reagent Factory (Beijing, China). Anhydrous sodium acetate, ninhydrin, ethylene glycol monomethyl ether, acetic acid, and phenol were analytical grade and were purchased from the Guangfu Fine Chemical Research Institute (Tianjin, China).

*Agrocybe chaxinggu* edible fungus powder, *Pleurotus citrinopileatus* edible fungus powder, *Flammulina velutipes* edible fungus powder, *Lentinus edodes* edible fungus powder, and *Hericiium erinaceus* edible fungus powder were supplied by Henan Longfeng Edible Fungi Industry Research Institute.

## 2.2. Methods

**2.2.1. Determination of Hydrolyzed Amino Acids.** Refer to GB 5009.124-2016 [29] for the determination of hydrolyzed amino acids. 0.5 g of each sample was hydrolyzed by an electric heating blast drying oven (Boxun GZX-9240MBE, China) with 10 mL of 6 mol/L hydrogen chloride at 110°C for 22 h under a nitrogen atmosphere, and then filtered through a 0.45  $\mu\text{m}$  membrane filter prior to analysis. The amino acid profiles of each sample were determined by an automatic amino acid analyzer (Hitachi L-8900, Japan). All determinations were carried out in triplicate.

**2.2.2. Determination of Free Amino Acids.** Refer to the first method in GB/T 30987-2020 [30] for the determination of free amino acids. 0.5 g of the sample was diluted with 100 mL of boiling water. The sample was water bathed by a water bath constant temperature oscillator (Runhua SHA-B, China) at 95°C for 10 min. and then filtered through a 0.45  $\mu\text{m}$  membrane filter prior to analysis. The amino acid profiles of each sample were determined by an automatic amino acid analyzer (Hitachi L-8900, Japan). All determinations were carried out in triplicate.

**2.3. Statistical Analysis.** All analyses were conducted in triplicate. The results reported were the average of these three replicates. Normal distribution tests of multielements and PCA analysis were performed with SPSS 25.0 software (SPSS, IBM Corp., USA).

## 3. Results and Discussion

**3.1. Hydrolyzed Amino Acid Concentrations in 5 Edible Fungus Powders.** The hydrolyzed amino acid is to hydrolyze the protein, polypeptide, and other amino acid chains in the plant to be tested into a single amino acid through acid hydrolysis. Therefore, the hydrolyzed amino acid can fully reflect the kind and content of all single amino acids in the sample. The hydrolyzed amino acid composition and content of 5 kinds of edible fungus powder are shown in Table 1. Results showed that 15 hydrolyzed amino acids were present in all samples tested. The total amount of hydrolyzed amino acids contained in the 5 edible fungus powders was between 2.583 and 14.656 g/100 g. The total hydrolyzed amino acid content of *Pleurotus citrinopileatus* edible fungus powder was the highest, reaching 14.656 g/100 g, and the total hydrolyzed amino acid content of *Hericiium erinaceus* edible fungus powder was the lowest, at 2.583 g/100 g. Glutamic acid was the most abundant among the 5 kinds of edible fungus powder, accounting for 17.41%, 19.75%, 25.16%, 24.92%, and 16.72% of the total hydrolyzed amino acids, respectively.

**3.2. Free Amino Acid Concentrations in 5 Edible Fungus Powders.** Free amino acids refer to amino acids that exist in a free state in plants as a single amino acid molecule and can be directly absorbed and utilized. The free amino acid composition and content of 5 kinds of edible fungus powder are shown in Table 2. The total amount of free amino acids

TABLE 1: Contents\* of hydrolyzed amino acids in 5 kinds of edible fungus powders.

Compound	<i>Agrocybe chaxinggu</i> edible fungus powder	<i>Pleurotus citrinopileatus</i> edible fungus powder	<i>Flammulina velutipes</i> edible fungus powder	<i>Lentinus edodes</i> edible fungus powder	<i>Hericium erinaceus</i> edible fungus powder
Aspartic acid and asparagine	1.571 ± 0.015	0.613 ± 0.001	0.531 ± 0.002	0.737 ± 0.002	0.247 ± 0.005
Threonine	0.744 ± 0.012	0.510 ± 0.009	0.147 ± 0.003	0.192 ± 0.002	0.107 ± 0.005
Serine	0.768 ± 0.003	0.469 ± 0.006	0.280 ± 0.006	0.399 ± 0.004	0.099 ± 0.003
Glutamic acid and glutamine	2.536 ± 0.012	2.894 ± 0.001	2.198 ± 0.031	2.969 ± 0.030	0.432 ± 0.001
Glycine	0.799 ± 0.008	0.867 ± 0.004	0.468 ± 0.004	0.650 ± 0.002	0.165 ± 0.003
Alanine	1.491 ± 0.004	1.427 ± 0.059	1.065 ± 0.024	1.859 ± 0.014	0.414 ± 0.005
Valine	1.021 ± 0.014	1.202 ± 0.023	0.585 ± 0.002	0.809 ± 0.014	0.207 ± 0.012
Methionine	0.022 ± 0.002	0.113 ± 0.011	ND	ND	ND
Isoleucine	0.583 ± 0.011	0.677 ± 0.003	0.301 ± 0.004	0.423 ± 0.005	0.068 ± 0.002
Leucine	1.379 ± 0.017	1.703 ± 0.037	0.821 ± 0.001	1.135 ± 0.009	0.298 ± 0.002
Tyrosine	0.507 ± 0.004	0.636 ± 0.008	0.414 ± 0.001	0.406 ± 0.015	0.111 ± 0.000
Phenylalanine	0.714 ± 0.010	0.849 ± 0.004	0.537 ± 0.003	0.567 ± 0.025	0.112 ± 0.006
Lysine	0.754 ± 0.002	1.082 ± 0.006	0.622 ± 0.002	0.710 ± 0.005	0.102 ± 0.001
Histidine	0.300 ± 0.004	0.410 ± 0.005	0.217 ± 0.003	0.257 ± 0.003	0.057 ± 0.003
Arginine	0.943 ± 0.009	1.204 ± 0.027	0.554 ± 0.009	0.799 ± 0.012	0.165 ± 0.001
Proline	0.434 ± 0.016	ND	ND	ND	ND
Total	14.567 ± 0.024	14.656 ± 0.287	8.739 ± 0.016	11.912 ± 0.092	2.583 ± 0.010

\* Value (g/100 g) = mean ± SD ( $n = 3$ ). ND: not detectable.

TABLE 2: Contents\* of free amino acids in 5 kinds of edible fungus powders.

Compound	<i>Agrocybe chaxinggu</i> edible fungus powder	<i>Pleurotus citrinopileatus</i> edible fungus powder	<i>Flammulina velutipes</i> edible fungus powder	<i>Lentinus edodes</i> edible fungus powder	<i>Hericium erinaceus</i> edible fungus powder
Aspartic acid	0.070 ± 0.001	0.016 ± 0.000	0.018 ± 0.000	0.022 ± 0.000	0.016 ± 0.001
Threonine	0.139 ± 0.003	0.286 ± 0.000	0.373 ± 0.001	0.327 ± 0.004	0.037 ± 0.001
Serine	0.079 ± 0.002	0.107 ± 0.000	0.068 ± 0.002	0.015 ± 0.000	0.004 ± 0.000
Glutamic acid	0.505 ± 0.003	0.396 ± 0.000	0.739 ± 0.003	0.448 ± 0.007	0.100 ± 0.002
Glycine	0.047 ± 0.000	0.032 ± 0.000	0.049 ± 0.000	0.022 ± 0.000	0.019 ± 0.001
Alanine	0.326 ± 0.002	0.207 ± 0.000	0.409 ± 0.001	0.135 ± 0.002	0.085 ± 0.003
Valine	0.164 ± 0.002	0.117 ± 0.000	0.118 ± 0.000	0.053 ± 0.001	0.047 ± 0.002
Methionine	ND	0.007 ± 0.000	ND	ND	ND
Isoleucine	0.101 ± 0.001	0.033 ± 0.000	0.060 ± 0.000	0.012 ± 0.000	0.022 ± 0.000
Leucine	0.168 ± 0.002	0.063 ± 0.000	0.103 ± 0.000	0.017 ± 0.000	0.064 ± 0.002
Tyrosine	0.064 ± 0.001	0.086 ± 0.001	0.159 ± 0.000	0.032 ± 0.001	0.038 ± 0.001
Phenylalanine	0.115 ± 0.002	0.131 ± 0.000	0.216 ± 0.001	0.046 ± 0.000	0.046 ± 0.003
Lysine	0.066 ± 0.002	0.079 ± 0.000	0.151 ± 0.001	0.035 ± 0.000	0.007 ± 0.000
Histidine	0.027 ± 0.000	0.028 ± 0.000	0.052 ± 0.000	0.009 ± 0.000	0.008 ± 0.000
Arginine	0.106 ± 0.002	0.062 ± 0.000	0.057 ± 0.001	0.055 ± 0.001	0.024 ± 0.001
Proline	0.026 ± 0.002	ND	0.039 ± 0.002	ND	0.034 ± 0.002
Total	2.003 ± 0.018	1.651 ± 0.001	2.612 ± 0.005	1.228 ± 0.017	0.550 ± 0.018

\* Value (g/100 g) = mean ± SD ( $n = 3$ ). ND: not detectable.

contained in the 5 edible fungus powders was between 0.550 and 2.612 g/100 g. The total free amino acid content of *Flammulina velutipes* edible fungus powder was the highest, reaching 2.612 g/100 g, and the total free amino acid content of *Hericium erinaceus* edible fungus powder was the lowest, at 0.550 g/100 g. Glutamic acid was the most abundant among the 5 kinds of edible fungus powders, accounting for 25.21%, 23.99%, 28.29%, 36.48%, and 18.18% of the total free amino acids, respectively.

3.3. *The Difference in the Ratio of Essential Amino Acids and Nonessential Amino Acids.* In order to scientifically evaluate the component structure of hydrolyzed amino acids, indicators such as the ratio of essential amino acids (EAAs) to nonessential amino acids (NEAAs) have been introduced. According to the essential amino acid model of protein nutritional value proposed by the World Health Organization (WHO) and the United Nations Food and Agriculture Organization (FAO) in 1973, the EAA/(EAA + NEAA)



TABLE 3: Comparative analysis of the mass fractions and composition of amino acids in 5 edible fungus powders.

Sample	EAA/NEAA	EAA/(EAA + NEAA)
<i>Agrocybe chaxinggu</i> edible fungus powder	55.81	35.82
<i>Pleurotus citrinopileatus</i> edible fungus powder	72.03	41.87
<i>Flammulina velutipes</i> edible fungus powder	52.62	34.48
<i>Lentinus edodes</i> edible fungus powder	47.48	32.20
<i>Hericium erinaceus</i> edible fungus powder	52.85	34.58

TABLE 4: Flavored amino acid content (g/100 g) in 5 kinds of edible fungus powders.

Sample	Umami amino acids	Sweet amino acids	Bitterness amino acids	Tasteless amino acids
<i>Agrocybe chaxinggu</i> edible fungus powder	0.574	0.616	0.682	0.131
<i>Pleurotus citrinopileatus</i> edible fungus powder	0.412	0.633	0.441	0.163
<i>Flammulina velutipes</i> edible fungus powder	0.757	0.969	0.606	0.310
<i>Lentinus edodes</i> edible fungus powder	0.469	0.499	0.193	0.067
<i>Hericium erinaceus</i> edible fungus powder	0.115	0.179	0.211	0.045

TABLE 5: The TAV of free amino acid in 5 kinds of edible fungus powders.

Compound	Taste characteristics	Taste threshold (mg/100 g) [34]	TAV of 5 kinds of edible fungus powders				
			<i>Agrocybe chaxinggu</i>	<i>Pleurotus citrinopileatus</i>	<i>Flammulina velutipes</i>	<i>Lentinus edodes</i>	<i>Hericium erinaceus</i>
Aspartic acid	Umami	3.00	23.22	5.30	6.03	7.29	5.24
Threonine	Sweet	260.00	0.53	1.10	1.44	1.26	0.14
Serine	Sweet	150.00	0.52	0.72	0.45	0.10	0.02
Glutamic acid	Umami	5.00	100.93	79.30	147.84	89.50	19.95
Glycine	Sweet	110.00	0.42	0.29	0.45	0.20	0.17
Alanine	Sweet	60.00	5.44	3.45	6.82	2.25	1.42
Valine	Bitterness	150.00	1.09	0.78	0.78	0.35	0.32
Methionine	Bitterness	30.00	0.00	0.24	0.00	0.00	0.00
Isoleucine	Bitterness	90.00	1.13	0.37	0.67	0.14	0.25
Leucine	Bitterness	380.00	0.44	0.17	0.27	0.04	0.17
Tyrosine	Tasteless	260.00	0.25	0.33	0.61	0.12	0.15
Phenylalanine	Bitterness	150.00	0.77	0.87	1.44	0.31	0.31
Lysine	Tasteless	50.00	1.33	1.59	3.02	0.69	0.14
Histidine	Bitterness	20.00	1.34	1.39	2.60	0.44	0.38
Arginine	Bitterness	10.00	10.64	6.23	5.73	5.53	2.38
Proline	Sweet	300.00	0.09	0.00	0.13	0.00	0.11

value in an ideal protein should reach about 40%, and the EAA/NEAA value should be above 60% [31]. The results (Table 3) showed that the value of EAA/(EAA + NEAA) was between 32.20% and 41.87%, and the value of EAA/NEAA was 47.48%–72.03%. In contrast, among the 5 kinds of edible fungus powders, *Lentinus edodes* edible fungus powder had the lowest EAA/(EAA + NEAA) and EAA/NEAA values, and *Pleurotus citrinopileatus* edible fungus powder best met the ideal protein standard.

**3.4. The Difference in Taste Characteristics and Taste Activity Values.** The determination of hydrolyzed amino acids was mainly to study their nutritional properties. The flavored amino acids in structural proteins are mostly in a combined state and have little effect on flavor, while free amino acids are mainly used to participate in the formation of taste substances. Therefore, the taste characteristics of free amino acids in the five test samples were compared, and they were divided into 4 categories: umami amino acids, sweet amino acids, bitterness amino acids, and tasteless

amino acids [32]. The results (Table 4) showed that *Pleurotus citrinopileatus* edible fungus powder, *Flammulina velutipes* edible fungus powder, and *Lentinus edodes* edible fungus powder had the highest content of sweet amino acids. *Agrocybe chaxinggu* edible fungus powder and *Hericium erinaceus* edible fungus powder had the highest content of bitterness amino acids.

The absolute content and relative ratio of flavored amino acids may be closely related to the taste of the food. Therefore, the taste active value (TAV) of 16 amino acids in 5 kinds of test samples was analyzed and compared. TAV is the ratio of the content of each taste amino acid in the sample to its corresponding taste threshold [33]. In general, when  $TAV > 1$ , the taste-producing substance is considered to have a significant impact on the taste-producing effect of the sample; when  $TAV < 1$ , it means that the substance has no significant taste-producing effect [34]. The results (Table 5) showed that among the 5 edible fungus powders, the TAV values of aspartic acid, glutamic acid, alanine, and arginine were also greater than 1. The TAV values of serine, glycine, methionine, leucine, tyrosine, and proline were also

TABLE 6: Correlation analysis of free amino acids in 5 kinds of edible fungus powders.

Amino acids	Aspartic acid	Threonine	Serine	Glutamic acid	Glycine	Alanine	Valine	Methionine	Isoleucine	Leucine	Tyrosine	Phenylalanine	Lysine	Histidine	Arginine	Proline
Aspartic acid	1															
Threonine	-0.320	1														
Serine	0.271	0.349	1													
Glutamic acid	0.200	0.783	0.502	1												
Glycine	0.519	0.333	0.680	0.819	1											
Alanine	0.385	0.457	0.624	0.888*	0.983**	1										
Valine	0.699	0.122	0.839	0.583	0.889*	0.799	1									
Methionine	-0.296	0.214	0.670	-0.101	-0.073	-0.106	0.195	1								
Isoleucine	0.842	-0.119	0.545	0.493	0.867	0.772	0.910*	-0.197	1							
Leucine	0.802	-0.276	0.493	0.353	0.807	0.702	0.860	-0.198	0.980**	1						
Tyrosine	-0.153	0.577	0.559	0.767	0.763	0.843	0.492	0.111	0.379	0.351	1					
Phenylalanine	0.007	0.557	0.682	0.808	0.856	0.908*	0.646	0.160	0.515	0.475	0.982**	1				
Lysine	-0.023	0.697	0.634	0.894*	0.833	0.906*	0.591	0.117	0.449	0.375	0.968**	0.981**	1			
Histidine	0.047	0.555	0.657	0.832	0.878	0.930*	0.655	0.100	0.546	0.501	0.978**	0.998**	0.983**	1		
Arginine	0.874	0.119	0.624	0.527	0.707	0.605	0.875	0.023	0.832	0.728	0.134	0.311	0.320	0.337	1	
Proline	0.146	-0.343	-0.173	0.118	0.419	0.431	0.159	-0.593	0.449	0.556	0.432	0.382	0.284	0.408	-0.102	1

Note: relevance is Pearson's type; \* significant correlation ( $p < 0.05$ ); \*\* extremely significant correlation ( $p < 0.01$ ).

TABLE 7: Results of principal component analysis.

Component	Initial eigenvalue			Rotate the sum of squares loading		
	Total	Variance (%)	Accumulate (%)	Total	Variance (%)	Accumulate (%)
1	9.241	57.759	57.759	7.125	44.532	44.532
2	3.455	21.592	79.351	5.259	32.869	77.402
3	2.183	13.645	92.996	1.916	11.977	89.378
4	1.121	7.004	100	1.699	10.622	100

TABLE 8: Contribution value of element principal component.

Amino acids	Component			
	1	2	3	4
Aspartic acid	0.432	0.854	0.178	-0.228
Threonine	0.417	-0.750	0.176	-0.482
Serine	0.745	-0.103	0.589	0.296
Glutamic acid	0.843	-0.301	-0.045	-0.443
Glycine	0.991	0.112	-0.064	-0.031
Alanine	0.984	-0.040	-0.148	-0.089
Valine	0.882	0.334	0.315	0.104
Methionine	0.037	-0.397	0.776	0.488
Isoleucine	0.809	0.587	-0.011	0.029
Leucine	0.743	0.634	-0.089	0.195
Tyrosine	0.814	-0.490	-0.256	0.176
Phenylalanine	0.902	-0.377	-0.131	0.163
Lysine	0.884	-0.454	-0.112	-0.017
Histidine	0.917	-0.344	-0.164	0.117
Arginine	0.675	0.510	0.443	-0.295
Proline	0.349	0.253	-0.847	0.311

less than 1. The TAV of free amino acid in *Agrocybe chaxinggu* edible fungus powder was between 0.00 and 100.93. The TAV of free amino acid in *Pleurotus citrinopileatus* edible fungus powder was between 0.00 and 79.30. The TAV of free amino acid in *Flammulina velutipes* edible fungus powder was between 0.00 and 147.84. The TAV of free amino acid in *Lentinus edodes* edible fungus powder was between 0.00 and 89.50. The TAV of free amino acid in *Hericium erinaceus* edible fungus powder was between 0.00 and 19.95. According to the TAV value, the most significant free amino acid that affects the taste of the 5 edible fungus powders that can be screened out was glutamic acid in the umami amino acid, followed by aspartic acid in umami amino acids, arginine in bitterness amino acids, and alanine in sweet amino acids. And *Flammulina velutipes* edible fungus powder has the most outstanding umami.

**3.5. Correlation Analysis and PCA of Free Amino Acids.** A correlation analysis was performed on the 16 free amino acid components of 5 edible fungus powders, and the results are shown in Table 6. There were positive correlations and negative correlations between amino acids, and most of them were positive. The results showed that there was a strong correlation between the free amino acids of the five edible fungus powders, which could be comprehensively evaluated by PCA.

PCA is a multivariate statistical analysis method that analyses a few variables which can reveal the internal structure sufficiently by studying the relationship between

multiple original variables [35]. According to the rule that the characteristic value is greater than 1 and the cumulative variance contribution rate is greater than 80%, four principal component factors were obtained through rotation and extraction factors, and the total contribution rate was 100%, indicating that the experimental data can fully reflect the original information (Table 7).

The first principal component was mainly composed of glycine, alanine, histidine, phenylalanine, lysine, valine, glutamic acid, tyrosine, isoleucine, serine, leucine, and arginine. The second principal component was mainly composed of aspartic acid, leucine, isoleucine, and arginine. And the third principal component was mainly composed of methionine and serine (Table 8).

### 3.6. Correlation Analysis and PCA of Hydrolyzed Amino Acids.

A correlation analysis was performed on the 16 hydrolyzed amino acid components of 5 edible fungus powders, and the results are shown in Table 9. The results showed that the correlation coefficients between most hydrolyzed amino acids were greater than 0.7, indicating that there were strong correlations among the 16 hydrolyzed amino acids in 5 kinds of edible fungus powders, so they could be further studied by PCA.

PCA was performed on the hydrolyzed amino acid content of the 5 samples, and the results are shown in Tables 10 and 11. It can be seen from Tables 10 and 11 that the cumulative contribution rate of the three principal components reaches 99.143%, indicating that three

TABLE 9: Correlation analysis of free amino acids in 5 kinds of edible funguses powder.

Amino acids	Aspartic acid	Threonine	Serine	Glutamic acid	Glycine	Alanine	Valine	Methionine	Isoleucine	Leucine	Tyrosine	Phenylalanine	Lysine	Histidine	Arginine	Proline
Aspartic acid	1															
Threonine	0.853	1														
Serine	0.953*	0.927*	1													
Glutamic acid	0.513	0.481	0.684	1												
Glycine	0.663	0.785	0.852	0.903*	1											
Alanine	0.576	0.444	0.692	0.948*	0.832	1										
Valine	0.607	0.783	0.817	0.875	0.995**	0.785	1									
Methionine	0.041	0.519	0.319	0.418	0.648	0.235	0.724	1								
Isoleucine	0.630	0.807	0.834	0.861	0.994**	0.769	0.999**	0.721	1							
Leucine	0.568	0.758	0.787	0.876	0.990**	0.780	0.999**	0.746	0.996**	1						
Tyrosine	0.515	0.688	0.734	0.889*	0.956*	0.734	0.964**	0.712	0.963**	0.967**	1					
Phenylalanine	0.573	0.714	0.779	0.910*	0.974**	0.777	0.975**	0.673	0.974**	0.975**	0.996**	1				
Lysine	0.435	0.612	0.673	0.917*	0.952*	0.777	0.962**	0.728	0.955*	0.970**	0.989**	0.985**	1			
Histidine	0.480	0.686	0.717	0.886*	0.969**	0.753	0.983**	0.769	0.979**	0.989**	0.988**	0.986**	0.993**	1		
Arginine	0.548	0.737	0.772	0.885*	0.988**	0.790	0.997**	0.746	0.993**	0.999**	0.966**	0.974**	0.974**	0.990**	1	
Proline	0.932*	0.817	0.824	0.178	0.414	0.245	0.369	-0.057	0.402	0.324	0.266	0.318	0.158	0.225	0.297	1

Note: relevance is Pearson's type; \* significant correlation ( $p < 0.05$ ); \*\* extremely significant correlation ( $p < 0.01$ ).

TABLE 10: Results of principal component analysis.

Component	Initial eigenvalue			Rotate the sum of squares loading		
	Total	Variance (%)	Accumulate (%)	Total	Variance (%)	Accumulate (%)
1	12.568	78.547	78.547	6.213	38.834	38.834
2	2.294	14.335	92.882	5.491	34.318	73.152
3	1.002	6.261	99.143	4.158	25.99	99.143

TABLE 11: Contribution value of element principal component.

Amino acids	Component		
	1	2	3
Aspartic acid	0.674	0.732	-0.100
Threonine	0.805	0.474	0.355
Serine	0.861	0.508	-0.018
Glutamic acid	0.889	-0.176	-0.419
Glycine	0.998	-0.017	-0.035
Alanine	0.805	-0.027	-0.562
Valine	0.994	-0.077	0.049
Methionine	0.657	-0.467	0.582
Isoleucine	0.996	-0.045	0.073
Leucine	0.989	-0.126	0.054
Tyrosine	0.964	-0.185	0.022
Phenylalanine	0.980	-0.126	-0.023
Lysine	0.952	-0.288	-0.037
Histidine	0.971	-0.232	0.047
Arginine	0.985	-0.152	0.036
Proline	0.436	0.889	0.131

TABLE 12: Comprehensive scores of 5 edible fungus powder.

Sample	Free amino acid		Hydrolyzed amino acid	
	Comprehensive score	Rank	Comprehensive score	Rank
<i>Agrocybe chaxinggu</i> edible fungus powder	2.040	1	2.027	1
<i>Pleurotus citrinopileatus</i> edible fungus powder	0.065	3	1.180	2
<i>Flammulina velutipes</i> edible fungus powder	0.733	2	-0.844	4
<i>Lentinus edodes</i> edible fungus powder	-1.424	5	-0.381	3
<i>Hericium erinaceus</i> edible fungus powder	-1.413	4	-1.979	5

components can represent the information of all hydrolyzed amino acids in 5 kinds of edible fungus powders and can better reflect the relationship of free amino acids in 5 kinds of edible fungus powders.

The first principal component was mainly composed of glycine, isoleucine, valine, leucine, arginine, phenylalanine, histidine, tyrosine, lysine, glutamic acid, serine, alanine, threonine, aspartic acid, and methionine. The second principal component was mainly composed of proline, aspartic acid, and serine. And the third principal component was mainly composed of methionine (Table 11).

**3.7. Comprehensive Evaluation.** A comprehensive evaluation model was established based on the contribution rates of the eigenvalues corresponding to the three principal components of hydrolyzed amino acids and the four principal components of free amino acids. The free amino acid model was  $F = 0.445F_1 + 0.329F_2 + 0.120F_3 + 0.106F_4$ . The hydrolyzed amino acid model was  $F' = 0.392F'_1 + 0.346F'_2 + 0.262F'_3$ . A comprehensive score was calculated for each sample, followed

by ranking and evaluating the amino acid content of each sample. It can be seen from Table 12 that the comprehensive scores of hydrolyzed amino acids and free amino acids of *Agrocybe chaxinggu* edible fungus powder were greater than those of other varieties, indicating that the comprehensive quality of hydrolyzed amino acids and free amino acids of this variety was higher, and it is a variety with better amino acid quality.

#### 4. Conclusions and Discussion

In this study, the composition and content of free amino acids and hydrolyzed amino acids of *Agrocybe chaxinggu* edible fungus powder, *Pleurotus citrinopileatus* edible fungus powder, *Flammulina velutipes* edible fungus powder, *Lentinus edodes* edible fungus powder, and *Hericium erinaceus* edible fungus powder were analyzed. The results showed that the total amount of hydrolyzed amino acids contained in the 5 edible fungus powders was between 2.583 and 14.656 g/100 g. The total amount of free amino acids contained in the 5 edible fungus powders was between

0.550 and 2.612 g/100 g. The total amount of hydrolyzed amino acids was relatively large, which may be caused by the simultaneous thermal degradation and Maillard reaction, which hydrolyzed macromolecular proteins or polypeptides into small molecular amino acids. Comparative analysis of the mass fractions and composition of amino acids indicated that *Pleurotus citrinopileatus* edible fungus powder best met the ideal protein standard. The delicious taste of edible fungus powder is determined by the balance and mutual influence of different free amino acids, which play an important role in the taste of edible fungus powder. In this study, the TAV of free amino acids of five edible fungus powders was evaluated. The TAV of amino acids is related to water solubility. Water-soluble amino acids may be partly due to hydrolysis, or may be due to water-solubility in nature, which was related to the structure and properties of the amino acids themselves [36]. The most significant free amino acid that affects the taste of the 5 edible fungus powders which can be screened out was the glutamic acid in the umami amino acid. And *Flammulina velutipes* edible fungus powder has the most outstanding umami. However, the amino acids alone might not be good enough to be responsible for the taste. Fatty acids might also contribute a lot in forming the taste. The taste of edible fungus powder was systematically evaluated, and the results of fatty acids need to be determined later [37]. PCA extracted four principal components from 16 free amino acids with a cumulative variance contribution rate of 100%, and extracted three principal components from 16 hydrolyzed amino acids with a cumulative variance contribution rate of 99.143%, which can better reflect the comprehensive information on the quality of the 5 edible fungus powders. A comprehensive evaluation model was established, and the comprehensive quality of amino acids in *Agrocybe chaxinggu* edible fungus powder was the best. This paper only studies the amino acid compositions and contents of 5 edible fungus powders at present. Further research will collect more edible fungus powder samples to determine their amino acid composition and content in order to establish a more detailed edible fungus powder quality evaluation system, laying a theoretical foundation for the development of edible fungus resources.

### Data Availability

The data used to support the findings of this study are included within the article.

### Disclosure

Jian Li and Junmei Ma are the co-first authors.

### Conflicts of Interest

The authors declare that they have no conflicts of interest.

### Authors' Contributions

Jian Li and Junmei Ma contributed equally to this paper. YZ and SQM conceived and designed the study. JL and JMM

performed the experiments. JL and JMM wrote the paper. YZ, SQM, and SSF reviewed and edited the manuscript. All authors read and approved the manuscript.

### Acknowledgments

This work was supported by National Key Research and Development Program of China (Project no. 2018YFC1311400).

### References

- [1] P Kalač, "A review of chemical composition and nutritional value of wild-growing and cultivated mushrooms," *Journal of the Science of Food and Agriculture*, vol. 93, no. 2, pp. 209–218, 2013.
- [2] Y. Zhang, C. Venkatasamy, Z. Pan, and W. Wang, "Recent developments on umami ingredients of edible mushrooms—a review," *Trends in Food Science & Technology*, vol. 33, no. 2, pp. 78–92, 2013.
- [3] S. T. Chang, "Overview of mushroom cultivation and utilization as functional foods," *Mushrooms as functional foods*, vol. 260, 2008.
- [4] T. Girish and M. K. Rai, "Biotechnological potential of mushrooms: drugs and dye production," *International Journal of Medicinal Mushrooms*, vol. 8, no. 4, 2006.
- [5] H. Kawagishi, "Function of mushrooms and their active principles," *Food Style*, vol. 7, no. 9, pp. 70–73, 2003.
- [6] H. Kawagishi, M. Ando, T. Mizuno, H. Yokota, and S. Konishi, "A novel fatty acid from the mushroom *Hericium erinaceum*," *Agricultural & Biological Chemistry*, vol. 54, no. 5, pp. 1329–1331, 1990.
- [7] V. M. Dembitsky, A. O. Terent'ev, and D. O. Levitsky, "Amino and fatty acids of wild edible mushrooms of the genus *boletus*," *Records of Natural Products*, vol. 4, no. 4, pp. 218–223, 2010.
- [8] R. Ana, B. Sunčica, and Š. Zdenko, "Analysis of nucleosides and monophosphate nucleotides from mushrooms with reversed-phase HPLC," *Journal of Separation Science*, vol. 33, no. 8, pp. 1024–1033, 2010.
- [9] S. J. M. Mdachi, M. H. H. Nkunya, V. A. Nyigo, and I. T. Urasa, "Amino acid composition of some Tanzanian wild mushrooms," *Food Chemistry*, vol. 86, no. 2, pp. 179–182, 2004.
- [10] R. Bonku and J. Yu, "Health aspects of peanuts as an outcome of its chemical composition," *Food Science and Human Wellness*, vol. 9, no. 1, pp. 21–30, 2020.
- [11] D. Tagkouli, A. Kaliora, G. Bekiaris et al., "Free amino acids in three pleurotus species cultivated on agricultural and agro-industrial by-products," *Molecules*, vol. 25, no. 17, p. 4015, 2020.
- [12] J. W. Xia, Y. R. Ma, Z. Li, and X. G. Zhang, "Acrodictys-like wood decay fungi from southern China, with two new families Acrodictyceae and Junewangiaceae," *Scientific Reports*, vol. 7888, pp. 1–21, 2017.
- [13] S.-Y. Tsai, T.-P. Wu, S.-J. Huang, and J.-L. Mau, "Nonvolatile taste components of *Agaricus bisporus* harvested at different stages of maturity," *Food Chemistry*, vol. 103, no. 4, pp. 1457–1464, 2007.
- [14] J.-L. Mau, Y.-L. Chen, R.-C. Chien, Y.-C. Lo, and S.-D. Lin, "Taste quality of the hot water extract from *Flammulina velutipes* and its application in umami seasoning," *Food Science and Technology Research*, vol. 24, no. 2, pp. 201–208, 2018.

- [15] J.-L. Mau, "The umami taste of edible and medicinal mushrooms," *International Journal of Medicinal Mushrooms*, vol. 7, no. 1-2, pp. 119–126, 2005.
- [16] Z. Chen, H. Gao, W. Wu et al., "Effects of fermentation with different microbial species on the umami taste of Shiitake mushroom (*Lentinus edodes*)," *Lebensmittel-Wissenschaft & Technologie*, vol. 141, Article ID 110889, 2021.
- [17] D. Kumari, M. S. Reddy, and R. C. Upadhyay, "Nutritional composition and antioxidant activities of 18 different wild *Cantharellus* mushrooms of Northwestern Himalayas," *Food Science and Technology International*, vol. 17, no. 6, pp. 557–567, 2010.
- [18] S.-Y. Chen, K.-J. Ho, Y.-J. Hsieh, L.-T. Wang, and J.-L. Mau, "Contents of lovastatin,  $\gamma$ -aminobutyric acid and ergothioneine in mushroom fruiting bodies and mycelia," *Lebensmittel-Wissenschaft & Technologie*, vol. 47, no. 2, pp. 274–278, 2012.
- [19] M. M. Poojary, V. Orlien, P. Passamonti, and K. Olsen, "Enzyme-assisted extraction enhancing the umami taste amino acids recovery from several cultivated mushrooms," *Food Chemistry*, vol. 234, pp. 236–244, 2017.
- [20] D. Luo, J. Wu, Z. Ma, P. Tang, X. Liao, and F. Lao, "Production of high sensory quality Shiitake mushroom (*Lentinus edodes*) by pulsed air-impingement jet drying (AID) technique," *Food Chemistry*, vol. 341, Article ID 128290, 2021.
- [21] D. Liu, Y.-Q. Chen, X.-W. Xiao et al., "Nutrient properties and nuclear magnetic resonance-based metabonomic analysis of macrofungi," *Foods*, vol. 8, no. 9, p. 397, 2019.
- [22] L. Y. Zhou, W. Li, and W. J. Pan, "Effects of thermal processing on nutritional characteristics and non-volatile flavor components from *Tricholoma lobayense*," *Emirates Journal of Food and Agriculture*, vol. 29, no. 4, pp. 285–292, 2017.
- [23] W. Tang, C. Liu, J. Liu et al., "Purification of polysaccharide from *Lentinus edodes* water extract by membrane separation and its chemical composition and structure characterization," *Food Hydrocolloids*, vol. 105, Article ID 105851, 2020.
- [24] X. Li, Y. Guo, Y. Zhuang, Y. Qin, and L. Sun, "Nonvolatile taste components, nutritional values, bioactive compounds and antioxidant activities of three wild *Chanterelle* mushrooms," *International Journal of Food Science and Technology*, vol. 53, no. 8, pp. 1855–1864, 2018.
- [25] Z. Qing, J. Cheng, X. Wang, D. Tang, X. Liu, and M. Zhu, "The effects of four edible mushrooms (*Volvariella volvacea*, *Hypsizygus marmoreus*, *Pleurotus ostreatus* and *Agaricus bisporus*) on physicochemical properties of beef paste," *Lebensmittel-Wissenschaft & Technologie*, vol. 135, Article ID 110063, 2021.
- [26] X. Wang, P. Zhou, J. Cheng, Z. Chen, and X. Liu, "Use of straw mushrooms (*Volvariella volvacea*) for the enhancement of physicochemical, nutritional and sensory profiles of Cantonese sausages," *Meat Science*, vol. 146, pp. 18–25, 2018.
- [27] D. Li, D. Wang, Y. Fang et al., "A novel phase change coolant promoted quality attributes and glutamate accumulation in postharvest shiitake mushrooms involved in energy metabolism," *Food Chemistry*, vol. 351, Article ID 129227, 2021.
- [28] T. Ming, J. Li, P. Huo, Y. Wei, and X. Chen, "Analysis of free amino acids in *russula griseocarnosa* harvested at different stages of maturity using iTRAQ-LC-MS/MS," *Food analytical methods*, vol. 7, no. 9, pp. 1816–1823, 2014.
- [29] GB 5009 124-2016, "National Food Safety Standards Determination of Amino Acids in Food," 2016.
- [30] GB/T 30987-2020, "Determination of Free Amino Acids in Plant," 2020.
- [31] J. Lv, L. Wei, Y. Yang et al., "Amino acid substitutions in the neuraminidase protein of an H9N2 avian influenza virus affect its airborne transmission in chickens," *Veterinary Research*, vol. 46, no. 44, pp. 44–10, 2015.
- [32] X. Yu, M. J. Chen, and C. H. Li, "Effects of culture substrates on nutritional and flavor components of *Volvariella volvacea*," *Mycosystema*, vol. 37, no. 12, pp. 1731–1740, 2018.
- [33] J. Y. Duan, Z. Y. Li, and J. Li, "Comparison of nutritional and flavor characteristics between four edible fungi and four fruits and vegetables based on components and characteristics of free amino acids," *Mycosystema*, vol. 39, no. 6, pp. 1077–1089, 2020.
- [34] M. Lu, H. M. An, and X. H. Zhao, "Analysis of amino acids in *Rosa sterilis* and *Rosa roxburghii* fruits," *Food Science*, vol. 36, no. 14, pp. 118–121, 2015.
- [35] Y. Ma, X. X. Yuan, L. N. Liu et al., "Multielement principal component analysis and origin traceability of rice based on ICP-ms/MS," *Journal of Food Quality*, vol. 2021, pp. 1–12, Article ID 5536241, 2021.
- [36] Y. Zhou and H. Yang, "Effects of calcium ion on gel properties and gelation of tilapia (*Oreochromis niloticus*) protein isolates processed with pH shift method," *Food Chemistry*, vol. 277, pp. 327–335, 2019.
- [37] M. Golebiowski, A. Ostachowska, and M. Paszkiewicz, "Fatty acids and amino acids of entomopathogenic fungus *Conidiobolus coronatus* grow on minimal and rich media," *Chemical Papers*, vol. 70, pp. 1360–1369, 2016.

## Research Article

# Structure and Menthone Encapsulation of Corn Starch Modified by Octenyl Succinic Anhydride and Enzymatic Treatment

Xuan Ji,<sup>1,2,3</sup> Jing Du,<sup>1,2,3</sup> Jiaying Gu,<sup>2</sup> Jie Yang,<sup>1,2,3</sup> Li Cheng,<sup>1,2,3</sup> Zhaofeng Li,<sup>1,2,3</sup> Caiming Li,<sup>1,2,3</sup> and Yan Hong<sup>1,2,3</sup> 

<sup>1</sup>Key Laboratory of Synthetic and Biological Colloids, Ministry of Education, Wuxi 214122, Jiangsu Province, China

<sup>2</sup>School of Food Science and Technology, Jiangnan University, Wuxi 214122, Jiangsu Province, China

<sup>3</sup>Collaborative Innovation Center of Food Safety and Quality Control, Jiangnan University, Wuxi 214122, Jiangsu Province, China

Correspondence should be addressed to Yan Hong; hongyan@jiangnan.edu.cn

Received 3 February 2022; Accepted 15 February 2022; Published 7 March 2022

Academic Editor: Tao Feng

Copyright © 2022 Xuan Ji et al. This is an open access article distributed under the Creative Commons Attribution License, which permits unrestricted use, distribution, and reproduction in any medium, provided the original work is properly cited.

In order to improve the ability of starch to absorb menthone, corn starch was modified by enzymatic treatment (amyloglucosidase and  $\alpha$ -amylase) combined with octenyl succinic anhydride (OSA) esterification. The oil absorption rate of starch modified by enzymatic treatment followed by OSA (P-OSA) reached 101.33%, whereas that of samples with reverse action sequences (OSA-P) was only 59.67%. The degree of substitution of OSA-P was also generally lower than that of P-OSA. At high OSA addition, OSA-P had a smaller specific surface area with fewer pores because octenyl succinic (OS) groups impeded the enzymatic treatment. Compared with OSA-P, the lamellar structure of P-OSA is sparser and less ordered. Owing to its pores, P-OSA was beneficial for the reaction to occur inside the granules, which was observed by Raman spectroscopy and laser confocal microscopy. At high OSA addition, the loading of P-OSA to menthone could reach 64.34 mg/g.

## 1. Introduction

Porous starch is characterized by numerous dents or pores extending to the interior of starch granules. It has higher absorption and slow-release properties than native starch owing to its higher specific surface area. In recent years, porous starch has attracted increasing attention due to its low price, valuable functions, and potential applications [1]. Several approaches, including physical, chemical, enzymatic, and synergic methods, have been used to promote the formation of pores in starch [2]. Porous starch prepared by traditional physical methods, such as mechanical extrusion, microwave, and ultrasonic methods, has a low yield and nonuniform pore size, whereas those derived from chemical methods, including solvent exchange, acid hydrolysis, and molecular insertion, result in porous starch with limited absorption capacity and formation of organic solvent residues during the preparation process. Enzyme catalysis has been widely used for the preparation of porous starch

because of the advantages of mild reaction conditions, high catalytic efficiency, and substrate specificity [3].

The absorption capacity of porous starch is influenced by the nature of the raw material, the method of preparation, the absorption conditions, and the nature of the adsorbate, while the absorption capacity per gram of porous starch is generally in the tens of milligrams [4]. Because starch is a hydrophilic substance, porous starch has a weaker absorption capacity for hydrophobic substances than for hydrophilic substances. To improve the porous starch absorption capacity of hydrophobic substances, hydrophobic groups can be introduced by chemical modification. Owing to its hydrophobicity and steric contribution, octenyl succinic anhydride (OSA) can be combined with starch to enhance its hydrophobicity, encapsulation, and emulsification properties [5]. Several studies have explored the combination of porous treatment with esterification modification on starch granules [6–8]. Such studies demonstrated that OSA-modified porous starch has significantly enhanced capacity



to absorb oils; thus, it could be applied to adsorb hydrophobic substances. Moreover, the presence of pores affects the reaction of the OSA reagent during the esterification modification process, which in turn impacts on the structure and properties of the starch.

Porous starch is mainly used for the absorption of hydrophilic substances, but its ability to adsorb hydrophobic substances is relatively weak. OSA, as a common emulsifier, can impart amphiphilicity to starch and improve its absorption ability to hydrophobic substances. However, there are few studies on the effect of esterification modification on the absorption performance of porous starch and its mechanism, and there is a lack of comparison of the effects of the two reversing treatments on the structure and properties of starch. In this study, amyloglucosidase and  $\alpha$ -amylase were used to prepare porous starch. The differences in the absorption properties of hydrophobic porous starches prepared by reversing the order of the two treatments were compared, and the influence of starch structure that caused the differences in absorption properties was investigated. Further, hydrophobic porous starch was applied to load menthone.

## 2. Materials and Methods

**2.1. Materials.** Native corn starch (moisture: 12.36 g/100 g; amylose content:  $21.73 \pm 0.81\%$ ) was provided from Juneng Golden Corn Co., Ltd. (Shandong, China). Amyloglucosidase (EC 3.2.1.3, 20,000 U/mL) was purchased from Genencor International (Palo Alto, CA, USA), and  $\alpha$ -amylase (EC 3.2.1.1, 10,000 U/mL) was purchased from Sukahan (Weifang) Bio-Technology Co., Ltd. Octenyl succinic anhydride (OSA) was provided by Huahao Huafeng Co., Ltd. (Guangdong, China). Menthone was purchased from Shanghai Aladdin Biochemical Technology Co., Ltd. Other reagents were purchased from China National Pharmaceutical Group Co., Ltd. (Shanghai, China) and were all of analytical grade.

### 2.2. Preparation of Hydrophobic Porous Starch

**2.2.1. Preparation of Porous Starch.** Porous starch preparation was based on the method described by Zhang et al. [9] with some modifications. First, a weighed quantity of native corn starch was suspended in phosphate buffer (pH 5.5, 30% w/w). A mixture (2:1, v/v) of glucoamylase and  $\alpha$ -amylase was added to the starch slurry at 2.0% (v/w) and was incubated at 50°C for 6 h. After the enzymatic reaction, the pH was adjusted to 3.5 by adding 0.1 M hydrochloric acid to inactivate the enzymes, and the solution was neutralized to pH 7.0 with 0.1 M NaOH solution. Next, the mixture was filtered and the precipitate was washed three times with deionized water. The final product was dried, milled, and stored for further use.

**2.2.2. Preparation of OSA Starch.** OSA starch was prepared based on the method described by Song et al. [10] with some modifications. A certain mass of starch was stirred and suspended in deionized water (30%, w/w) at 35°C. The pH of

the suspension was adjusted up to 8.5 by adding 3% NaOH solution. A weighed quantity of OSA (3, 6, and 9% of the dry starch basis) was diluted with absolute ethanol (1:3, v/v) added slowly over a period of 2 h while maintaining the pH at 8.5. The reaction was allowed to continue for additional 2 h, after which the pH was adjusted to 6.5 with 3% HCl solution. The mixture was centrifuged and washed twice with deionized water and twice with 70% aqueous alcohol. The precipitate was oven-dried at 40°C for 24 h and then passed through a 100-mesh sieve.

OSA-modified porous starch (P-OSA) samples were prepared using corn starch that was first transformed into porous starch and then modified with OSA, whereas OSA-P samples were prepared with reversed treatment sequences (corn starch was first modified with OSA and then hydrolyzed by enzymes).

**2.3. Degree of Substitution.** The OSA content in starch granules is indicated by the degree of substitution (DS). DS was examined according to a previously described method with some modifications [5]. The starch sample (5 g) was dispersed in 2.5 M HCl/isopropyl alcohol solution (25 mL) by stirring for 30 min. An aqueous 90% (v/v) isopropanol solution (100 mL) was added, and the mixture was stirred for 10 min. After filtration, the residue was washed with 90% isopropanol until no more  $\text{Cl}_2$  could be detected (using 0.1 M  $\text{AgNO}_3$  solution). The starch was redispersed in 300 mL of deionized water in a boiling water bath for 20 min. The starch was titrated with a 0.1 M NaOH solution using phenolphthalein as an indicator. Native starch was used as blank control. The DS was calculated according to the following equation:

$$DS = \frac{0.162 \times (A \times M)/W}{1 - [0.210 \times (A \times M)]/W}, \quad (1)$$

where  $A$  is the titration volume of NaOH solution (mL),  $M$  is the molarity of the NaOH solution, and  $W$  is the dry weight (g) of the OSA starch.

### 2.4. Absorption Properties

**2.4.1. Oil Absorption Rate.** A quantity of starch was dried at 105°C for 4 h and immersed in 30 mL of soybean salad oil. After stirring at 25°C for 30 min, the mixture was placed in a sand core funnel of known mass and filtered until no oil drops fell. The total mass of the sand core funnel and starch was weighed, and the oil absorption rate was calculated according to the following equation:

$$\text{oil absorption rate (\%)} = \frac{m_2 - m_1 - m_0}{m_1} \times 100, \quad (2)$$

where  $m_0$  and  $m_1$  represent the weight of the sand core funnel and the starch, respectively, and  $m_2$  is the weight of the mixture after filtration.

**2.4.2. Absorption of Methylene Blue.** The absorption of methylene blue (MB) of starch samples was measured in terms of the method described by Xie et al. [11] with some

modifications. The starch samples (0.5 g) were dried at 105°C for 4 h and immersed in 30 mL of MB solution (40 mg/L). After stirring for 2 h, the samples were centrifuged at 3,000 rpm for 10 min, and the absorbance of the supernatant was measured at 665 nm using a spectrophotometer (T-6V; Persee Analytics, Auburn, CA, USA). The equilibrium absorption capacity was calculated according to the following equation:

$$Q_e = \frac{V(C_0 - C_e)}{m}, \quad (3)$$

where  $Q_e$  represents the equilibrium absorption capacity of starch sample (mg/g),  $C_0$  and  $C_e$  represent the initial and equilibrium concentrations of MB solution (mg/L), respectively, and  $V$  and  $m$  represent the volume of MB solution (mL) and the weight of starch sample (g), respectively.

**2.5. Contact Angle.** The hydrophobicity of the starch samples is indicated by the magnitude of the contact angle. The starch samples were pressed into sheets. The contact angle was measured using an OCA15EC optical contact angle meter equipped with a CDD camera and WINDROP software, and the measurement method was a sitting drop method with a volume of 2.5  $\mu$ L of injection water [12].

**2.6. Starch Granule Morphology Assessment.** The morphology of starch samples was observed by using a field-emission scanning electron microscope (SU8100; Hitachi Int., Japan) as described by Xie et al. [2]. Starch samples were spilled on a carrier table with a silver plate and coated with a layer of gold in vacuum prior to observation. Samples were examined at an accelerating voltage of 1.0 kV, and images were taken at 2000x and 5000x magnifications.

**2.7. Specific Surface Area and Pore Diameter Assessment.** The specific surface area and pore diameter of the starch samples were estimated using the Autosorb-iQ surface area and pore size analyzer (Quantachrome Instruments, Boynton Beach, FL, USA) by measuring the absorption of liquid nitrogen. Before measurement, the starch samples were dried under vacuum at 150°C for 2 h. The isotherm of nitrogen absorption-desorption at liquid nitrogen temperature (77.35 K) was determined. The specific surface area and the pore size were analyzed by the Barrett–Joyner–Halenda method [13].

**2.8. Lamellar Structure Evaluation.** The lamellar structure of the starch samples was determined by small-angle X-ray scattering (SAXSpoint 2.0, Anton Paar, Graz, Austria). The starch samples were configured as starch paste with 50% moisture content equilibrated at room temperature for 24 h. The acceleration voltage was 50 kV, and the current was 1 mA. The scattering intensity  $I(q)$  was obtained as a function of the scattering vector  $q$  by radially averaging each homogeneous scattering intensity and subtracting the blank group [14].

**2.9. Relative Crystallinity.** The crystalline features were analyzed using an X-ray diffractometer (Bruker AXS, D2 PHASER, Germany). The diffraction angle ( $2\theta$ ) ranged from 4 to 40°. The scanning speed was set to 2°/min with a step size of 0.05°. The relative crystallinity was calculated using JADE 7.0 software (Materials Data Inc., Livermore, USA) based on the ratio of the area of the crystalline peaks to the total area of the diffractogram.

#### 2.10. Distribution of Octenyl Succinic Groups on Starch Granules

**2.10.1. Raman Spectroscopy Analysis.** Spectral data were recorded in the 400–2,000  $\text{cm}^{-1}$  range with a 532 nm laser using LabRAM HR Evolution (HORIBA Jobin Yvon SAS, Longjumeau, France). An area of 1.2 mm  $\times$  1.2 mm was selected, and 100 points and two spectral images were randomly acquired with a single point acquisition time of 15 s, an accumulation time of 2 s, and a Real Time Display time of 2 s. The synthesized two-dimensional images in the  $x$  and  $y$  directions provided spatial information, while the third dimension ( $z$ ) indicated intensity [15].

**2.10.2. Laser Confocal Microscopy Analysis.** Distribution of the octenyl succinic (OS) groups within the starch granules was determined using a confocal laser scanning microscope (LSM880; Carl Zeiss, Oberkochen, Germany) equipped with an argon ion laser, as previously described [16, 17]. The lens used was 40 $\times$ /1.25, and the gas laser argon laser emission wavelength was 514 nm. The samples (0.5 g) were suspended in 30 mL of deionized water. The starch suspension at pH 8.0 was stained with 1% MB solution. The mixture was incubated in a shaking water bath at room temperature for 8 h, and the excess dye was removed with methanol.

**2.11. Preparation of Menthone Complexes.** A certain mass of starch sample was weighed in a centrifuge tube with cap, about 2–3 times the mass of menthone was added, shaken for a period of time to make it dispersed, and then centrifuged at 3000 r/min for 10 min, and the precipitate was washed quickly with anhydrous ethanol to remove the unadsorbed menthone. The precipitate was dried to obtain the starch-menthone complex.

**2.12. Menthone Loading Determination.** After weighing 100 mg of the complex and dispersing it in 5 ml of methanol, the mixture was sealed, sonicated for 30 min, left overnight to dissolve menthone in methanol, and then centrifuged at 4000 r/min for 10 min to obtain a clarified supernatant. The absorbance of the supernatant was measured, and the content of menthone in the complex was calculated using the regression equation.

**2.13. Statistical Analysis.** All experiments were performed at least in triplicate. All results were expressed as mean  $\pm$  standard deviation (SD). Data were analyzed by one-way analysis of variance (ANOVA) followed by Tukey's test using

the SPSS 17.0 statistical software program (SPSS Inc., Chicago). Values of  $P < 0.05$  were considered statistically significant.

### 3. Results and Discussion

**3.1. Absorption Properties, Contact Angles, and DS.** The starch absorption capacity of hydrophobic substances was determined by the absorption of oil and MB (Table 1). The presence of pores increased the oil absorption rate by 3-fold that of corn starch; however, no significant increase in oil absorption was observed for OSA starch produced by esterification modification only. When PS was esterified to produce P-OSA, it was observed that P-OSA had a higher oil absorption capacity than PS, and the oil absorption rate gradually increased with the further addition of OSA. Compared with PS, the enhancement of the absorption performance of P-OSA prepared at lower OSA additions (3% and 6%) was not significant, which was due to the fact that there were fewer OS groups attached to the starch granules at this time, so the absorption of hydrophobic substances could not be significantly increased. A significant improvement in the absorption of hydrophobic substances was observed when the amount of OSA addition was increased to 9%. In contrast, the oil absorption of OSA-P was lower than that of P-OSA. This was related to the different hydrophobic features of the samples. The interfacial wettability of solid granules can reveal the hydrophobicity of the granules. After hydrolysis of two enzymes and esterification modification, the water-oil interface contact angle of the starch granules increased (Table 1). The contact angle of the products increased with the increase of OSA addition under the same enzymatic conditions, indicating that the presence of long-chain alkenyl groups increased the hydrophobicity of the starch, which would be beneficial to increase the affinity of the starch granules to oil. In contrast, the contact angle of OSA-P was lower than that of P-OSA, and this difference led to the difference in the absorption capacity of the samples on the oil. However, the contact angle was not the only indicator affecting the absorption capacity, which resulted in a lower contact angle for PS samples than OSA samples, but a higher oil absorption capacity for PS samples than OSA samples. The contact angle of OSA9-P sample was the second highest, but its oil absorption capacity was the lowest from all dual modified samples. The causes of this phenomenon were further analyzed and discussed through the observation of starch granule morphology and specific surface area values. The absorption capacity of MB showed a similar variation pattern. The amount of MB adsorbed by porous starch was greatly increased compared with that of corn starch [18]. By comparing the DS values of different samples, the DS values after compound modification were smaller than those of OSA starch at the same OSA addition, regardless of the treatment sequences. This phenomenon may be due to the removal of amorphous regions during pretreatment [19]. Notably, the DS of OSA-P was lower than that of P-OSA with the same amount of OSA added. The decrease of DS indicated the decrease of OSA content in starch granules,

which suggests that it was difficult to avoid the part with OS groups being cut off when enzymatically digesting OSA starch.

**3.2. Morphology of Starch Granules.** Micrographs of the starch samples are shown in Figure 1. Native corn starch exhibited a spherical granular structure with a smooth surface. P-OSA and OSA-P showed a granular morphology with pores distributed on the surface, and different treatment sequences resulted in different pore distribution outcome. The degree of starch morphological variation is highly dependent on the source and properties of the starch, which is in turn due to the differences in the susceptibilities among the starches [18]. Field-emission scanning electron microscopy (FESEM) data showed that the formation of the pores was not effective when esterification modification was performed first. The number of particles with pores in the field of view gradually decreased in the presence of increasing amount of OSA. When OSA (9%) starch was treated enzymatically, only a small portion of the starch formed a structure with pores, which resulted in a weak absorption capacity of OSA9-P. The increase in the OS groups hindered the formation of additional pores. In contrast, a prior enzymatic treatment followed by OSA modification did not have a significant negative impact on the presence and distribution of pores. This was consistent with Chang et al. [6] report, which suggested that heat during the esterification reaction may alter the structure of pores already formed before the esterification modification.

**3.3. Specific Surface Area and Pore Size.** Data on the specific surface area and pore size of starch samples with different sequences of OSA modification and enzymatic treatment are shown in Table 2. Compared with porous starch, the specific surface area of P-OSA decreased, whereas the pore size increased after OSA modification. With increased OSA amount, the specific surface area of P-OSA also tended to increase, but the pore size gradually decreased. This may be due to the temperature during the reaction between OSA and the porous starch, as well as the flaking reaction of organic solvents [6]. P-OSA9 had great differences on surface area and pore size from P-OSA3 and P-OSA6. This may be due to the high concentration of OSA during the reaction process which caused the starch granules to swell, bringing about a higher specific surface area and affecting the pore size. For P-OSA, the higher specific surface area had a positive effect on its absorption performance. Although the pore size of the starch decreased at high OSA addition, the higher specific surface area and the presence of hydrophobic groups at this time ensured the superior absorption performance of the samples.

Comparing the specific surface area and pore size of starch samples obtained from two different treatment sequences, it was found that the specific surface area of OSA-P was smaller than that of P-OSA, but the pore sizes were similar. This could be related to the previous FESEM imaging data that the surface pores of OSA-P were less than those of P-OSA, which resulted in a smaller specific surface

TABLE 1: Absorption properties, DS, and contact angle of CS, PS, P-OSA, and OSA-P.

Samples	Oil (%)	MB (mg/g)	DS	Contact angle (°)
CS	25.33 ± 7.50 <sup>e</sup>	23.23 ± 0.31 <sup>j</sup>	—	19.9 ± 0.35 <sup>h</sup>
PS	82.67 ± 4.72 <sup>bc</sup>	42.53 ± 0.17 <sup>f</sup>	—	60.7 ± 0.37 <sup>g</sup>
OSA3	29.33 ± 6.03 <sup>c</sup>	25.50 ± 0.10 <sup>i</sup>	0.0122 ± 0.0023 <sup>d</sup>	63.5 ± 0.39 <sup>g</sup>
OSA6	34.00 ± 7.81 <sup>e</sup>	34.73 ± 0.56 <sup>h</sup>	0.0252 ± 0.0023 <sup>b</sup>	74.53 ± 0.41 <sup>f</sup>
OSA9	39.67 ± 6.81 <sup>e</sup>	40.76 ± 0.66 <sup>g</sup>	0.0314 ± 0.0006 <sup>a</sup>	96.6 ± 0.72 <sup>e</sup>
P-OSA3	88.00 ± 5.29 <sup>abc</sup>	45.32 ± 0.23 <sup>e</sup>	0.0054 ± 0.0003 <sup>e</sup>	125.3 ± 4.6 <sup>c</sup>
P-OSA6	92.67 ± 3.51 <sup>ab</sup>	49.66 ± 0.09 <sup>d</sup>	0.0161 ± 0.0015 <sup>cd</sup>	127.4 ± 2.1 <sup>c</sup>
P-OSA9	101.33 ± 6.43 <sup>a</sup>	57.16 ± 0.11 <sup>a</sup>	0.0232 ± 0.0007 <sup>b</sup>	143.3 ± 0.3 <sup>a</sup>
OSA3-P	79.33 ± 2.52 <sup>bc</sup>	42.04 ± 0.70 <sup>f</sup>	0.0051 ± 0.0008 <sup>e</sup>	75.6 ± 3.1 <sup>f</sup>
OSA6-P	74.67 ± 4.93 <sup>cd</sup>	51.91 ± 0.27 <sup>c</sup>	0.0136 ± 0.0015 <sup>cd</sup>	117.0 ± 0.7 <sup>d</sup>
OSA9-P	59.67 ± 7.02 <sup>d</sup>	54.43 ± 0.36 <sup>b</sup>	0.0172 ± 0.0013 <sup>c</sup>	136.2 ± 0.2 <sup>b</sup>

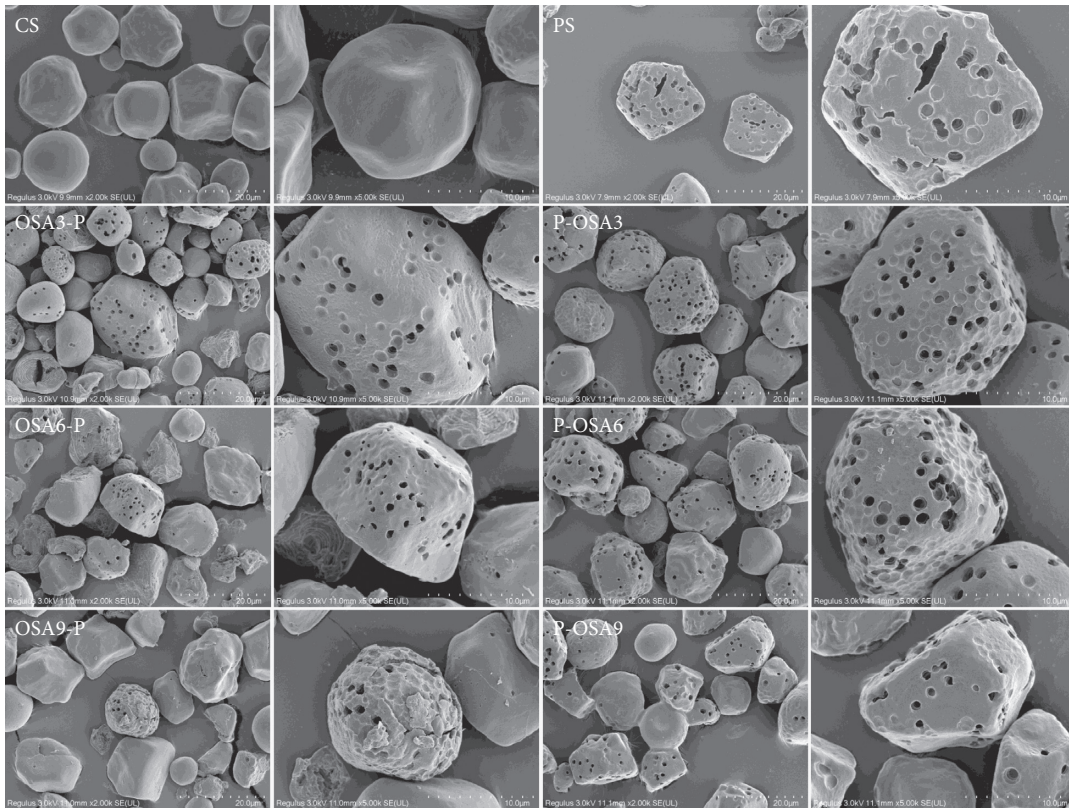


FIGURE 1: Field-emission micrographs of CS, PS, P-OSA, and OSA-P.

TABLE 2: Specific surface area and pore size of CS, PS, P-OSA, and OSA-P.

Samples	Specific surface area (m <sup>2</sup> /g)	Pore size (nm)
CS	0.516 ± 0.018 <sup>c</sup>	—
PS	0.980 ± 0.019 <sup>a</sup>	3.059 ± 0.034 <sup>b</sup>
P-OSA3	0.621 ± 0.004 <sup>cd</sup>	3.395 ± 0.016 <sup>a</sup>
OSA3-P	0.619 ± 0.018 <sup>cd</sup>	3.400 ± 0.033 <sup>a</sup>
P-OSA6	0.651 ± 0.009 <sup>c</sup>	3.398 ± 0.014 <sup>a</sup>
OSA6-P	0.613 ± 0.008 <sup>d</sup>	3.400 ± 0.036 <sup>a</sup>
P-OSA9	0.845 ± 0.012 <sup>b</sup>	3.073 ± 0.061 <sup>b</sup>
OSA9-P	0.606 ± 0.006 <sup>d</sup>	3.061 ± 0.014 <sup>b</sup>

area value for OSA-P. This indicated that the formation of pores had an important effect on the change in the specific surface area. The presence of substituents had a significant hindering effect on enzymatic treatment, and this resistance was proportional to the DS of samples [16]. When

esterification modification was performed first, followed by the hydrolysis of two enzymes, where the OS groups are located or nearby may not be subjected to enzymatic treatment. It was more difficult to produce pores, especially at high OSA levels, resulting in a smaller overall specific

TABLE 3: The lamellar structural dimensions of CS, PS, P-OSA, and OSA-P obtained from SAXS analysis.

Samples	$q_{\max}$	$D_{\text{bragg}}$	$I$ (a.u.)	$\alpha$	Peak area
CS	$0.619 \pm 0.002^b$	$10.145 \pm 0.033^c$	$5.273 \pm 0.065^a$	$2.839 \pm 0.042^{bc}$	$1.881 \pm 0.038^a$
PS	$0.616 \pm 0.003^{bc}$	$10.195 \pm 0.050^{bc}$	$2.539 \pm 0.062^e$	$3.683 \pm 0.051^a$	$0.902 \pm 0.026^d$
P-OSA3	$0.615 \pm 0.001^{bc}$	$10.211 \pm 0.017^{bc}$	$3.748 \pm 0.069^c$	$2.821 \pm 0.035^{bc}$	$1.311 \pm 0.041^c$
OSA3-P	$0.628 \pm 0.003^a$	$10.000 \pm 0.048^d$	$3.842 \pm 0.067^c$	$3.501 \pm 0.044^a$	$1.416 \pm 0.057^c$
P-OSA6	$0.619 \pm 0.002^b$	$10.145 \pm 0.033^c$	$2.672 \pm 0.054^e$	$2.463 \pm 0.036^{cd}$	$1.318 \pm 0.036^c$
OSA6-P	$0.589 \pm 0.001^d$	$10.662 \pm 0.018^a$	$4.363 \pm 0.072^b$	$2.926 \pm 0.033^b$	$1.594 \pm 0.043^b$
P-OSA9	$0.612 \pm 0.002^c$	$10.261 \pm 0.034^b$	$3.530 \pm 0.066^d$	$2.356 \pm 0.036^d$	$1.330 \pm 0.027^c$
OSA9-P	$0.616 \pm 0.002^{bc}$	$10.195 \pm 0.033^{bc}$	$5.417 \pm 0.079^a$	$2.922 \pm 0.031^b$	$1.968 \pm 0.033^a$

surface area. Moreover, the lower specific surface area resulted in weaker absorption performance of OSA-P samples than P-OSA.

**3.4. Lamellar Structure Analysis.** The SAXS scattering profiles of starch with different treatment sequences and different OSA amounts are shown in Supplementary Figure 1. The peak position of each starch was approximately  $0.6 \text{ nm}^{-1}$ , and the peak was generated by the alternation of crystalline and amorphous layers inside the starch granule [20]. According to the Wulff-Bragg formula [ $D_{\text{bragg}} = 2\pi/q$ ], the thickness of the semicrystalline lamellae of starch granules, also called the Bragg layer spacing, can be calculated [21]. In particular, after esterification and enzymatic treatment, the thickness of the starch semicrystalline lamellae  $D_{\text{bragg}}$  was between 10.000 and 10.662 nm (Table 3).

The peak intensity  $I$  at  $q_{\max}$  reflected the consistency of the double helix structure arrangement in the crystalline region of the starch lamellar structure, and the peak intensity decreased after enzymatic action. This was due to the fact that enzymes more easily attack the accessible and amorphous lamellae and growth rings of starch, whereas more crystalline and organized structures remain unaltered.

The fractal theory could be used to describe the self-similarity of the aggregate structure between geometrically ordered and geometrically disordered structures in starch granules [22]. The  $\alpha$  values of each curve were calculated using Power's theorem:  $I \sim q^{-\alpha}$  (shown in Table 3). The  $\alpha$  values of P-OSA were generally smaller than those of OSA-P at the same OSA level, which implies a sparser and less ordered aggregate structure.

The area of the peak at  $q_{\max}$  was calculated, with larger peak area indicating that the degree of ordering in the crystalline region of the lamellar structure was higher. The peak areas of P-OSA were generally smaller than those of OSA-P, suggesting that the enzymatic treatment disrupted the order of the crystalline region of the lamellar structure of the starch, but the degree of ordering did not easily decrease when esterified starch was subjected to enzymatic action.

**3.5. Relative Crystallinity.** The X-ray diffraction spectra and relative crystallinity of the samples are shown in Figure 2. A typical A-type diffraction peak was shown for all starch samples, with diffraction peaks at  $15^\circ$ ,  $17^\circ$ ,  $18^\circ$ , and  $23^\circ$ , respectively. Minor differences between the esterified modified porous starch samples and PS indicated that the esterification reaction does not change the crystalline type of starch.

The sharper diffraction peak of PS compared to CS implies that the enzymatic hydrolysis process reduces the amorphous region, which is also indicated by the increase in relative crystallinity [23]. The relative crystallinity of the samples decreased slightly after the esterification modification, but the difference between the samples with different OSA additions was not obvious, which indicated that the crystalline morphology of the starch granules changed less during the esterification modification [24–26]. Comparison of the samples obtained by reversing the order of action shows that the relative crystallinity of P-OSA was higher than that of OSA-P, which indicates a more effective enzymatic hydrolysis of P-OSA during the action. Such more efficient enzymatic hydrolysis resulted in P-OSA having a higher specific surface area than OSA-P at the same OSA addition and led to a superior absorption capacity of P-OSA.

**3.6. Distribution of Octenyl Succinic Groups on Starch Granules.** Confocal Raman spectroscopy can be used to assess the internal vibrations of molecules; thus, it can be used to characterize the distribution of OS groups on starch granules.

For starch granules, the characteristic peaks at  $1,300\text{--}800 \text{ cm}^{-1}$  are derived from the absorption peaks of native starch molecules. Supplementary Figure 2 shows that the starch modified by esterification had a characteristic peak at  $1,670 \text{ cm}^{-1}$  caused by the carbonyl stretching vibration in the OS groups, indicating the presence of a carbonyl group. The distribution of the OS groups on the whole starch granule can be effectively characterized by scanning the whole starch granule, layer by layer, within an X-Y two-dimensional Raman spectral scan matrix under  $532 \text{ nm}$  laser excitation with the carbonyl group characteristic peak at  $1,670 \text{ cm}^{-1}$  as the target peak. Figure 3(a) shows the two-dimensional Raman spectra of OSA starch. The distribution of OS groups on the whole starch granules was not uniform, and their concentration on the surface of OSA starch granules was higher than that on the inside [16, 19]. The distribution of OS groups in P-OSA was more uniform than that in OSA starch, and the signal of the OS groups inside the starch granules was enhanced (Figures 3(a) and 3(b)), indicating that the presence of pores facilitated the reaction inside the granules during the esterification process. Figure 3(c) shows the Raman spectra of OSA-P. Overall, the distribution of OS groups in OSA-P was similar to that of OSA starch. The two-dimensional Raman spectra of the remaining samples are presented in Supplementary Figure 3.

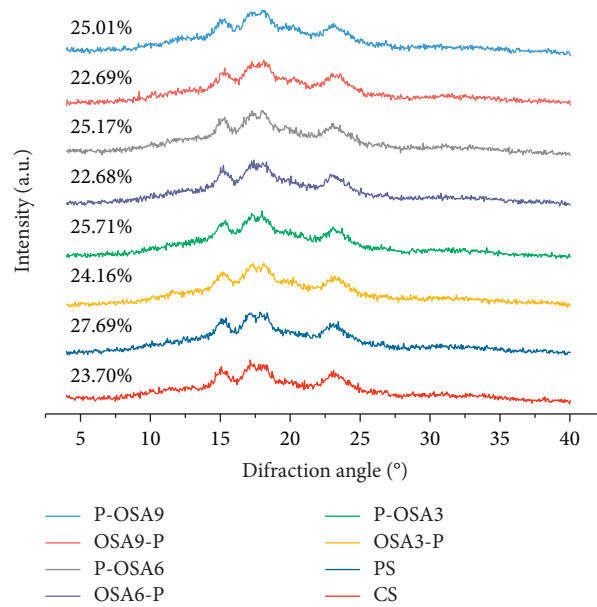


FIGURE 2: XRD patterns and relative crystallinity.

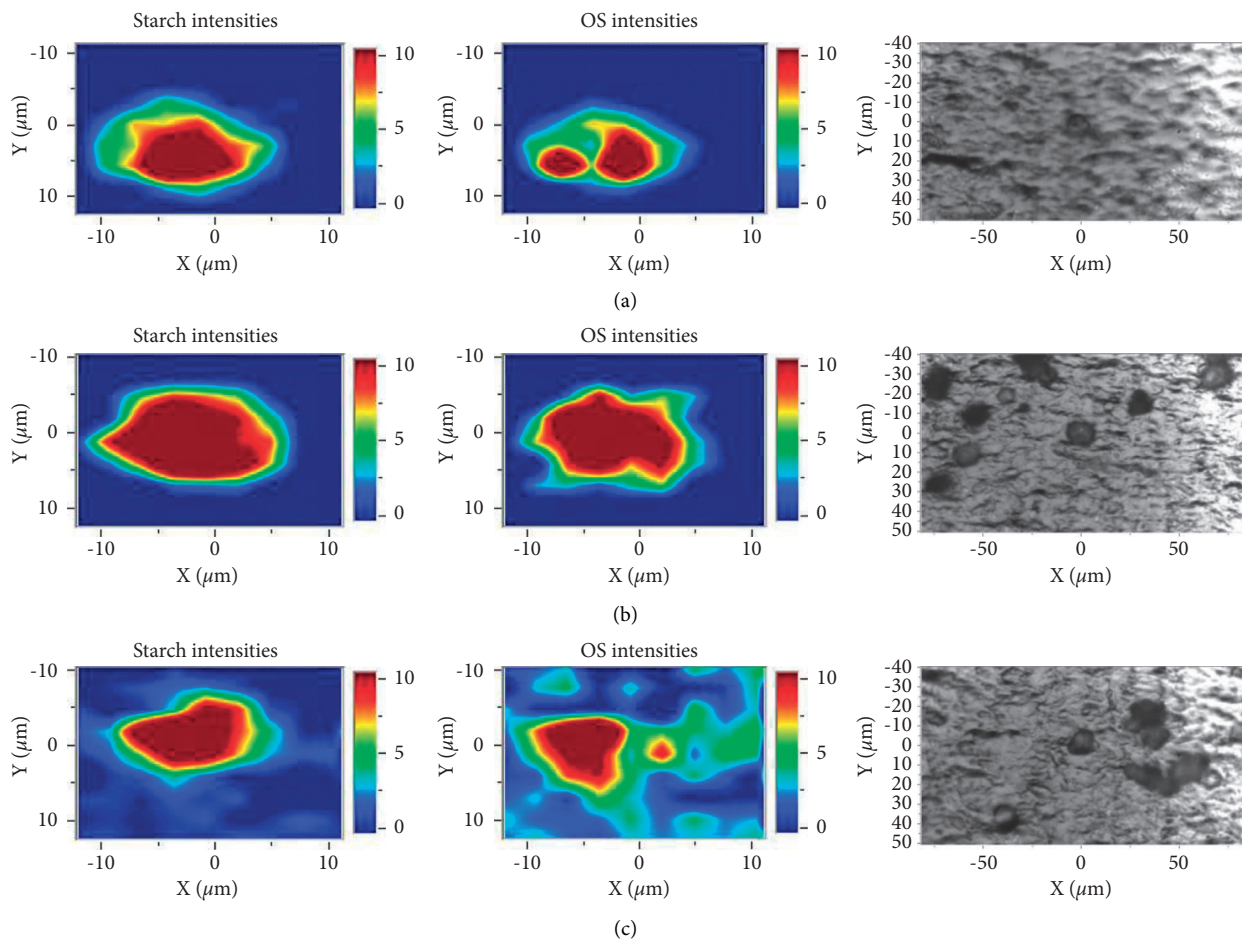


FIGURE 3: 2D Raman spectra of OSA9 (a), P-OSA9 (b), and OSA9-P (c).

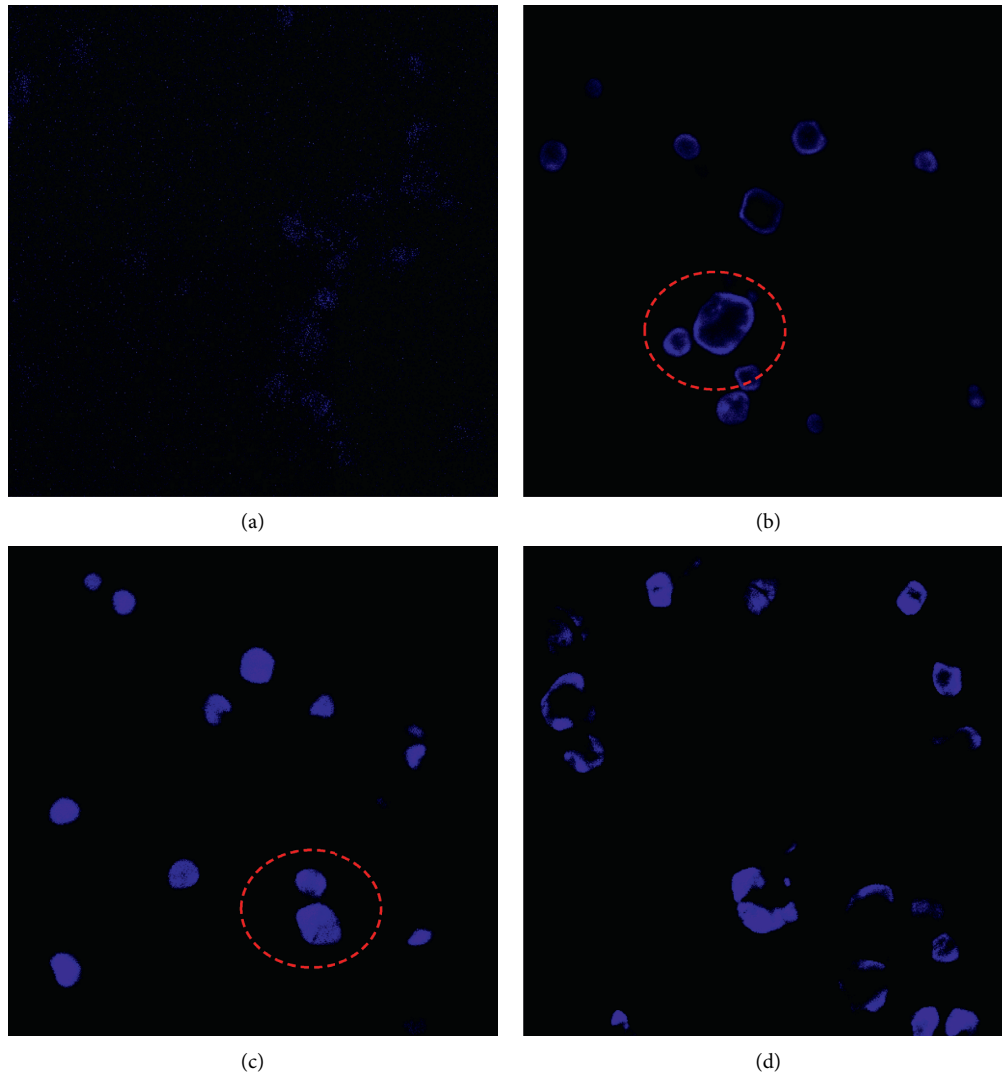


FIGURE 4: Laser confocal microscopy images of PS (a), OSA9 (b), P-OSA9 (c), and OSA9-P (d).

The laser confocal microscopy images are shown in Figure 4. Starch without OSA modification could not be stained by MB because it did not have OS groups, so the fluorescence intensity was very low. In contrast, the starch granules with OS groups were positively stained with MB (Figures 4(b) and 4(d)), further demonstrating that the OS groups were mainly distributed on the surface of the granules, as the fluorescence intensity inside the granules was weaker than that on the surface. The P-OSA internal part of the granules also showed fluorescent signal (Figure 4(c)), suggesting that the distribution of OS groups was affected when the porous starch was esterified, with the presence of pores being beneficial for the reaction to occur inside the granules. OS groups were not only mainly distributed on the surface of P-OSA granules, but there were also more OS groups inside the granules compared to the OSA starch.

**3.7. Analysis of Menthone Loading.** Under the action of enzymes, the pores on the surface of starch increased and the loading of menthone increased, and the PS loading of

TABLE 4: Menthone load of CS, PS, P-OSA, and OSA-P.

Samples	Loading (mg/g)
CS	$7.72 \pm 0.80^c$
PS	$31.83 \pm 0.41^d$
P-OSA3	$31.80 \pm 0.88^d$
P-OSA6	$52.76 \pm 1.09^b$
P-OSA9	$64.34 \pm 1.23^a$
OSA3-P	$46.57 \pm 0.69^c$
OSA6-P	$47.11 \pm 1.67^c$
OSA9-P	$51.30 \pm 0.96^b$

menthone reached 4 times of CS (Table 4). The OSA modification of porous starch further increased the loading of menthone due to the increased hydrophobicity. The sequential comparison showed that except for the low OSA addition (3%), the P-OSA had higher loading of menthone than OSA-P with the same OSA-esterification addition. At high OSA addition, P-OSA showed a higher loading of menthone, indicating that P-OSA possesses the potential for menthone loading applications.

## 4. Conclusion

Hydrophobic porous starch with different OSA amounts was prepared by the hydrolysis of amyloglucosidase and  $\alpha$ -amylase and OSA esterification modification, and the structures and properties of the hydrophobic porous starch obtained by different treatment sequences were compared. With the subsistence of OS groups, the hydrophobicity of starch was enhanced, which in turn improved the affinity of starch for oil. The DS of OSA-P was generally lower than that of P-OSA, which affected the absorption performance of the samples. The presence of more OS groups could hinder enzyme activity, thus leading to differences in structure and properties of samples under different treatment sequences. The relative crystallinity of the starch and SAXS data showed that for P-OSA, the relative crystallinity was higher and the aggregated structure was less ordered compared to OSA-P. The surface of P-OSA is still widely distributed with pores, and its specific surface area was larger than that of OSA-P, resulting in a better absorption capacity. However, the OSA-P did not easily form pores due to the inhibitory effect of the OS groups on the enzyme, and the absorption capacity was not ideal. In addition, the OSA reagent may react with the inside of the starch granules during the preparation process due to the presence of the pores of PS, resulting in a more uniform distribution of OS groups in the starch granules of P-OSA. The results of loading on menthone showed that P-OSA showed higher loading on menthone at high OSA additions, indicating that P-OSA possesses the potential to load menthone for application.

## Abbreviations

DS:	Degree of substitution
FESEM:	Field-emission scanning electron microscopy
MB:	Methylene blue
OS:	Octenyl succinic group
OSA:	Octenyl succinic anhydride
CS:	Native corn starch
PS:	Porous starch
OSAS:	OSA starch
P-OSA:	Starch modified by enzymatic hydrolysis followed by OSA
OSA-P:	Starch modified by OSA followed by enzymatic hydrolysis. The numbers following OSA (3, 6, and 9) represent the amount of OSA added as a percentage of the dry starch weight (w/w) during preparation.

## Data Availability

The data used to support the findings of this study are included within the article.

## Conflicts of Interest

The authors declare that they have no conflicts of interest.

## Acknowledgments

This research was supported by the National Natural Science Foundation of China (nos. 31571794 and 31560437), National First-Class Discipline Program of Food Science and Technology (JUFSTR20180204), Science and Technology Major Project of Guangxi (no. guikeAA17202029), and Postgraduate Research & Practice Innovation Program of Jiangsu Province (no. KYCX21\_2046).

## Supplementary Materials

Supplementary Figure 1: the  $I \sim q$  curves of CS, PS, P-OSA, and OSA-P obtained from SAXS analysis. Supplementary Figure 2: Raman spectra of OSAS. Supplementary Figure 3: 2D Raman spectra of OSA3 (a), P-OSA3 (b), OSA3-P (c), OSA6 (d), P-OSA6 (e), and OSA6-P (f). Supplementary Figure 4: the morphology of samples after oil absorption. Supplementary Figure 5: the morphology of samples after MB absorption. Supplementary Figure 6: field-emission micrographs of samples after MB absorption. Supplementary Figure 7: absorption amount in pre-experiment. Supplementary Figure 8: field-emission micrographs of CS and PS in pre-experiment. Supplementary Table 1: absorption properties and DS of samples with the same degree of esterification and different enzyme additions and order of action. (*Supplementary Materials*)

## References

- [1] X. Ma, X. Liu, D. P. Anderson, and P. R. Chang, "Modification of porous starch for the adsorption of heavy metal ions from aqueous solution," *Food Chemistry*, vol. 181, pp. 133–139, 2015.
- [2] Y. Xie, M.-N. Li, H.-Q. Chen, and B. Zhang, "Effects of the combination of repeated heat-moisture treatment and compound enzymes hydrolysis on the structural and physicochemical properties of porous wheat starch," *Food Chemistry*, vol. 274, pp. 351–359, 2019.
- [3] J. Liu, X. Wang, H. Yong, J. Kan, and C. Jin, "Recent advances in flavonoid-grafted polysaccharides: synthesis, structural characterization, bioactivities and potential applications," *International Journal of Biological Macromolecules*, vol. 116, pp. 1011–1025, 2018.
- [4] J. Chen, Y. Wang, J. Liu, and X. Xu, "Preparation, characterization, physicochemical property and potential application of porous starch: a review," *International Journal of Biological Macromolecules*, vol. 148, pp. 1169–1181, 2020.
- [5] Q.-Q. Lv, G.-Y. Li, Q.-T. Xie et al., "Evaluation studies on the combined effect of hydrothermal treatment and octenyl succinylation on the physicochemical, structural and digestibility characteristics of sweet potato starch," *Food Chemistry*, vol. 256, pp. 413–418, 2018.
- [6] P. R. Chang, D. Qian, D. P. Anderson, and X. Ma, "Preparation and properties of the succinic ester of porous starch," *Carbohydrate Polymers*, vol. 88, no. 2, pp. 604–608, 2012.
- [7] Y. Bai, R. C. Kaufman, J. D. Wilson, and Y.-C. Shi, "Position of modifying groups on starch chains of octenylsuccinic anhydride-modified waxy maize starch," *Food Chemistry*, vol. 153, pp. 193–199, 2014.
- [8] Y. Bai and Y.-C. Shi, "Structure and preparation of octenyl succinic esters of granular starch, microporous starch and



- soluble maltodextrin," *Carbohydrate Polymers*, vol. 83, no. 2, pp. 520–527, 2011.
- [9] B. Zhang, D. Cui, M. Liu, H. Gong, Y. Huang, and F. Han, "Corn porous starch: preparation, characterization and adsorption property," *International Journal of Biological Macromolecules*, vol. 50, no. 1, pp. 250–256, 2012.
- [10] X.-y. Song, Q.-h. Chen, H. Ruan, G.-q. He, and Q. Xu, "Synthesis and paste properties of octenyl succinic anhydride modified early Indica rice starch," *Journal of Zhejiang University-Science B*, vol. 7, no. 10, pp. 800–805, 2006.
- [11] Y. Xie, B. Zhang, M.-N. Li, and H.-Q. Chen, "Effects of cross-linking with sodium trimetaphosphate on structural and adsorptive properties of porous wheat starches," *Food Chemistry*, vol. 289, pp. 187–194, 2019.
- [12] Y. Zheng, Y. Ou, C. Zhang et al., "The impact of various exogenous type starch on the structural properties and dispersion stability of autoclaved lotus seed starch," *International Journal of Biological Macromolecules*, vol. 175, pp. 49–57, 2021.
- [13] R. Bardestani, G. S. Patience, and S. Kaliaguine, "Experimental methods in chemical engineering: specific surface area and pore size distribution measurements-BET, BJH, and DFT," *Canadian Journal of Chemical Engineering*, vol. 97, no. 11, pp. 2781–2791, 2019.
- [14] Z. Yang, X. Xu, Y. Hemar, G. Mo, L. de Campo, and E. P. Gilbert, "Effect of porous waxy rice starch addition on acid milk gels: structural and physicochemical functionality," *Food Hydrocolloids*, vol. 109, Article ID 106092, 2020.
- [15] X. Chen, R. Liang, F. Zhong et al., "Effect of high concentrated sucrose on the stability of OSA-starch-based beta-carotene microcapsules," *Food Hydrocolloids*, vol. 113, Article ID 105472, 2021.
- [16] B. Zhang, Q. Huang, F.-x. Luo, X. Fu, H. Jiang, and J.-l. Jane, "Effects of octenylsuccinylation on the structure and properties of high-amylose maize starch," *Carbohydrate Polymers*, vol. 84, no. 4, pp. 1276–1281, 2011.
- [17] W. Gao, J. Sui, P. Liu, B. Cui, and A. M. Abd El-Aty, "Synthetic mechanism of octenyl succinic anhydride modified corn starch based on shells separation pretreatment," *International Journal of Biological Macromolecules*, vol. 172, pp. 483–489, 2021.
- [18] Y. Benavent-Gil and C. M. Rosell, "Morphological and physicochemical characterization of porous starches obtained from different botanical sources and amylolytic enzymes," *International Journal of Biological Macromolecules*, vol. 103, pp. 587–595, 2017.
- [19] Q. Huang, X. Fu, X.-w. He, F.-x. Luo, S.-j. Yu, and L. Li, "The effect of enzymatic pretreatments on subsequent octenyl succinic anhydride modifications of cornstarch," *Food Hydrocolloids*, vol. 24, no. 1, pp. 60–65, 2010.
- [20] J. Blazek and E. P. Gilbert, "Application of small-angle X-ray and neutron scattering techniques to the characterisation of starch structure: a review," *Carbohydrate Polymers*, vol. 85, no. 2, pp. 281–293, 2011.
- [21] L. Zhang, X. Li, S. Janaswamy, L. Chen, and C. Chi, "Further insights into the evolution of starch assembly during retrogradation using SAXS," *International Journal of Biological Macromolecules*, vol. 154, pp. 521–527, 2020.
- [22] T. Suzuki, A. Chiba, and T. Yarno, "Interpretation of small angle x-ray scattering from starch on the basis of fractals," *Carbohydrate Polymers*, vol. 34, no. 4, pp. 357–363, 1997.
- [23] L. Guo, J. Li, Y. Gui et al., "Porous starches modified with double enzymes: structure and adsorption properties," *International Journal of Biological Macromolecules*, vol. 164, pp. 1758–1765, 2020.
- [24] B. Zhang, J.-Q. Mei, B. Chen, and H.-Q. Chen, "Digestibility, physicochemical and structural properties of octenyl succinic anhydride-modified cassava starches with different degree of substitution," *Food Chemistry*, vol. 229, pp. 136–141, 2017.
- [25] H. Hu, W. Liu, J. Shi et al., "Structure and functional properties of octenyl succinic anhydride modified starch prepared by a non-conventional technology," *Starch-Stärke*, vol. 68, no. 1-2, pp. 151–159, 2015.
- [26] Z. Yi, L. Hu, D. Ning, L. Ping, and H. Zhang, "Physicochemical and structural characteristics of the octenyl succinic ester of ginkgo starch," *International Journal of Biological Macromolecules*, vol. 94, pp. 566–570, 2017.